Suspended Carbon Nanotube Beams Fabricated by a Low Temperature Surface Micromachined Process for Humidity and Gas Sensing

by

Shiva Ram ARUNACHALAM

MANUSCRIPT BASED THESIS PRESENTED TO ÉCOLE DE TECHNOLOGIE SUPÉRIEURE IN PARTIAL FULFILLMENT FOR THE DEGREE OF DOCTOR OF PHILOSOPHY
Ph.D.

MONTREAL, MARCH 29, 2020

ÉCOLE DE TECHNOLOGIE SUPÉRIEURE
UNIVERSITÉ DU QUÉBEC

BOARD OF EXAMINERS

THIS THESIS HAS BEEN EVALUATED

BY THE FOLLOWING BOARD OF EXAMINERS

Mr. Frédéric Nabki, Thesis Supervisor
Department of Electrical Engineering, École de Technologie Supérieure

Mr. Ricardo Izquierdo, Thesis Co-supervisor
Department of Electrical Engineering, École de Technologie Supérieure

Mr. Guy Gauthier, President of the Board of Examiners
Department of Systems Engineering, École de Technologie Supérieure

Mr. Ricardo Zednik, Member of the jury
Department of Mechanical Engineering, École de Technologie Supérieure

Mr. Thomas Szkopek, External Evaluator
McGill University

THIS THESIS WAS PRESENTED AND DEFENDED

IN THE PRESENCE OF A BOARD OF EXAMINERS AND PUBLIC

26 FEBRUARY 2020

AT ÉCOLE DE TECHNOLOGIE SUPÉRIEURE

ACKNOWLEDGMENT

Neither this Ph.D., nor these past five years in Montreal, nor me would be the same without the help and company of many people.

First, I would like to express my sincere gratitude to my research supervisor Professor Frederic Nabki and my co-supervisor Professor Ricardo Izquierdo, for giving me the opportunity to pursue a Ph.D. and keeping faith in me through some challenging times. I will never forget your words of encouragement and support. This Ph.D. would not have been possible without your guidance, knowledge and intuitive insights. Thank you for teaching me, inspiring me and patiently listening to me. I could not have asked for better guidance. I am especially thankful to Professor Nabki for continually pushing me towards excellence in my research. His work-ethic and passion for science is infectious. It is something that I will strive to carry with me throughout my professional life.

Secondly, I would like to thank all the members of the thesis committee for their encouragement, time and insightful comments. I would also like to express my sincere gratitude to the technical staff at ETS and UQAM, Alexandre Robichaud and Normand Gravel for helping me train on the lab equipment and addressing any difficulties that I may have faced. Without their support, thesis research project would not have been possible. My friends who formed a large part of my life in Montreal and have become more like family: Anubha, Michiel, Lakshay, Pankaj, Devika, Mohammed and many others. Thank you for all the love and support. I will fondly remember the conversations and parties that we had over the years

Finally, and most importantly, I want to thank my family, my biggest pillars of strength, support and inspiration. I would not be where I am today if not for their sacrifice, encouragement, patience and advice when I needed it most. Although I live thousands of miles away, I feel their love, warmth and presence constantly and it helps me push through life's obstacles. I wouldn't be who I am if it wasn't for you.

Mom, Dad, Hari, this thesis is dedicated to you.

Faisceaux de nanotubes de carbone suspendus fabriqués par un procédé micromachiné en surface à basse température pour la détection d'humidité et de gaz

Shiva Ram ARUNACHALAM

RÉSUMÉ

Le monde dans lequel nous vivons aujourd'hui est connecté de plus de façons que nous ne pouvons l'imaginer. Les appareils intelligents et les réseaux sont au cœur de notre vie quotidienne. L'avènement de l'Internet des objets et de l'industrie 4.0 nécessite différents types de capteurs fonctionnants conjointement. Gardant cela à l'esprit, cette thèse explore l'application des nanotubes de carbone à simple paroi en suspension pour la détection de gaz. Les détecteurs de gaz sont utilisés dans une variété d'environnements tels que les hôpitaux, les navettes spatiales et les cuisines domestiques pour détecter et empêcher les fuites de gaz dangereux. Une variété de matériaux tels que les polymères, la céramique et les oxydes métalliques et les mécanismes de détection ont été utilisés pour identifier divers gaz. Plus récemment, les nanotubes de carbone ont suscité une attention considérable pour les applications de détection de gaz en raison de leurs excellentes propriétés électriques et de leur facilité de modification de surface. Avec les progrès des techniques de production, le coût de production des nanotubes de carbone a considérablement diminué, ce qui a permis le développement de capteurs de gaz à base de nanotubes de carbone. Bien que plusieurs capteurs de gaz à base de nanotubes de carbone aient été étudiés dans le passé, la structure globale du dispositif reste globalement similaire. De plus, ces dispositifs offrent souffrent de grands effets hystérétiques, souvent en raison de l'effet du substrat sur le mécanisme de détection global, ce qui peut conduire à des sorties de mesure peu fiables.

Ce travail vise à résoudre le problème de l'hystérésis en utilisant des nanotubes de carbone en suspension et ainsi isoler l'élément de détection des effets du substrat. Pour ce faire, tout d'abord, un procédé de micro-usinage de surface à basse température est développé pour obtenir des dispositifs suspendus. Une fois le processus bien développé, le dispositif suspendu est utilisé pour détecter l'humidité. Les performances du dispositif suspendu sont comparées à celles d'un dispositif non suspendu pour démontrer les avantages des nanotubes de carbone suspendus.

Ensuite, les mesures de performance du capteur suspendu sont améliorées en fonctionnalisant chimiquement les nanotubes pour les rendre plus sensibles à la vapeur d'eau. Les nanotubes sont obtenus dans le commerce, pré-fonctionnalisés et utilisés dans le processus de fabrication. Une étude comparative entre les capteurs à base de nanotubes fonctionnalisés suspendus et non suspendus est également réalisée. Enfin, la conception de l'appareil a été modifiée pour fabriquer un capteur de gaz d'ionisation basé sur des nanotubes de carbone suspendus alignés horizontalement. Le potentiel d'ionisation de divers gaz est identifié et d'autres paramètres tels que la répétabilité, la stabilité à long terme, etc. ont été étudiés.

Mots-clés: Nanotubes de carbone; Suspendu; humidité; Ionisation

Suspended Carbon Nanotube Beams Fabricated by a Low temperature Surface Micromachined Process for Humidity and Gas sensing

Shiva Ram ARUNACHALAM

ABSTRACT

The world we live in today is connected in more ways than we can imagine. Smart devices and networks form the core of our everyday lives. The advent of the Internet of Things and Industry 4.0, which are terms defined to make the world around us more connected via the internet at a domestic and industrial setting respectively, necessitates various kinds of sensors working in conjunction with each other. Keeping this in mind, this thesis explores the application of Suspended Single walled Carbon Nanotubes for Gas Sensing. Gas Sensors are used in a variety of environments such as hospitals, space shuttles and domestic kitchens to detect and prevent the leakage of hazardous gases. A variety of materials such as Polymers, ceramics and metal oxides and detection mechanisms have been used to identify various gases. More recently, Carbon nanotubes have garnered considerable attention for gas sensing applications due to their excellent electrical properties and ease of surface modification. With advancements in production techniques, the cost of Carbon Nanotube production has reduced significantly which has enabled the development of Carbon Nanotube based gas sensors. Although multiple Carbon Nanotube based gas sensors have been studied in the past, the overall device structure remains broadly similar. Additionally, these devices offer suffer from large hysteretic effects, often because of the effect of the substrate on the overall sensing mechanism, which can lead to unreliable measurement outputs.

This work aims to solve the issue of hysteresis by using suspended Carbon Nanotubes and thereby isolating the sensing element from the effects of the substrate. To do this, first, a low temperature surface micromachining process is developed to obtain suspended devices. Once the process is well developed, the suspended device is used to detect humidity. The performance of the suspended device is compared to a non-suspended device to demonstrate the advantages of suspended Carbon nanotubes.

Next, the performance metrics of the suspended sensor are improved by chemically functionalizing the nanotubes to make them more sensitive to water vapor. The nanotubes are obtained commercially, pre-functionalized, and used in the fabrication process. A comparative study between suspended and non-suspended functionalized nanotube-based sensors is also done. Lastly, the device design has been modified to fabricate an ionization gas sensor based on horizontally aligned suspended carbon nanotubes. The ionization potential of various gases is identified and other parameters such as the repeatability, long term stability, etc. have been studied.

Keywords: Carbon Nanotubes; Suspended; Humidity; Ionization.

TABLE OF CONTENTS

Page

LIST OF TABLES

Page

LIST OF FIGURES

Page

LIST OF ABREVIATIONS

MEMS	Microelectromechanical Systems
IC	Integrated Circuits
CNTs	Carbon Nanotubes
SWCNT	Single-walled Carbon Nanotubes
MWCNT	Multi-walled Carbon Nanotubes
NEMS	Nanoelectromechanical Systems
in^3	Cubic inch
CMOS	Complementary metal-oxide semiconductor
PMMA	Poly Methyl Methacrylate
TEM	Transmission Electron Microscope
nm	Nanometers
FET	Field Effect Transistor
ChemFET	Chemical Field Effect Transistor
MHz	Megahertz
CVD	Chemical Vapor Deposition
ppm	Parts per Million
ppb	Parts per billion
DMMP	Dimethyl Methyl Phosphate

PAA	Polyacrylic acid
RH	Relative Humidity
DI	Deionized
SEM	Scanning Electron Microscope
min	Minutes
rpm	Rounds per minute
s	Second
VOCs	Volatile Organic Compounds
SDS	Sodium Dodecyl Sulfate
Wt%	Weight %
Tpa	Tera Pascal
DC	Direct current
DRIE	Deep Reactive Ion Etching
I_{sd}	Source-drain current
PVA	Poly Vinyl Alcohol

LIST OF SYMBOLS

μm	Micrometers
°C	Degrees Celsius
GaAs	Gallium Arsenide
InP	Indium Phosphide
V	Volts
eV	Electron-volt
K	Kelvin
mK	milli-Kelvin
C	Chiral Vector
d	Diameter
σ	Stress
σ_c	Film thickness
ε	Strain
σ_s	Tensile Strength
Sm^{-1}	Siemens per meter
aN	Atto-newton
$cm^2V^{-1}s^{-1}$	centimeter squared per volt per second
NH_3	Ammonia

Cr	Chromium
Au	Gold
Ar	Argon
He	Helium
N_2	Nitrogen
CO	Carbon Monoxide
Si	Silicon
COOH	Carboxylic acid group
HF	Hydrofluoric acid
KOH	Potassium Hydroxide
HNO_3	Nitric acid
CO_2	Carbon dioxide
g	Gram
kΩ	Kilo-ohm
Gpa	Giga-Pascal
R	Resistance
R_H	Resistance at any measured humidity
R_o	Baseline resistance
mA	Milliampere

INTRODUCTION

Motivation

During the past two decades, the field of Micro-electromechanical systems (MEMS) has attracted significant attention from academic researchers as well as the electronics industry. MEMS can be described as a process technology that can be used to create miniature components ranging in size from a few micrometers to a few millimeters. These miniature devices can be used in various applications such as sensing, actuation, etc. Over the years, MEMS has become an interdisciplinary field in which expertise from different areas such as materials science, electrical engineering, IC design, etc. MEMS technology has matured to the point where its applications can now be found in a variety of systems ranging from automotive, medical and defense applications. Some everyday MEMS devices that we come across include accelerometers in automobile airbags, printheads for ink-jet printers, etc. MEMS is one of the most promising technologies of the 21st century and has the potential to revolutionize many aspects of industrial and consumer products.

Gas sensors enable the detection of various gaseous components in the ambient air. Gas sensors find their use in a variety of applications such as process control and packaging facilities, domestic kitchens, environment control in automobiles and space shuttles, etc. Gas sensors primarily consist of a sensing element and a component to transfer the signal, namely, a transducer. Various sensing elements such as metal oxides, polymers, biomaterials, etc. have been used for gas detection (Baratto et al. 2005; Yang et al. 1999). The sensing mechanism is a characteristic of change in the material properties due to the interaction between the analyte and the sensing element. The type of interaction can be chemical or physical depending on the type of analyte-sensor interaction. Transduction mechanisms include optical, capacitive, resistive, etc. (Barone et al. 2004; Yang et al. 1999). Gas sensors are not the only tools that can be used for gas detection and analysis. Tools like Gas chromatography, Spectrometry, etc. have also been used extensively for a similar purpose (Ballschmiter and Zell 1980). However, these tools are cumbersome to operate, expensive and can have sub-optimal performance in some conditions.

Carbon Nanotubes (CNTs), which are essentially rolled up sheets of Graphene, have been actively used as gas sensing elements in the past few years, owing to their excellent electrical properties. The ability to tailor the sensitivity of CNTs to specific gases by chemical functionalization of the sidewalls makes them suitable candidates for gas sensing applications. CNTs have been used to detect gases such as NH_3, CO, etc. CNT sensors have demonstrated fast response and recovery times, long shelf life and high selectivity which are essential factors to make a good gas sensor. Thus, the electrical properties of CNTs in combination with MEMS fabrication technologies has the potential to result in high performance, cost-effective gas sensors which can be widely used in various applications.

Problem Statement

Although CNTs make for a great sensing material, CNT based gas sensors often suffer from hysteretic effects, often due to the role played by the substrate in the overall sensing mechanism. A detailed study by Soares et al. (Soares and Jorio 2012) have shown that the substrate sometimes limits the charge transfer in case of chemical sensors. Hysteresis often leads to unreliable measurements and subsequently unreliable results, which are not desirable. Interestingly, not a lot of research has been done to study and eliminate hysteretic effects in gas sensors. One way to eliminate the unwanted effects is to use a suspended architecture wherein the sensing element is suspended above the substrate. Suspended CNT devices have been studied and published previously to study the intrinsic properties of CNTs such as transport mechanism and scattering phenomena. Muoth et al. (Muoth et al. 2010) first fabricated a hysteresis free CNT transistors. The hysteresis free operation of the transistors in this work is attributed to the absence of substrate effects on the CNT. (Chikkadi et al. 2014a) in their work further proved that a suspended architecture is instrumental in eliminating hysteretic effects.

Although suspended CNT sensors exist in literature, their application to gas sensing has been limited to detecting NO_2 (Chikkadi, Muoth, and Hierold 2013). Thus, it would be interesting to see if combining a suspended architecture and the intrinsic properties of CNTs can solve the issue of hysteresis and lead to improved reliability.

It will also be interesting to see if adopting a suspended architecture also improves other aspects of device performance such as the response time, recovery time and sensitivity. Fabrication of suspended devices involves use of expensive equipment such as vapor deposition tools and lithography tools such as e-beam lithography which also adds to the time consumption. Even by using these expensive techniques, obtaining a usable device yield and repeatability remains a challenge.

Thus, this Ph.D. work aims to study and address the problem of device reliability while also trying to improve other sensor aspects such as response time, long term stability and sensitivity. The primary focus of research in this Ph.D. is the design and fabrication of suspended CNT beams using a photoresist sacrificial layer by a low-temperature process that is integrable with above IC processes aiding in maximum sensor integration. To the author's best knowledge, there has not been an attempt yet to fabricate suspended CNT beam sensors by a low-temperature process.

Research Goals

MEMS fabrication technology has been at the forefront of sensor fabrication for the past few years. Bulk and surface micromachining techniques have been used to fabricate various types of sensors over the past few decades, with bulk micromachining being preferred in the industry since it results in cleaner devices, without stiction issues and high aspect ratio structures (Aimi et al. 2004). The fabrication costs associated with bulk micromachining are often on the higher side due to the use of dry etch setups and expensive lithography machines. However, the costs involved can be justified in the long run due to mass production and market demand. However, bulk micromachining is not amenable to monolithic integration above ICs which is why this research work was done by surface micromachining.

The primary aim of this Ph.D. work is to develop suspended CNT based gas sensors based on a MEMS surface micromachining process. Specifically, the inherent advantages of suspended CNTs for gas sensing is studied and demonstrated.

One of the objectives of the fabrication process is to have a low temperature budget preferably under 115°C and without the use of any expensive equipment like e-beam and chemical vapor deposition and by using a photoresist as a sacrificial layer.

The development of the microfabrication process and fabrication of a device constitutes the first part of the project. Further, the device is tested under humidity to gauge its response. Then, the device design and fabrication process are evolved by placing a metal electrode underneath the suspended beam, and thus an ionization sensor based on suspended CNTs is fabricated and tested. This further process the versatility of the envisioned fabrication process.

Thus, the main objectives of this thesis can be summarized as follows:

- Identify the challenges with current humidity and gas sensing materials and methods.
- Design, fabrication and testing of a novel suspended CNT beam humidity sensor to eliminate hysteretic effects.
- Improving the performance metrics of the fabricated humidity sensor by using readily obtained chemically functionalized CNTs as the sensing material.
- Evolution of device design to fabricate a CNT based ionization gas sensor.

Thesis Outline

This thesis is organized into 6 chapters.

Chapter 1 aims to familiarize the reader about MEMS techniques and includes discussions about commonly used materials and MEMS fabrication methodologies.

Chapter 2 gives a brief introduction about CNTs, which is the sensing material used in this PhD work. The electrical and mechanical properties of CNTs are discussed followed by a brief description of the potential applications of CNTs in various fields such as electronics, energy harvesting and sensing. Finally, the challenges currently facing the commercial application of CNTs is discussed.

Chapter 3 discusses the application of CNTs to gas sensing by reviewing various peer published works. A section discussing the application of suspended CNTs for gas sensing is presented. Further, a section pertaining to humidity sensing is presented with an overview of the most popular materials used, including CNTs is presented. Further, CNT based ionization sensors are reviewed.

Chapter 4 presents a humidity sensor using suspended CNT beams. The developed surface micromachining-based microfabrication process is described in detail. Then, the humidity sensing capabilities of suspended CNTs is studied and the results are reported. This work constitutes the first journal publication of this Ph.D. work published in MDPI Sensors.

In **Chapter 5**, a functionalized suspended CNT humidity sensor is presented. In this work, a remarkable improvement in all performance metrics is reported. The CNTs in this work were obtained pre-functionalized to increase their affinity to water vapor directly correlating to the improved performance. This work forms the second journal publication of this Ph.D. work published in MDPI Sensors.

In **Chapter 6**, a concept for the evolution of the sensor structure and design is presented. This work constitutes the third journal publication. In this work, an ionization sensor based on a suspended CNT beam is fabricated and tested for sensitivity to various gases. This further proves that the developed process can be easily modified and adopted for fabricating different types of sensors. The resultant ionization sensor has good performance metrics and good long-term stability as compared to other works in literature but by eliminating use of any high temperature CNT growth techniques.

CHAPTER 1

INTRODUCTION TO MEMS TECHNOLOGY

The 20th century gave birth to major technological accomplishment such as manned flight, lasers, information technology, the internet, integrated circuits (ICs) and Microelectromechanical Systems (MEMS). The conception of the transistor using Germanium by John Bardeen and Walter Barttain of Bell Labs in 1947 ignited a spark and research in electrical engineering spiked interest, eventually leading to the field known as Microelectromechanical Systems (MEMS). Soon after the discovery of the transistor, the piezoresistive property of Silicon was discovered and the first silicon strain gauge was fabricated in 1954 followed by its commercialization in 1959 by Kulite Semiconductors. Further, the first Integrated Circuit (IC) was developed by Jack Kilby of Texas Instruments in 1958 consisting of 1 transistor, 3 resistors and 1 capacitor on one Germanium chip. Not long after, Fairchild Semiconductor commercialized the IC after Robert Noyce's invention of the first Silicon integrated circuit. The 1960's and 1970's saw rapid progress in the area of pressure sensors fabricated by etching Si using bulk micromachining. Kurt Petersen of IBM developed a pressure sensor using a Si diaphragm by micromachining. The rate of advancement in MEMS associated technologies has been nothing short of outstanding with applications in displays, sensing, computing, etc., which affect our lives every day.

1.1 Microelectromechanical Systems (MEMS)

Richard Feynman, during his talk at the American Physical Society in 1959 claimed that "There is plenty of room at the bottom". This famous quote can be credited to the development of cutting-edge technologies at the micro and nano scale. Feynman pointed out that there was lack of research to explore the micro-dimension and that it might be of interest to investigate for potential applications. Feynman famously challenged the scientists to print the contents of a page of a book in an area 1/25,000 smaller and to make a working motor measuring less than 1/64 in^3.

Table 1.1 A Brief History of MEMS

1950's	1960's	1970's	1980's	1990's
"There's plenty of room at the Bottom"	Silicon Piezoresistive Sensors (Honeywell)	Silicon Pressure Transducers (Honeywell)	Polysilicon Surface Micromachining	Commercial Accelerometer (Analog Devices) Digital Mirror Display
Metal Sacrificial Process	Resonant gate transistor	Integrated Gas Chromatograph	Polysilicon Micrometers	Optical Network Switch (Lucent) Silicon Gyroscope (Draper Labs)
	HNA &EDP Etching	Ink Jet Nozzles (IBM) KOH Etching	Silicon wafer bonding LIGA	RF MEMS Optical MEMS Bio MEMS TMAH Etching Deep Reactive Ion etching (DRIE)

Consequently, the motor was developed in 1960 by William McLellan (Science and Society 2004) and the book was reproduced by Thomas Newman of Stanford in 1985 (Archives.caltech.edu 2016).

Table 1 shows a brief history of MEMS and significant milestones in the area across each decade. One can clearly notice the significant progress in various areas and applications. Significant developments and innovations based on MEMS devices are still being reported as the technology evolves continuously.

1.2 MEMS Technology

MEMS is the technology of microscopic devices. At the nanoscale, it merges into Nano-electromechanical systems (NEMS). MEMS are also sometimes referred to as microdevices or micro-systems technology. MEMS are made up of components that range in size between 1 and 100 μm in size and the device sizes usually range from micrometers to sometimes a few millimeters. Once the first MEMS device was fabricated and published, a lot of visionary researchers in both academic and industrial domains took notice and immediately began developing a variety of micro-devices such as micro-cantilevers, micro-gears, etc. MEMS systems have been used in devices such as RF switches, sensors, actuators and accelerometers.

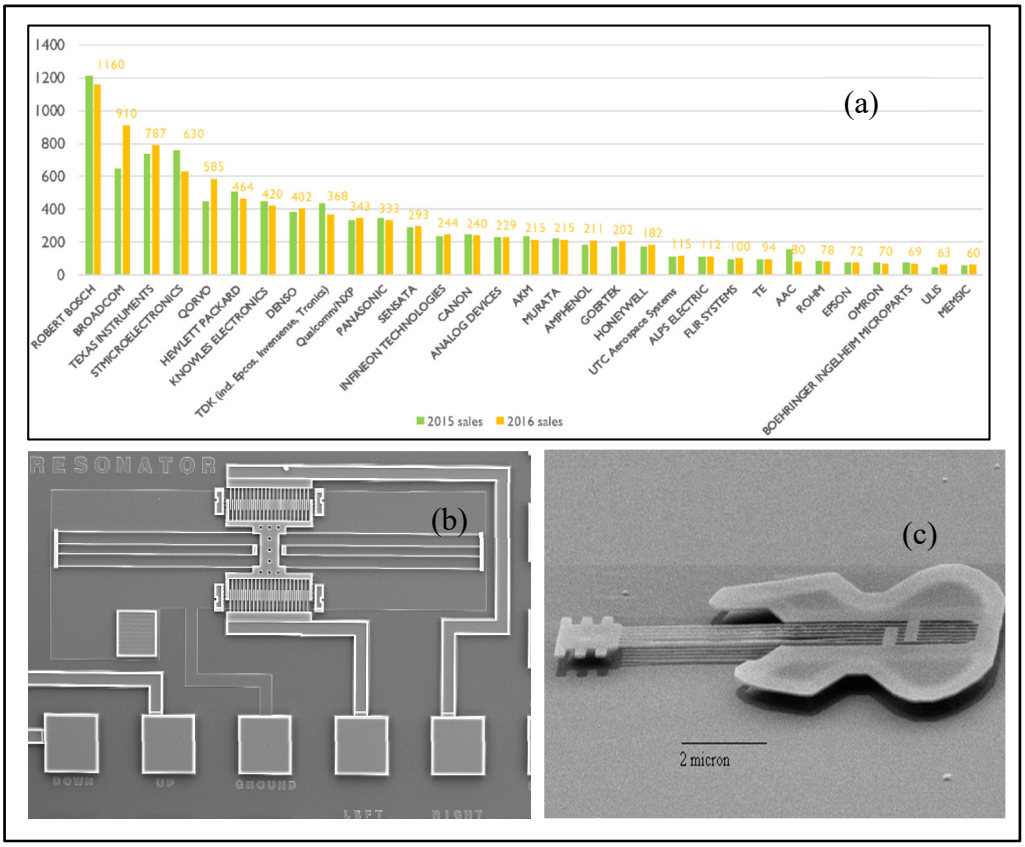

Figure 1.1 (a) MEMS sales in the USA for 2015 and 2016, and,
(b) SEM Micrograph of a typical MEMS device Taken from Smith et al. (2001), and,
(c) The world's smallest guitar, fabricated by MEMS fabrication technologies
Taken from http://news.cornell.edu/stories/1997/07/worlds-smallest-silicon-mechanical-devices-are-made-cornell
(Consulted in December 2019)

With advancements in microfabrication techniques, the field eventually split into a variety of sub-categories such as Radiofrequency MEMS, Optical MEMS, microfluidic MEMS, etc. Figure 1 (a) shows the progression of MEMS device research and sales in the USA for the years 2015 and 2016 in US$ millions. The clear increase in market value of MEMS is mainly due to advancements made in the areas of packaging, device performance and miniaturization.

1.3 Materials used in MEMS

Some popular materials used to fabricate MEMS devices are as follows:

1.3.1 Silicon

Silicon is the go-to material for fabrication of MEMS devices. Silicon in crystalline form is a great Hookean material, meaning, it has minimal energy dissipation. This property also contributes to reliability as it suffers from very little fatigue and shows no mechanical hysteresis. The high melting point of 1400°C also makes it a good candidate for high temperature operation. Added to this, the ready availability of high-quality silicon, cost of scaling and the ability to incorporate electronic functionality make silicon an attractive proposition for MEMS applications. Silicon is mostly used as a substrate material in MEMS applications in a single-crystal form. Other compounds of Silicon such as Silicon dioxide, Silicon carbide and Silicon Nitride are also used in various applications. In this work, Silicon has been used primarily as a substrate and is not an active component of the device.

1.3.2 Polymers

Polymers play a major role in MEMS and microelectronics. They can be found in the packaging of IC chips, intermetallic dielectric layers, etc. Polymers are one of the essential elements in microfabrication of MEMS devices as photoresists for lithographic patterning. The ease of processing, relatively low cost and ease of production and high stability makes them a great choice for use in MEMS. Polymers are generally insulators but there are ways like Pyrolysis and metal doping to make them conductive. These conductive polymers are used as substrates in MEMS. Some popular polymers used in cleanrooms include SU-8, an epoxy-based photoresist consisting of 8 epoxy groups, Polymethyl Methacrylate (PMMA), Parylene, etc. This work uses SU-8, a polymer as a sacrificial material to obtain suspended CNT devices.

1.3.3 Ceramics

Ceramics materials like silicon nitride and silicon carbide are also being increasingly used in MEMS fabrication for piezoelectric devices where electrical and mechanical properties are coupled. Electrostatic MEMS are fabricated using ceramic materials owing to their large elastic modulus. Other favorable properties of ceramics include their chemical inertness, resistance to corrosion, etc.

1.4 Fundamental MEMS Techniques

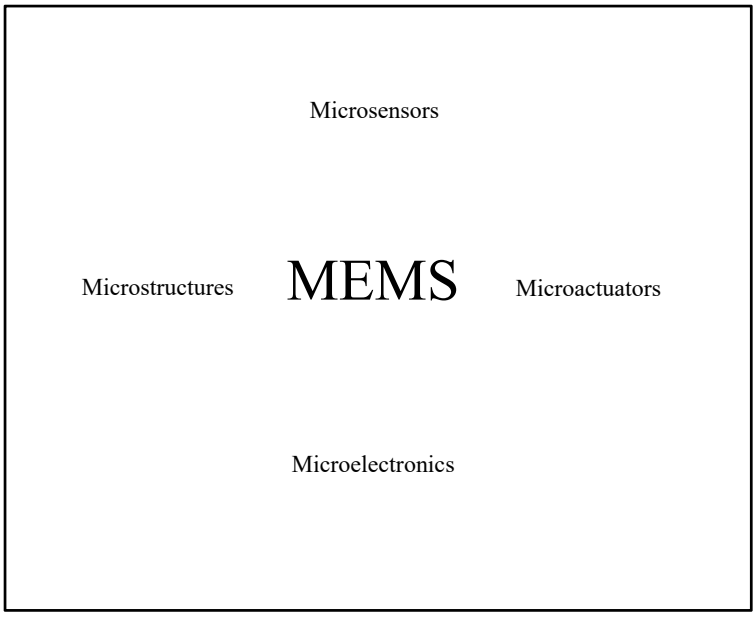

Figure 1.2 MEMS Components

Generally, MEMS can be divided into four major components as shown in Figure 1.2. Most of the times, all the four components are integrated onto a single chip. Micro-sensors detect changes in the environment by measuring changes in mechanical, thermal or chemical properties or phenomena and convert them to an electrical signal. Sensors generally operate by monitoring displacement of structures like beams and diaphragms. These elements are manufactured using several processing techniques, some of which are described briefly in the following section.

1.4.1 Lithography

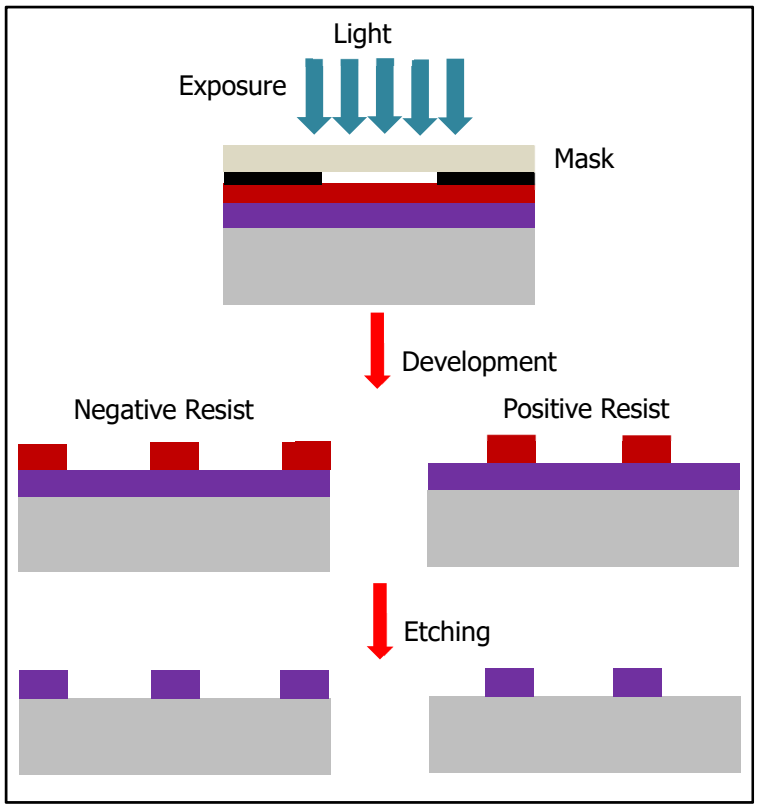

Figure 1.3 Lithography in MEMS

Lithography or photolithography is the process of transferring a pattern on a photomask onto a substrate using a photosensitive polymer. The photosensitive polymer is coated on the substrate using spin coating. Photoresists can be of two types: positive and negative depending on their reaction to UV light. Photolithography is a very common step and, in most cases, one of the first steps in MEMS processing. With the demand for increased resolution in the semiconductor industry, new methods such as X-ray lithography, e-beam lithography ion beam lithography and more recently Extreme UV Lithography have been developed. A schematic of the basic steps for lithography using both positive and negative photoresists is shown in Figure 1.3.

1.4.2 Bulk Micromachining

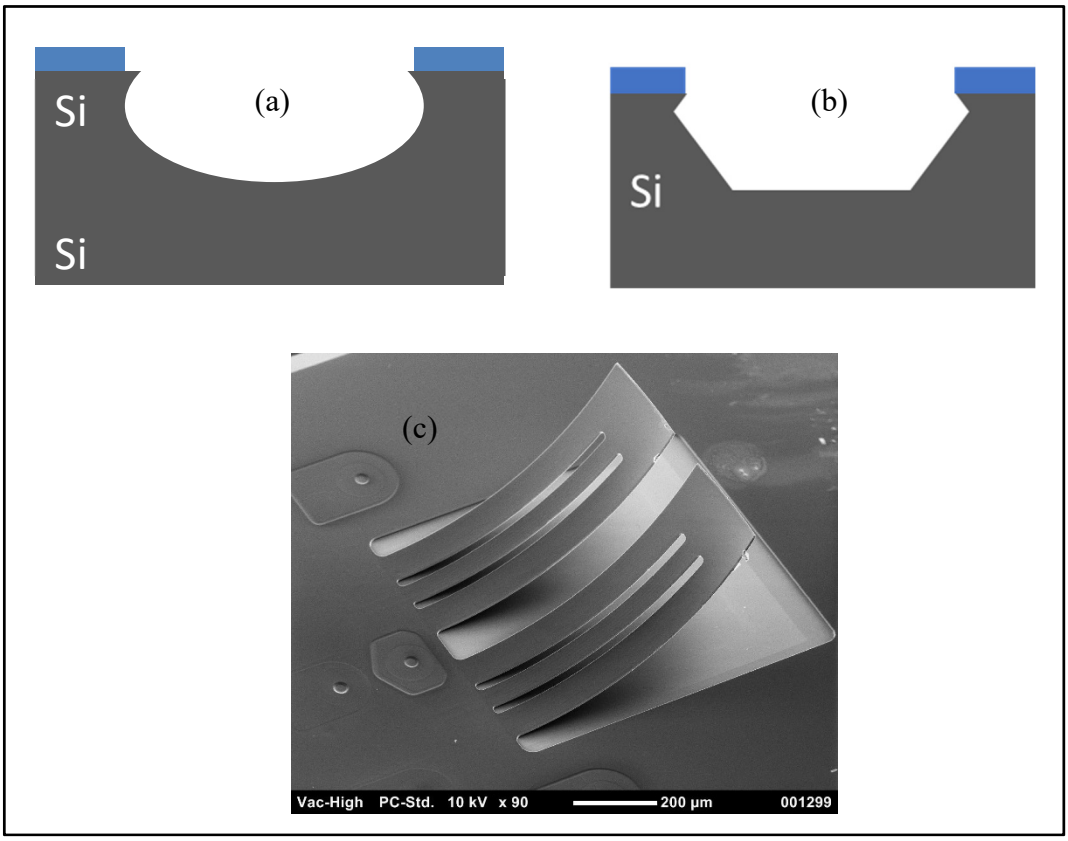

Figure 1.4 (a) Isotropic, and (b) Anisotropic etch profile, and,
(c) Cantilever beam fabricated by Bulk Micromachining
Taken from https://www.memsjournal.com/2011/01/mems-contributions-grow-forthe-control-of-atrial-fibrillation.html (Consulted in December 2019)

In Bulk micromachining, the substrate is selectively etched to create microstructures such as micro-cavities, channels. It is a subtractive process and generally, wet etch methods are preferred for cost effectiveness. The etchants used for wet etching can be either isotropic or anisotropic in nature. Isotropic etchants etch in multiple directions within the substrate and are limited by the geometry of the substrate. Examples of isotropic etchants include hydrofluoric acid (HF), Nitric acid (HNO_3). Anisotropic etchants, like Potassium Hydroxide (KOH) on the other hand, etch in one direction depending on the etchant's affinity to the crystallographic orientation. Dry etching is based on vapor or plasma states of various reactive gases at high temperatures for etching.

Reactive Ion Etching, which utilizes additional energy in the form of Radio Frequency power is the most common dry etching technique used. More recently, Deep Reactive Ion Etching (DRIE) is used sometimes to create structures with complex geometries and high aspect ratios. Some examples of devices fabricated by bulk micromachining include pressure sensors, cantilevers and accelerometers.

1.4.3 Surface Micromachining

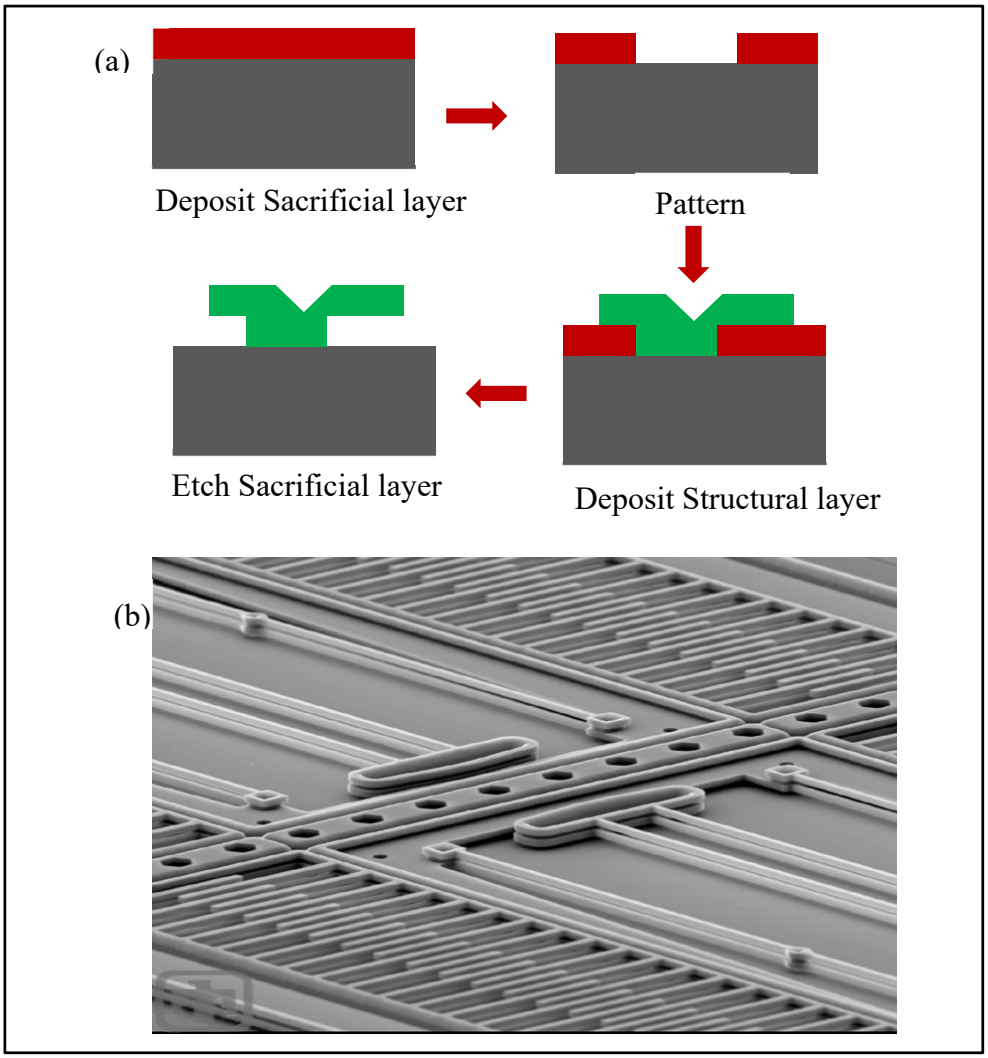

Figure 1.5 (a) Schematic of Surface Micromachining and,
(b) SEM image of a com-drive fabricated by a surface micromachining process
Taken from Sandia National Laboratories SUMMiT™ Technologies
www.sandia.gov/mstc (Consulted in December 2019)

In surface micromachining, thin films are deposited as structural and sacrificial layers on top of a substrate, making it an additive process. The substrate in this case does not play a major role like in bulk micromachining. Examples of sacrificial layers include polymers, metals, polysilicon, etc. Added structural layers are usually deposited that may vary in thickness from 2 to 5 µm. These layers are generally patterned using photolithography and etched using either wet or dry etching techniques depending on the requirement.

Examples of MEMS devices fabricated by surface micromachining include micromotors, comb drives and springs. An important advantage of surface micromachining over bulk micromachining is that it is compatible with CMOS processing. This compatibility allows integration of mechanical components to logic circuits. Surface micromachining is also cost-effective as compared to bulk micromachining. One major issue that devices suffer is stiction. Close attention should be paid to the compatibility of different layers to reduce the effect of stiction in the devices. Surface micromachining techniques are primarily used for fabrication in this Ph.D. work.

1.4.4 LIGA

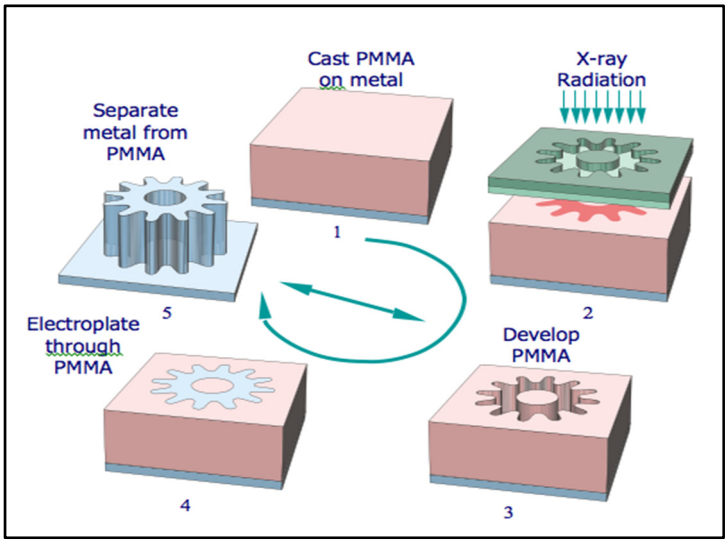

Figure 1.6 Schematic of the LIGA Process.
Taken from http://www.x-ray-optics.de/index.php/en/10-hauptkategorie-en/208-

LIGA, which is acronym for Lithographie, Galvanoformung, Abformung was developed in Germany to overcome the two-dimensionality of Surface Micromachining. LIGA forms a part of High Aspect Ratio Micromachining technique which sometimes uses molding techniques to form microstructures (Saile et al. 2009). LIGA uses X-rays instead of Ultraviolet light to expose a photosensitive layer such as polymethyl methacrylate (PMMA) that is normally a few hundred micrometers thick. The exposed areas are then stripped away chemically and metallized. The resulting component is generally used as a structural layer. A variety of structures with high aspect ratios ranging in height from a few microns to centimeters can be realized using this method. A variety of devices such as accelerometers and microfluidic devices have been fabricated by this method. Since this process is carried out on a Silicon substrate, this technique can be used to integrate the control electronics and circuitry for the MEMS sensor on the same chip. LIGA is limited by the need to have expensive X-ray synchrotron facility which adds to the production costs.

1.4.5 Wafer Bonding

Wafer Bonding is a way to join multiple wafers together and is an integral step in MEMS processing. It is one way to circumvent the limitations of wafer thickness on devices. Wafer bonding can be used to create multi-layer devices using either surface or bulk micromachining. Wafer bonding can be divided into:

- Direct bonding.
- Intermediate layer bonding.

In the direct bonding technique, two wafers are brought together under specific temperature and pressure conditions. Fusion bonding that bonds two Si surfaces together is the most common type of direct bonding. Another common direct bonding technique is anodic bonding that is used to fuse Si with glass.

On the other hand, intermediate bonding requires an intermediate layer such as an adhesive, polymer or metal between two wafers. The common type of intermediate bonding is eutectic bonding. Eutectic bonding uses a metallic intermediate layer to fuse two layers.

Wafer bonding has been used to fabricate MEMS devices, to heretically seal them or to transfer bond a MEMS device to a wafer with integrated circuits thereby becoming an important part of MEMS processing.

1.5 Summary

This chapter briefly summarizes the important aspects of MEMS technology and various fabrication methodologies. MEMS devices have been extensively used in sensor applications such as pressure sensing, mass sensing and gas sensing. In particular, MEMS based gas sensors integrate gas-sensitive materials in a MEMS architecture to enhance the sensing capabilities of the devices. This Ph.D. also incorporates MEMS fabrication methodologies in combination with SWCNTs as sensing materials for gas sensing. The envisioned gas sensor will have excellent performance metrics, operable at room temperature and can be easily integrated with above CMOS technologies.

CHAPTER 2

CARBON NANOTUBES – PROPERTIES AND APPLICATIONS

Preface

The discovery of Carbon Nanotubes was a result of an observation of needle like structures under an electron microscope. CNTs were first discovered by Sumio Iijima in 1991 at NEC's Fundamental Research lab. An individual CNT is composed of a single sheet of a honeycomb network of carbon atoms. The first reported structures were Multi-walled CNTs (MWCNTs) (Iijima 1991), while Single walled CNTs (SWCNTs) were discovered in 1993 (Iijima and Ichihashi 1993). After the first reports about CNTs, scientists began theoretically investigating the electronic band structures for SWCNTs and found excellent electrical and mechanical properties depending on to their diameter and chirality. This was later proved by many experiments and various electrical and optical measurements. In the past few, considerable research has been done to map out the applications of CNTs. The applications range from the concept of a space elevator to biomedical applications such as targeted drug delivery and building transistors of individual SWCNTs. The inherent properties of CNTs also make them excellent candidates for sensing applications. Devices such as pressure sensors, mass sensors, flow sensors and gas sensors have been developed with noteworthy results.

In the following chapter, a brief introduction to CNTs is presented where a discussion of the electrical and mechanical properties is presented in a bit more detail. This is followed by a discussion about their applications where a brief literature review of the different applications of CNTs is presented and discussed. Finally, the challenges facing the real-world application of CNTs is discussed briefly.

2.1 Introduction

The rapid development of the semiconductor industry has successfully extended the boundaries and capabilities of science and technology beyond what was perceived as science fiction only a few decades ago. To think that a modern cellular phone packs more computing power and capability than a supercomputer from the 70's is an ode to the progress of semiconductor research and scaling achievements. As scaling continues to evolve beyond the 20 nm node, it faces a variety of problems that could hinder performance of the devices. Lithography and process variations, leakage, short channel effects, etc. prevent scaling beyond 20 nm. Devices such as fin-FETs and multi-core processors can be developed to mitigate the mentioned issues. However, to scale beyond the envisioned 10 nm, a new channel material is required.

Compound semiconductors such as GaAs and InP are promising materials and have been studied for a while due to high electron mobilities (~8000 cm^2/Vsec for GaAs and 5400 cm^2/Vsec for InP). However, low hole mobilities (~300 cm^2/Vsec) mean that there is an asymmetric transport mechanism in these materials. Another material that is of interest is Germanium due to its high electron (3600 cm^2/Vsec) and hole mobility (1800 cm^2/Vsec) values. However, Germanium has been found to suffer from leakage and short channel effects (Eneman et al. 2008) due to its small energy gap (0.67 eV) which can inhibit performance of nanoscale devices. Innovations in device designs can help overcome material limitations. However, the unavoidable complexity of devices and fabrication costs involved have left the industry hunting on for the next wonder material. Recently, Carbon based electronics have emerged as a complimentary technology for other semiconductor materials. Carbon Nanotubes and Graphene have especially received considerable attention from both academia and the industry due to their remarkable electronic and mechanical properties. The following sections delve more into the properties of Carbon Nanotubes, which is the material of interest to this thesis.

2.2 Carbon Nanotube Basics

Carbon Nanotubes, first discovered by Iijima (Iijima 1991) in 1991 are essentially cylindrical sheets of graphene. CNTs typically have a diameter ranging from 1-5 nm with each Carbon atom sharing a sp^2 covalent bond with three neighboring atoms that provides them with an good tensile strength. Tens of concentric cylinders rolled onto each other with a uniform spacing between layers firm MWCNTs. Depending on the number of layers, the inner diameter of MWCNTs varies from ~0.4 nm upto a few nanometers while the outer diameter ranges from 2 nm to around 20 nm (Monthioux et al. 2007). In the case of SWCNTs, diameters range from 2 to 3 nm with lengths extending upto a few micrometers.

2.3 Carbon Nanotubes: Structure and Properties

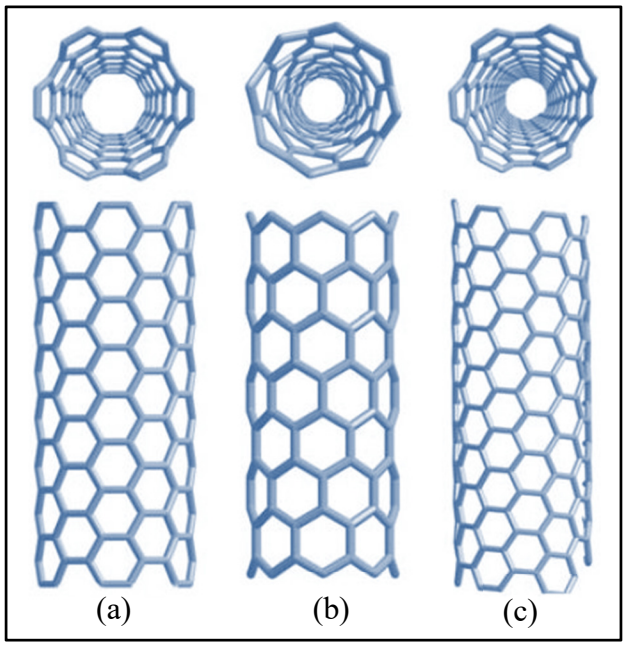

Figure 2.1 Types of CNTs based on chirality,
(a) Armchair, (b) Zigzag and (c) Chiral
Taken from (Bandaru 2007).

The orientation of the graphene sheets that constitute CNTs can be represented by a pair of indices *(n, m)*, that describe the chiral vector.

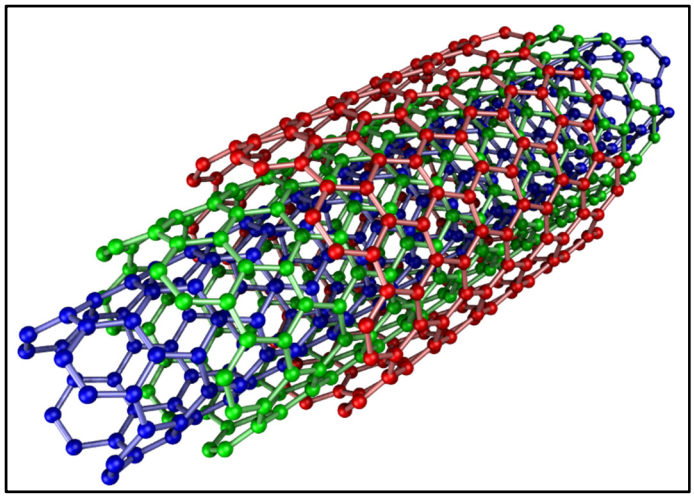

Figure 2.2 MWCNT Structure
Taken from (Weiser 2013)

The relationship between the indices can have a direct effect on the CNT electrical properties and thus results in three categories of CNTs -namely, Zigzag, armchair and chiral nanotubes. *n* and *m* determine the determine the number of unit vectors in the crystal lattice of graphene in two directions. For the condition *n=0 and m=0* and the chiral angle is 0º, the resultant nanotubes are zigzag. For the condition *n=m* and chiral angle being 30º, the resultant nanotubes are armchair. Lastly, for other values of *n* or *m* and chiral angle is between 0º and 30º, the resultant nanotubes are called chiral nanotubes. The chiral vector (*C)* can be expressed as:

$$C = na_1 + ma_2 \tag{2.1}$$

Where a_1 and a_2 are the base cell vectors. The chiral vector also determines the diameter of the CNT and can also be used to gauge the direction of the graphene sheet rolling. The diameter, *d*, of a CNT can thus be calculated using the equation:

$$d = \frac{a\sqrt{m^2+mn+n^2}}{\pi} \tag{2.2}$$

Where a = $1.42x\sqrt{3}$ is the lattice constant of the graphite sheet.

MWCNTs can be described using two models, namely the Russian Doll Model and the Parchment model. In the Russian Doll model, individual CNTS are arranged concentrically with the outer nanotube having a greater diameter than the inner nanotube.

On the other hand, if a single graphene sheet is rolled onto itself multiple times, it is known as the Parchment model. An advantage of MWCNTs is the ability of the outer walls to protect the inner walls from any unwanted chemical interactions and contamination.

2.4 Electrical Properties of Carbon nanotubes

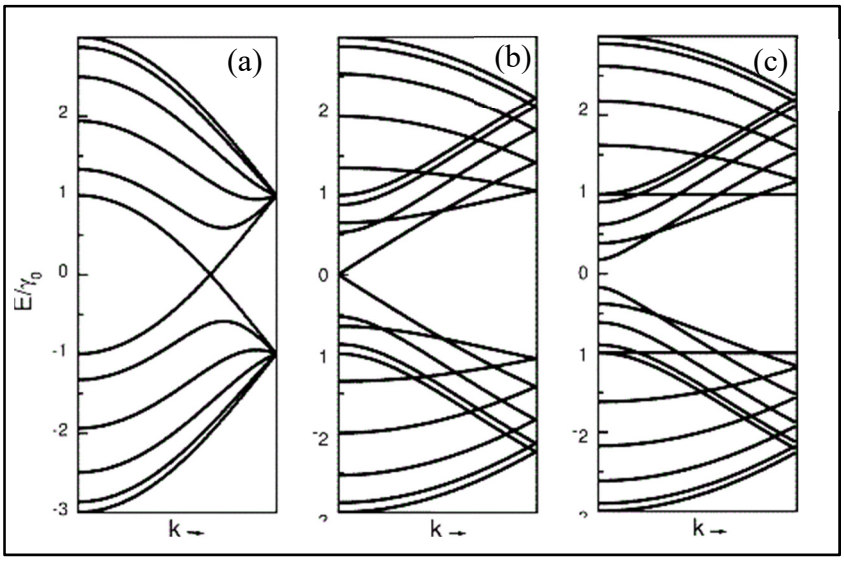

Figure 2.3 Electronic band structure of CNTs (a) (5,5), (b) (9,0) and, (c) (10,0) obtained by folding of a graphene sheet
Taken from Reich, Thomsen et al. (2002)

The band structure of CNTs can be studied by considering the band structure of a single sheet of graphene. A unit cell of the sheet consists of two carbon atoms with four valence electrons each. According to the tight-binding model (Saito et al. 1992), this yields eight bands in total, four valence and four conduction bands. On rolling the sheet of graphene into a cylindrical shape, periodic boundary conditions are imposed. Thus, transport occurs only along the axis of the tube making CNT a 1D conductor in case of a single walled CNT.

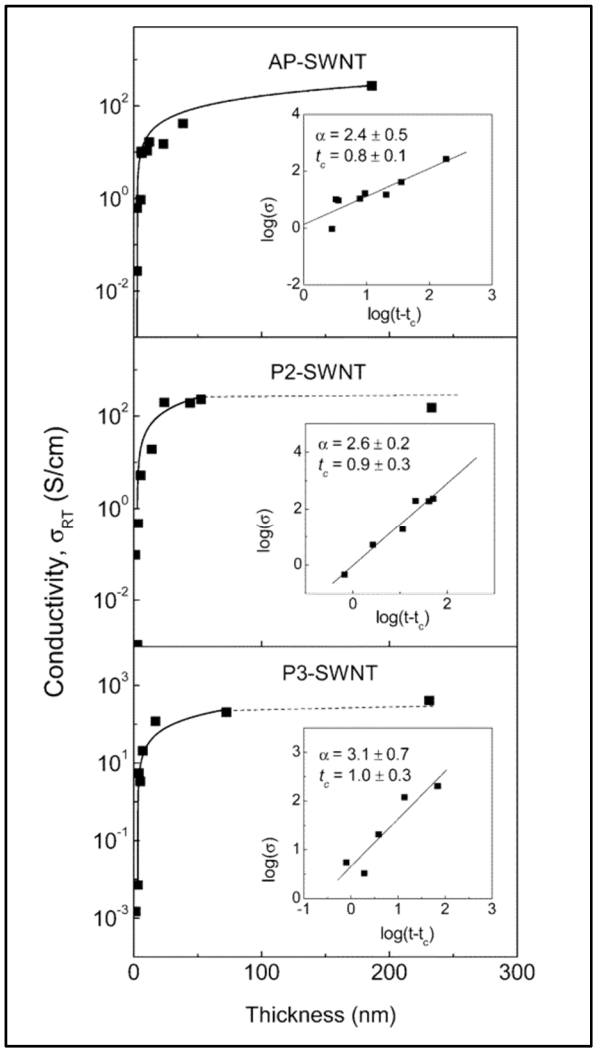

Figure 2.4 Conductivity of various types of SWNT films as a function of film thickness
Taken from Bekyarova et al. (2005)

A range of conductivities have been reported in case of SWCNT films ranging from 12.5 S/cm (Meitl et al. 2004) to ~10,000 S/cm (Hone et al. 2000). The conductivity of SWCNT mats has also been reported in the range of 200 to 500 S/cm (Fischer et al. 1997; Kaiser, Düsberg, and Roth 1998). Lower conductivities for SWNT films are also possible due to the existence of high resistance Schottky barriers at the intertube junctions. The non-uniformity in length, diameter and chirality of the SWCNTs in a network further leads to complications in the electronic properties of the films.

The conduction in thin films is a characteristic of the percolation effect (Kumar, Murthy, and Alam 2005). The conductivity of a CNT film is also influenced by the film density and is given by:

$$\sigma_c = (T - Tc)^a \tag{2.3}$$

Where σc is the conductivity, T is the film thickness and T_c is the critical thickness for the percolation threshold and a is the critical component. In a network of SWNTs, the overall resistance is usually dominated by the tube-tube/bundle-bundle contact resistance.

Therefore, the concentration of the conducting channels is proportional to the concentration of the low resistance intertube junctions. From equation 2.3 it is evident that the conductivity of CNT films is also dependent on the film thickness. In one study, the conductivity is shown to saturate at a film thickness of 50 nm (Bekyarova et al. 2005). Near the percolation threshold, the SWNT networks behave as 2D systems. In this Ph.D. work, the SWNT networks are above the percolation threshold evident by the dense networks thereby forming multiple conductive paths.

2.5 Mechanical Properties of Carbon nanotubes

The graphitic hexagonal ring based on sp^2 C-C bond is one of the strongest chemical bonds known due to hyperconjugation. Hyperconjugation is the stabilizing interaction that results from the interaction of the electrons in a σ-bond (usually C-H or C-C) with an adjacent empty or partially filled p-orbital or a π-orbital to give an extended molecular orbital that increases the stability of the system. The elastic modulus (E) which describes the slope of a stress (σ) vs strain (ε) curve given by:

$$\sigma = \varepsilon E \tag{2.4}$$

And the tensile strength (σ_s) defined as the maximum stress that a material can be subjected to before fracture or irreversible plastic deformation. The exceptional mechanical properties have been proved by numerous theoretical simulations and experimental measurements.

The Young's modulus of individual CNTs was first calculated by Treacy et al. (Treacy, Ebbesen, and Gibson 1996) to be of 1.8 TPa by measuring the amplitude of intrinsic vibrations using a transmission electron microscope (TEM). Other research groups (Krishnan et al. 1998) followed suit and measured it to be around 1.2 TPa experimentally. Wong et al. (Wong, Sheehan, and Lieber 1997) measured the elastic modulus of clamped single MWNTs to be of 1.3 TPa using an AFM cantilever. Plastic deformation of SWNTs was studied by Yu et al. (Yu et al. 2000) and it was determined that the breaking strength for SWNTs was of 30 GPa and an average of 3.1% for breaking strain. Many varying reports of the values of Young's modulus and other mechanical parameters can be found in literature.

The difference in values reported mainly arise due to the presence of varying amount and different kinds of defects, arrangement of the nanotubes, etc. Since the electronic properties of CNTs are sensitive to the geometrical arrangement of atoms in the lattice, it enables us to study the effect of mechanical changes in the CNT on its electronic properties.

Theoretical studies (Heyd, Charlier, and McRae 1997) have shown that the bandgap of a semiconducting CNT can be modified by applying strain. Indeed, it has been experimentally proven that the bandgap of a semiconducting NT can be tuned by applying a small mechanical strain (σ) (Minot et al. 2003).

2.6 Applications of Carbon Nanotubes

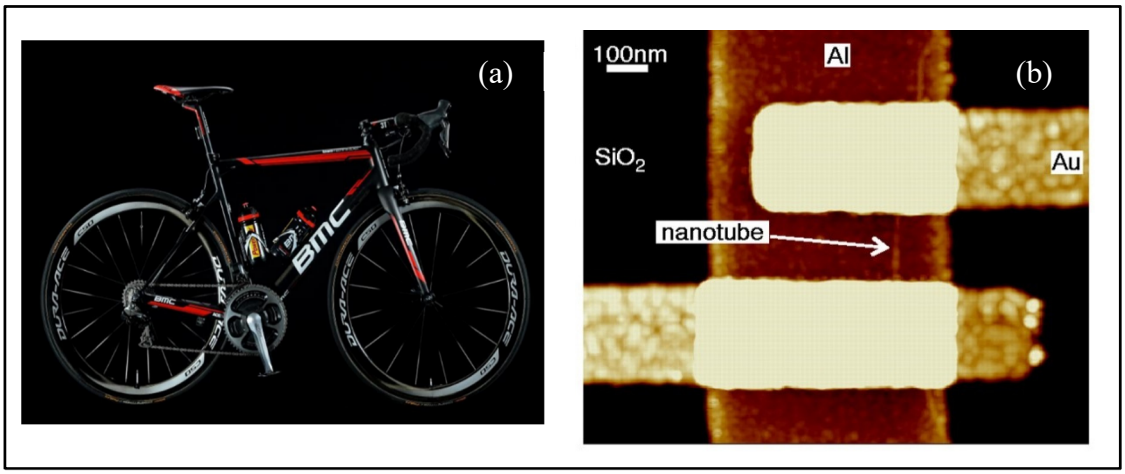

Figure 2.5 (a) Bicycle made of CNT reinforced metal and,
(b) AFM image of a CNT FET
Taken from Bachtold et al. (2001)

The worldwide commercial interest in CNTs has grown considerably in the past two decades. Factors contributing to this include advancements in scientific research and improved production capacity. This has ultimately paved the way for an array of emerging applications in medical therapy (Hong et al. 2015), microelectronics (Park, Vosguerichian, and Bao 2013; Cao and Rogers 2009), chemical sensors (Schroeder et al. 2018). Although CNTs have been studied intensely and the properties are well understood, by no means has the field saturated and our understanding keeps growing continually. Advances in production techniques have enabled the preferential production of CNTs with either semiconducting or metallic properties.

The high surface area to volume ratio of CNTs makes them a perfect candidate for manufacturing composite materials. MWNT-polymer composites have shown to reach conductivities as high as 10,000 Sm^{-1} (Bauhofer and Kovacs 2009).

Conductive CNT plastics have been used in the automotive industry for electrostatic assisted painting for fuel lines that may dissipate electrostatic charge. CNTs mixed with resins and polymers increase overall rigidity and toughness. These enhancements can be achieved by

minimal increase in weight percentage (Gojny et al. 2004). CNTs have also been used build lightweight turbines for windmills and hulls for naval boats.
CNT sheets have been demonstrated as materials for fuel cell electrodes and self-cleaning textiles (Lima et al. 2011). The addition of CNTs to metals has shown to increase the tensile strength and modulus. This can be used in aerospace and automobile applications.

It is well known that mechanical deformation can alter the electrical conductance of CNTs. This forms the basis for the application of CNTs in pressure sensing. A lot of works in the literature have been published about pressure and strain sensors based on CNTs. Electrical transition in SWNTs by radial deformation induced by hydrostatic pressure was studied using first principle calculations was studied by Wu et al. (Wu, Zang, et al. 2004). Kang et al. (Inpil et al. 2006) fabricated a CNT based strain sensor for applications in structural health monitoring. This work compared device performance between Buckypaper and a composite of SWCNT/Polymethylmethacrylate. A MWCNT based MEMS pressure sensor was developed and studied by Fung et al. (Fung et al. 2005) using dielectrophoresis to position the MWCNT network across a PMMA membrane. Deflection of the PMMA membrane under pressure induced bending in the MWNTs which was detected by fold electrodes with 3 μm to 10 μm spacing. This work uses conventional micromachining process without resorting to low throughput processes like electron beam lithography.

2.7 Carbon Nanotubes: Applications in MEMS and NEMS

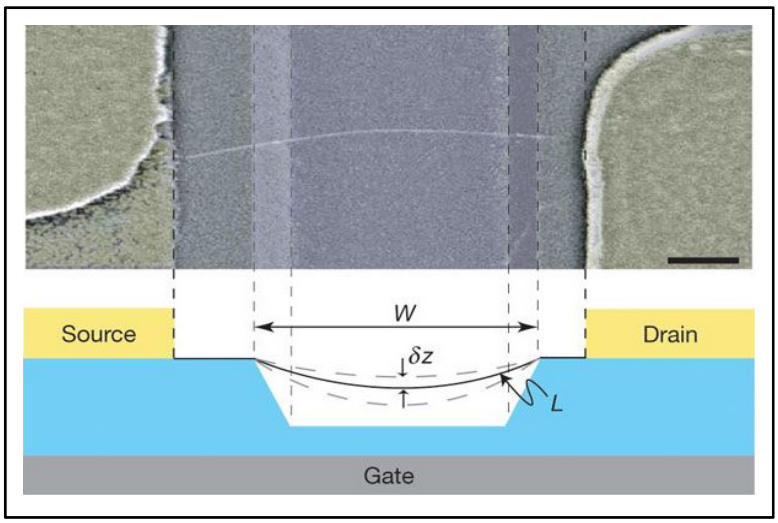

Figure 2.6 (Top) A false-colored SEM image of a suspended device and, (Bottom) Device geometry
Taken from Sazonova et al. (2004)

CNTs have been extensively used to fabricate Nano and microscale resonators for applications in mass sensing. Jensen et al. (Jensen, Kim, and Zettl 2008) fabricated one of the most sensitive mass sensors using CNT as a resonator. The density of CNTs is lower than other materials fabricated by a similar method and thus the resonance frequency is lower which results in a larger magnitude of response at lower resonance frequencies, especially useful for sensing applications. The high carrier mobility in CNTs has been used to develop FETs. For example, CNT-FETs with conductance as high as the ballistic limit have been demonstrated previously with on/off ratios as high as 10^9 (Javey et al. 2003). The chirality and the metallic properties of CNTs highly influence the performance of the FETs. The metal contact to the FETs is also found to have a significant impact on the performance (Chen et al. 2005). Reproducibility for large scale applications remains a major challenge to overcome in this area since there is no process to produce CNTs with uniform electrical properties. Another example of such an application was a self-detecting nanotube resonator reported by Sazonova et al. (Sazonova et al. 2004) using the CNTs as transistors. The device design again consisted of an individual CNT suspended over a trench.

Additionally, a gate electrode is used to induce an oscillatory motion using an AC voltage resulting in a resonant frequency of 55 MHz and a quality factor of 80. Upon subjecting the CNT to tension, a shift in the oscillation frequency was observed and thus the authors were able to tune the device to scale the resonant frequency from 3 to 200 MHz. The force sensitivity of the device was measured to be 1 $fN/Hz^{-1/2}$ which is one of the best force sensitivities determined to date. The authors predict that at temperatures of 1 kelvin, forces below 5 aN can be detected.

An important issue hindering the large-scale application of CNT FETs is that single CNT based devices can only be fabricated using e-beam lithography which is not feasible for large scale manufacturing. Many alternate methods have been proposed to overcome this challenge. For instance, highly aligned unipolar SWNTs grown by a CVD process have been demonstrated. The SWNTs are used as transistors with a conductance of 1000 $cm^2V^{-1}s^{-1}$. Having an array of highly aligned SWNTs improves the uniformity and reproducibility by reducing the role played by the chirality and defects in the SWNTs. However, determination of the number of active SWNTs during the FET operation remains an issue.

2.8 Carbon Nanotube Application Challenges

Even though the potential applications of CNTs are endless and there is an ever-growing interest in CNT research from thousands of researchers around the world, there are very few mass-produced products made from CNTs. One of the major challenges facing the commercial use of CNTs is cost. Even though the price of CNTs have reduced significantly in the past decade, the overall cost to manufacture CNTs on a large scale is still perceived to be too high. Another issue of concern is the growth and purity. To date, a technique to grow only a single species of CNTs with controlled chirality and diameter has not been developed fully, although techniques to sort nanotubes have certainly be developed (Janas 2018). Another issue is assembly. Billions of nanotubes are required for fabricating CNT based transistors or circuits. Manipulating billions of individual nanotubes is not an easy task and no techniques currently exist for doing so. However, with the speed of advancement in research, one can hope that it is only a matter of time that we can see CNTs in commercial applications such as sensors.

CHAPTER 3

GAS SENSING USING CARBON NANOTUBES

Preface

The electrical and mechanical properties of CNTs have been studied and put to good use in many applications, especially sensing, as described in the previous chapter. One area of sensing that CNTs have been widely used is gas sensing. CNTs, both single and multiwalled, have been used successfully to detect gas concentrations as low as 1 ppb and gases such as Ammonia, Methane, CO_2, etc. Many sensing principles such as change in capacitance, resistance and thermal transfer mechanisms have been used in gas sensing applications.

In the following chapter, a brief literature review of different gas sensors using CNTs as the sensing element is presented. Each reviewed work is then critically analyzed to determine the advantages and drawbacks of the as proposed device. In lieu of the theme of this Ph.D. work, a separate section about humidity sensing and humidity sensors is presented. A literature review for the common materials used for humidity sensing and a brief review about CNT based humidity sensors is presented.

Finally, a review of the CNT based ionization gas sensors is covered. The fabrication of an ionization sensor demonstrates the evolution of the device sensor. The discussion presents the working principle, advantages and disadvantages of ionization gas sensors.

3.1 Introduction

Gas sensors find widespread applications in space exploration, pharmaceutical industries and environmental monitoring. Sensors with high sensitivity and selectivity are of paramount importance to detect leakage of highly explosive gases such as hydrogen and other toxic gases such as methane. The basic criteria for a good gas sensor are:

1) Sensitivity, defined as the lowest concentration of the analyte that the sensor can detect,
2) Selectivity, defined as the ability of the sensor to detect a particular gas analyte in a mixture,
3) Fast response and recovery, defined as the time taken by the sensor to detect a minimum concentration of the analyte and recovery time is the time it takes for the sensor signal to return to its initial value after a step concentration change from a certain value to zero,
4) Long term stability.

The change in electrical properties of CNTs upon exposure to certain gases forms the basis of their application in gas sensing (Sinha, Ma, and Yeow 2006; Li et al. 2003).

3.2 Pristine Carbon Nanotube Gas Sensors

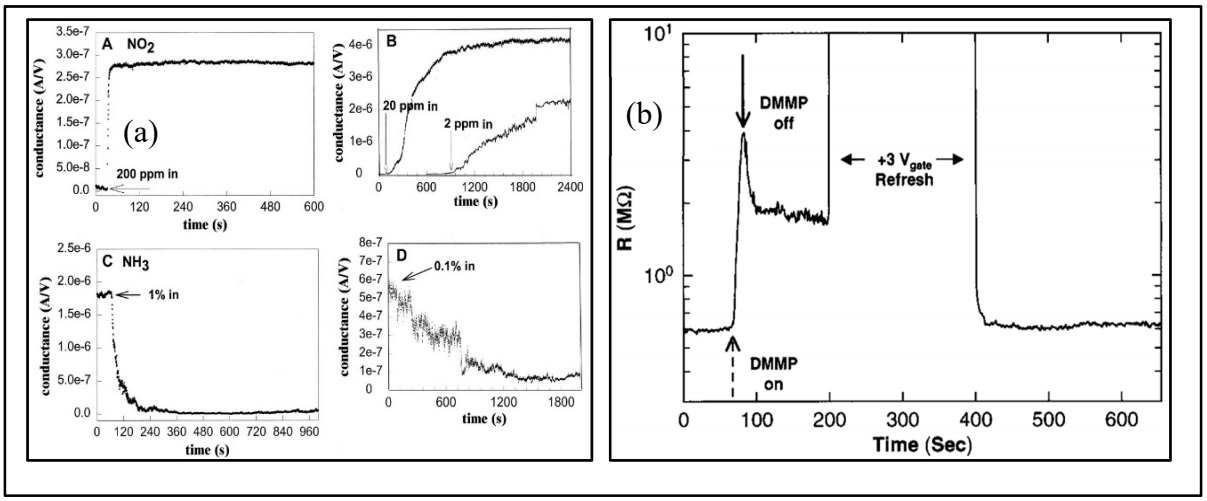

Figure 3.1 (a) Response of SWNTs to NO_2 and NH_3 Taken from Kong et al. (2000) and, (b) Device response of the ChemFET Sensor
Taken from Novak et al. (2003)

The presence of surface atoms on CNTs is ideal for the electrical detection of trace chemical elements. Two different configurations of CNT based gas sensors exist: chemiresistors and back-gated chemical field effect transistor (ChemFET).

In a chemiresistor configuration, CNTs are bridged between two electrodes. The analytes bind on the CNT surface resulting in charge transfer between the adsorbed molecule and the CNT surface resulting in change of electrical resistance. In the ChemFET configuration, the conductance of the CNT is modulated using a third gate electrode coupled by a thin dielectric layer. The ChemFET configuration is deemed a bit more sensitive than the Chemiresistor configuration due to the ability to tune the CNT conductance which makes them ideal candidates for electrical sensing, the downside being the requirement of complicated ancillary electronics.

Kong et al. (Kong et al. 2000) first demonstrated the use of semiconducting SWNTs can be used for gas sensing as ChemFETs. SWNTs were grown using Chemical Vapor Deposition (CVD) followed by patterning metal electrodes over individual SWNTs. The nanotubes

showed good sensitivity to NO_2 and NH_3. The conductance of the CNTs increased by three orders of magnitude when exposed to NO_2 and decreased by two orders of magnitude when exposed to NH_3.

Novak et al. (Novak et al. 2003) also used CNTs in a chemFET configuration to detect dimethyl methylphosphonate (DMMP), a simulant for Sarin. The sensors demonstrated quick recovery on application of a gate voltage of 3 V. The fast desorption time was explained by Coulombic interaction, where application of a positive gate voltage induced a negative charge which interacted with DMMP, a strong electron donor and decreases the desorption barrier. For such applications, it is important for the CNT to have chemical selectivity against agents like water vapor. This has been addressed using polymers to filter out other vapors from air during testing. However, it remains to be seen how such a filtering system can be translated for commercial applications.

One of the potential drawbacks of using pristine nanotubes for gas sensing applications could be the lack of selectivity towards specific gaseous analytes and lack of sensitivity to species that do not interact with CNTs. This problem is solved by chemical functionalization.
There are two main types of functionalization possible: covalent and non-covalent functionalization. Most covalently functionalized CNTs are based either on amidation or esterification of carboxylic acid groups found on defect sites during acid treatment (Chen et al. 1998).

On the other hand, non-covalent functionalization is based on forces such as Van der Waal's interactions and π – interactions without actually influencing the physical properties of the CNTs (Star et al. 2001). A Carbon monoxide (CO) sensor using SWNTs modified with thiolated heme (Dong et al. 2007) was fabricated in a ChemFET configuration. The sensor exhibited greater sensitivity to CO when contacted with Cr than Au showing that the CNT-metal interface is an important factor for determining sensor performance. The sensor had a response time of less than 100 s with a detection limit of 4.9 ppm. One potential drawback of this work is the repeatability. The authors report that the sensors perform optimally for 40 cycles after which there is a performance degradation. This can be a problem for long term applications.

CNT-polymer nanocomposites are also promising hybrid materials for use in gas sensing. For example, An et al. fabricated a polymer-CNT sensor for NO_2 sensing (An et al. 2004). A uniform film of polypyrrole on the surface of SWNT was achieved by in-situ chemical polymerization. The sensitivity of the SWNT-Polymer hybrid was 10x higher than the polymer alone. SWNTs functionalized with poly-(m-aminobenzene sulfonic acid) (PABS) were shown to have better sensitivity to NH_3 than simple carboxylated SWNTs (Zhao, Hu, and Haddon 2004). The better sensitivity was attributed to the protonation and deprotonation of the PABS which altered the charge carrier density in the SWNTs.

A multifunctional chemical sensor based on CNTs that are vertically aligned was fabricated (Wei et al. 2006). The vertically aligned CNTs were coated with different polymers. The sensor showed fast and reversible sensing of volatile organic solvents (VOCs).

The sensing mechanism was explained based on charge transfer interaction with the gas molecules and the change in inter-tube distance due to polymer swelling during gas adsorption.

3.3 Suspended Carbon Nanotubes for Gas Sensing

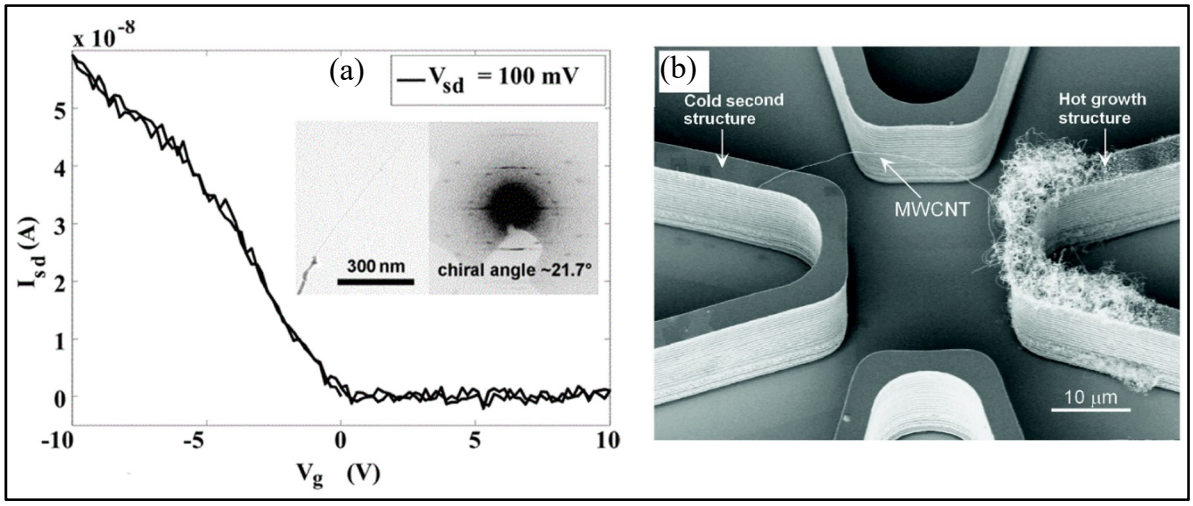

Figure 3.2 (a) Hysteresis free operation of a suspended NO_2 gas sensor fabricated Taken from Chikkadi et al. (2013) and,
(b) SEM micrograph of an individual suspended MWCNT acting as an electrothermal gas sensor Taken from Kawano et al. (2007)

In the previous section, a survey about CNT based gas sensors was discussed. Here, a review

of suspended CNT-based gas sensors is presented. Suspended CNT devices are generally difficult to fabricate, requiring expensive equipment and complex fabrication processes. Generally, suspended devices are fabricated by growing CNTs by high temperature vapor deposition techniques over prefabricated electrodes. Another way to obtain suspended structures is to deposit them on a substrate and then selectively etching the substrate using bulk micromachining techniques to release the CNTs. In recent times, attempts to precisely place individual CNTs across a trench have also been reported. However, suspended CNTs are normally fabricated to study the intrinsic properties and mechanisms within the tubes such as super-conduction and ballistic transport. Very few works have reported their application in gas sensing. Mostly, the application is limited to studying the mechanism of NO_2 gas adsorption on CNTs (Chikkadi et al. 2014b; Helbling, Pohle, et al. 2008).

One of the first instances of suspended carbon nanotubes for use in gas sensing was by Chikkadi et al. (Chikkadi, Muoth, and Hierold 2013) where a single SWCNT was used to detect NO_2 with zero gate hysteresis. The signal to noise ratio was 31 for a concentration of 1 ppm from which a detection limit of 32 ppb was extrapolated. The sensor showed a rise time of 3 minutes and exhibited complete recovery after 14 hours.

Gas sensing capabilities of suspended multiwalled CNTs based on electrothermal effects was demonstrated (Kawano et al. 2007) with fast response times and good reversibility. Individual CNTs were placed across prefabricated silicon microstructures. The MWCNT is shown to behave like a Pirani gauge. The temperature of the MWCNT increased on exposure to Argon and Nitrogen ambient. The selectivity of the gases is established by the different thermal conductivity values of the MWCNT under different ambient. For instance, the thermal conductivity for nitrogen is of 25.83 mW/mK and 17.72 mW/mK for argon. The authors predict fast response times for the sensor since the sensing mechanism is not adsorption based.

A qualitative comparison of suspended and non-suspended CNT NO_2 sensor was done in both chemiresistor and transistor configurations (Helbling, Hierold, et al. 2008). The rise time of the suspended device was of 16 minutes at 180 ppm compared to 25 min at 120 ppm for the

non-suspended device. The suspended CNT is shown to exhibit p-type behavior. The authors suggest using the shift in suspended FET gate characteristic in sensor applications.

3.4 Humidity Sensing

Humidity Sensors have a lot of potential applications in industrial processes, agriculture and civil engineering. Humidity sensors are used in monitoring humidity levels in the semiconductor industry for wafer processing. Commercially available humidity sensors use metal oxides or polymers as humidity sensing materials. Properties such as resistivity of these materials change drastically on interacting with water vapor.

Capacitive type humidity sensors rely on the change in capacitance due to change in humidity. These devices often need very little power to operate. However, they need to be calibrated very often to get accurate measurement results. Resistive type sensors depend on the change in resistivity of the sensing element to detect humidity. The resistivity increases if the sensing material is p-type and decreases if the material is n-type. Both capacitive and resistive type sensors are widely used, cheap and can measure a wide range of humidity. However, the sensor response is dependent on the temperature ambient and can be easily affected by the presence of other chemical species in the vicinity of the sensor, which is undesirable.

The humidity sensing material in a sensor plays a key role in developing any high-performance sensor. Carbon based materials have attracted attention due to their large surface area and resistance to chemical cross-sensitivity (Chu et al. 2013). Materials like graphene, CNTs and

carbon nanofibers have been used extensively for developing high performance gas sensors. A few other advantages of using Carbon based materials include room temperature operation, low power consumption, ability to functionalize for chemical specificity, etc. Sticking to the theme of this Ph.D. work, a brief overview of CNTs used for humidity sensing has been discussed in the following section.

3.5 Carbon Nanotubes for Humidity Sensing

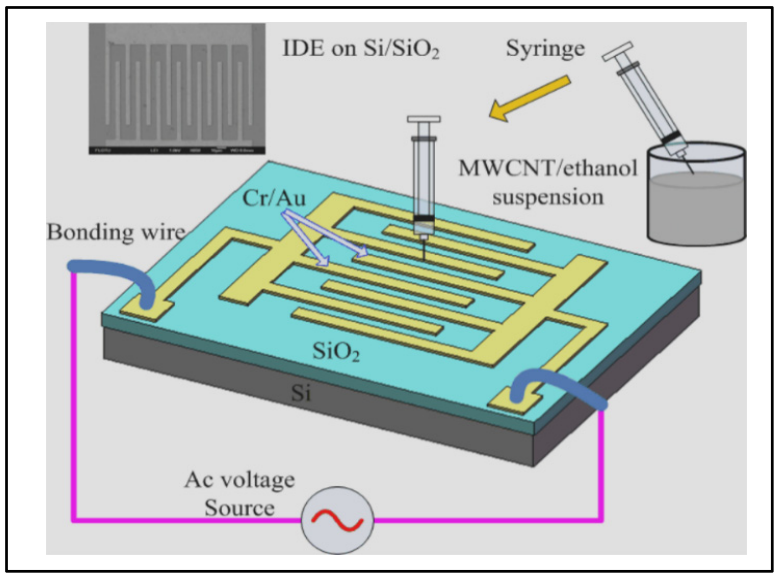

Figure 3.3 Schematic of the interdigitated humidity sensor
Taken from Liu et al. (2009)

Carbon Nanotubes with their high aspect ratio and superior electrical properties also constitute for good humidity sensing materials. Various methods have been discussed in literature for CNT based humidity sensors. Generally, CNTs are acid-treated with a mixture of Sulfuric and Nitric acid to functionalize them with Carboxylic acid (-COOH) groups (Chen et al. 2009a). A MWCNT humidity sensor with a response time of 2-3 minutes with recovery time of the order of hours.

In another instance, MWCNTs dispersed in Poly-acrylic acid (PAA) have been found to have sensitivity to low RH levels. The volume of the MWCNT-PAA film changes depending on adsorption or desorption of water vapor which causes a change in distance between

neighboring MWCNTs. Therefore, the electrical resistance of the film is dependent on volume change caused by adsorption or desorption of water vapor.

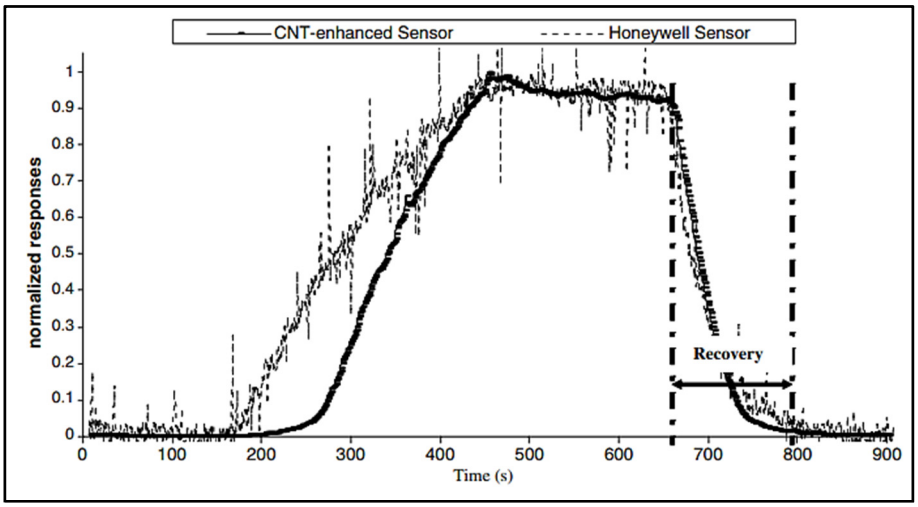

Figure 3.4 Normalized response of MWCNT sensor and the Honeywell sensor
Taken from Yeow et al. (2006)

The humidity sensing in CNTs occurs because of charge transfer between the water molecules and the CNTs. An ultrafast humidity sensor with a response time of 5 s was fabricated (Tang, Chan et al. 2011) using composite films of polyimide and CNTs. Another CNT humidity sensor was fabricated by CNTS deposited by dielectrophoresis on prefabricated interdigitated electrodes with a response time of 3 s and recovery time of 25 s with a humidity range of 25% to 95% RH (Liu, Ye et al. 2009).

A resistive type MWCNT-hydroxyethyl cellulose composite humidity sensor was developed using Ma et al. (Ma et al. 2015). The amount of MWCNT loading in the composite was varied and the effect on the overall sensitivity was studied. The sensitivity increased with increased MWCNT concentration. The sensor showed stable and repeatable performance over multiple humidity cycles. A capacitive humidity sensor using multi-walled carbon nanotubes (MWCNTs) deposited on a stainless-steel substrate (Yeow and She 2006). The MWCNTs are porous in nature and experience condensation of water molecules at lower RH levels. The sensor response time is 75 s with a sensitivity of 35.86%. The performance of the MWNT

sensor is compared to a commercial Honeywell sensor and the performance gains of the MWNT sensor is attributed to the capillary condensation effect.

A humidity sensor based on Single walled Carbon Nanotubes (SWCNT) in a Field Effect Transistor (FET) configuration was developed (Mudimela, Grigoras et al. 2012). Change in the gate voltage triggered the sensing response of the SWCNTs. For positive gate voltages, the source-drain current (I_{sd}) increases and vice-versa. This behavior was attributed to the electron-donating nature of the water molecules. No details on the response and recovery time of the sensor was provided. However, the sensor experienced a large hysteresis during operation in humid conditions which is undesirable.

A wearable humidity sensor based on high strength SWCNT-Polyvinyl alcohol (PVA). A weight ratio of 1:5 SWCNT-PVA showed the best performance. The electrical resistance increased by approximately 24 times under 100% RH with a response time of 40 s. The sensor response decreased by 50% as the operating temperature was increased to 75ºC. (Zhou et al. 2017). MWCNTs grown via pyrolysis and deposited on quartz substrate with interdigitated electrodes were used to detect humidity. The response time of the sensor was around 2 minutes while the recovery time was of the order of a few hours which is not ideal for real world use.

3.6 Carbon Nanotube based Ionization Gas Sensors

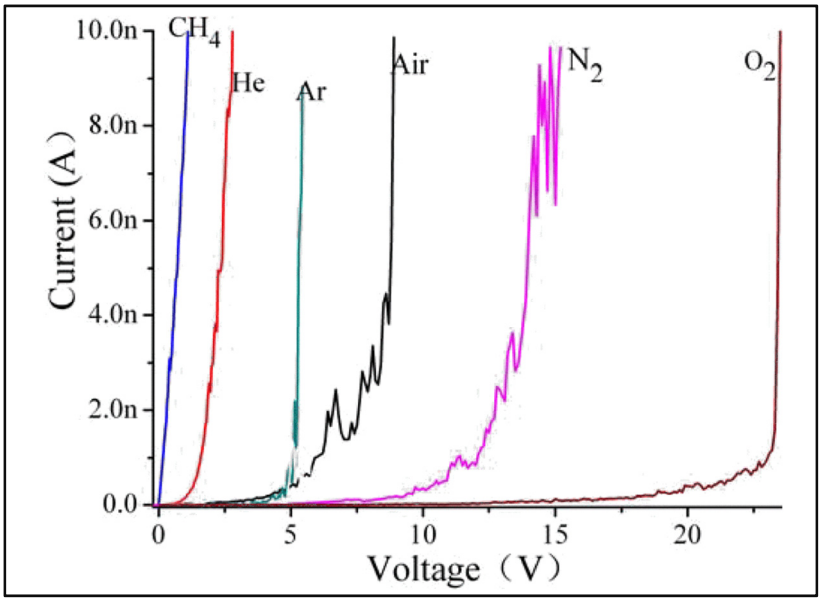

Figure 3.5 Breakdown Voltages of various gases for the MEMS based ionization sensor
Taken from Jiahao et al. (2008)

Ionization sensors work by identifying the field ionization characteristics of various gases. In comparison to chemical sensors which work based on adsorption or desorption of gaseous analytes, ionization gas sensors are not limited by factors such as the absorption energies and affinity of the gas molecules to the sensing elements. Traditional ionization sensors are bulky, have high power consumption and risk very high voltage operation. Ionization sensors usually consist of two electrodes separated by a certain distance across which a voltage is applied. The applied voltage creates an electric field which is instrumental in ionizing the gas. The inter-electrode distance has also been shown to affect the onset voltage of the gas discharge. The breakdown voltage of the gas has been shown to reduce with decreasing gap size (Slade and Taylor 2001). The one-dimensional nature of the CNTs helps in converging the electric field more efficiently and thus reduces the discharge voltage (Modi et al. 2003).

Modi et al. (Modi et al. 2003) proposed one of the first CNT based ionization gas sensors. In this work, MWCNTs grown vertically on an SiO_2 substrate with a diameter of 25-30 nm act as the anode while an Al sheet is used as a cathode. The anode and cathode are separated by a glass insulator with the separation between the electrodes of the order of 150 μm. At this separation, the breakdown for air occurred at 346 V with CNTs as one of the electrode as compared to 946 V when two metal electrodes were used. Multiple gases were tested, and their breakdown voltages were established in this work.

A MEMS based CNT ionization sensor was also developed (Jiahao et al. 2008) with electrode spacing between 2 μm to 10 μm. The CNTs were deposited by electrophoresis onto patterned 10 μm Ni beams on a Cr/Cu seed layer. The breakdown in air occurred at 28 V accompanied by an exponential increase in the discharge current from 200 nA to 10 μA which could potentially damage the device and hamper repeatability. This can be addressed by the addition of a dielectric barrier layer such as TiO_2. A single CNT was used to detect pre-ionized gases by Jiangbao et al. (Jiangbo et al. 2006). The CNT is deposited by dielectrophoresis on a pre-patterned electrode. As mentioned above, pre-ionized gas is tested in this work to achieve low response and recovery times. The device is primarily used as an oxygen sensor.

The tested oxygen is ionized using a “needle-point” method where a high voltage is applied to a conductive needle that is not grounded. The build-up of electrons within the needle leads to discharge which subsequently ionizes the oxygen gas. A porous silicon-based CNT field ionization sensor was also fabricated by growing CNTs within the pores of the silicon. The macropores on the Si substrate enables the growth of a highly dense CNT film. The CNT film acts as the cathode while a steel bar is used as the anode. The breakdown for air occurred at 1766 V. The breakdown voltage reduced as the inter-electrode distance. The authors report that the discharge current experiences a 60-fold increase when 4% hydrogen is introduced in a nitrogen ambient thereby exhibiting hydrogen sensitivity. The sensor showed degradation in performance after 100 breakdown cycles.

3.7 Summary

CNTs have been used extensively as the sensing material for detecting various gases. In this section, some of the published works based on CNT gas sensors have been reviewed. Further, a review of gas sensors based on suspended CNTs is provided. Mostly, suspended CNTs have been used to sense NO_2 and study the mechanism of NO_2 adsorption on the CNT surface. Further, suspended CNTs use expensive equipment and complex fabrication processes. Next, a discussion centered on CNT based humidity sensors is presented. Most of the humidity sensors based on CNTs work based on chemical interaction and charge transfer between the CNTs and the water molecules leading to change in properties such as resistivity, capacitance, etc. Although some works have managed to achieve impressive response and recovery times, issues with repeatability and shelf life of the sensor persist, in addition to unreliable measurements due to hysteresis. Next, ionization gas sensors have been reviewed and described. Ionization sensors can be an alternative to chemical sensors for gas sensing since ionization sensors do not depend on any chemical interaction, the possibility of cross-sensitivity is nullified. Further, the sensor response to gases is almost instantaneous which is another advantage. Various materials have been used as sensing elements as ionization gas sensors including polymers, ceramics, metals and CNTs. Since CNTs are the sensing material in this Ph.D. work, a brief survey of CNT based ionization sensors is also presented.

CHAPTER 4

SUSPENDED CARBON NANOTUBES FOR HUMIDITY SENSING

Shivaram Arunachalam[1], Frederic Nabki[1] Anubha Gupta[1], Ricardo Izquerdo[1],

[1]Department of Electrical Engineering, École de Technologie Supérieure,
1100 Notre Dame West, Montréal, Quebec, Canada H3C 1K3

Paper published in *MDPI Sensors*, May 2018

Preface

Humidity sensors play a key role in many environmental monitoring applications. The previous chapter described the methods and materials that have been used to develop humidity sensors, including CNTs. CNTs have the potential to be excellent materials for humidity sensing. MWNTs, both individual and thin films have been used widely as sensing materials. However, one major drawback of almost all sensors published in literature is hysteresis and repeatability. Hysteresis is an unwanted phenomenon in which the sensor gives different output in one complete sensing cycle (adsorption and desorption) against a measured parameter. This can ultimately lead to unreliable measurements which could have potentially dire consequences.

In the following chapter, the issue of hysteresis is addressed by fabricating a suspended CNT based humidity sensor. A novel fabrication process based on SU8, a commonly available photoresist as a sacrificial material has been developed. The entire fabrication has a thermal budget of around 115°C which makes the process compatible with CMOS integration. The resultant sensor showed minimal hysteresis and excellent repeatability and consistency even after multiple sensing cycles.

4.1 Abstract

A room temperature microfabrication technique using SU8, an epoxy-based highly functional photoresist as a sacrificial layer, is developed to obtain suspended aligned carbon nanotube beams. The humidity-sensing characteristics of aligned suspended single-walled carbon nanotube films are studied. A comparative study between suspended and non-suspended architectures is done by recording the resistance change in the nanotubes under humidity. For the tests, the humidity was varied from 15% to 98% RH. A comparative study between suspended and non-suspended devices shows that the response and recovery times of the suspended devices was found to be almost 3 times shorter than the non-suspended devices. The suspended devices also showed minimal hysteresis even after 10 humidity cycles and exhibit enhanced sensitivity. Repeatability tests were performed by subjecting the sensors to continuous humidification cycles. All tests reported here have been performed using pristine non-functionalized nanotubes.

Keywords: carbon nanotubes; non-suspended; suspended; humidity sensor

4.2 Introduction

Ever since their discovery in 1991 by Iijima (Iijima 1991) carbon nanotubes have been studied intensively due to their remarkable electrical and mechanical properties. A number of potential applications of carbon nanotubes have been well catalogued in the literature (Baughman, Zakhidov et al. 2002) (Schnorr and Swager 2011). Owing to their excellent electrical properties, the application of nanotubes in the area of sensing has been intensively studied (Saino Hanna, Remya et al. 2010). Enough theoretical and experimental proofs now exist that have led to the notion that carbon nanotubes are one of the future go-to materials of the sensing industry. Over the years, the cost of nanotube manufacturing has significantly decreased, which further makes them an attractive proposition to be used in sensors. Many different types of sensors ranging from pressure sensors (So et al. 2013) to optical sensors (Barone et al. 2004) have been demonstrated.

Other applications where nanotubes are used as sensing materials are solar cells (Klinger, Patel, and Postma 2012), displays (Choi et al. 1999) and transistors (Rosenblatt et al. 2002). Humidity Sensors play a major role in environment monitoring in various locations such as homes, automobiles and in medicine (Ma et al. 1995). A host of materials and methods have been researched upon to improve sensor parameters such as response times, shelf life, selectivity and more importantly to bring down manufacturing costs (Chou, Lee, and Liu 1999; Qi et al. 2008; Gu, Huang, and Qin 2004). To date, a majority of the work based on carbon nanotube humidity sensors published in the literature have been fabricated using chemically functionalized multiwalled carbon nanotubes (Cao et al. 2011; Chen et al. 2009b; Tsai, Lu, and Li 2010).

However, few works have investigated single-walled nanotubes for humidity sensing. For instance, (Mudimela et al. 2012) fabricated a humidity sensor based on networks of single-walled carbon nanotubes Field Effect Transistors (FETs). More recently, (Zhou et al. 2017) developed a textile-based humidity sensor based on Poly vinyl alcohol (PVA) functionalized single-walled nanotubes with a response time of 40 s. Carboxylic acid functionalized single-walled nanotube networks were used on a cellulose paper template to sense humidity by (Han et al. 2012) with a fast response time of about 6 s. All the above-mentioned works have used either single or a network of substrate bound carbon nanotubes. The one common problem that all the devices experience is hysteresis which can lead to reduced reliability. One way to eliminate the problem of hysteresis is to use suspended carbon nanotubes as the sensing material. Suspended carbon nanotubes were used to detect NO_2 with minimal hysteresis (Chikkadi et al. 2014a). However, suspended nanotubes are difficult to fabricate, leading to only a few suspended nanotube sensors in the literature. Suspended aligned nanotube networks were fabricated by (Lee et al. 2012) using a microfluidic template. Well aligned nanotube networks have shown to have better electrical and mechanical properties (Ko and Tsukruk 2006; Camponeschi et al. 2007). More recently, suspended carbon nanotubes were obtained using a transfer approach (Li et al. 2015). However, it is interesting to note that there has very little work done to investigate how aligned suspended carbon nanotube networks would react to humidity.

Having a suspended architecture can be very useful in sensing applications due to the increased surface area for adsorption. In this work, we have used SU8, an epoxy-based negative photoresist as a sacrificial material in a low-temperature surface micromachining process to obtain suspended beams comprising of networks of carbon nanotubes. The low temperature of the process makes it notably suitable for the integration of the suspended beam directly above CMOS integrated circuits. The suspended nanotubes beams were then tested to quantify their sensitivity to humidity. We compare the performance of the suspended nanotubes beam humidity sensor to a non-suspended nanotube beam sensor. Our results indicate that the response and recovery times of a suspended architecture are almost three times lower than a non-suspended architecture without any chemical modification to the nanotubes.

4.3 Materials and Methods

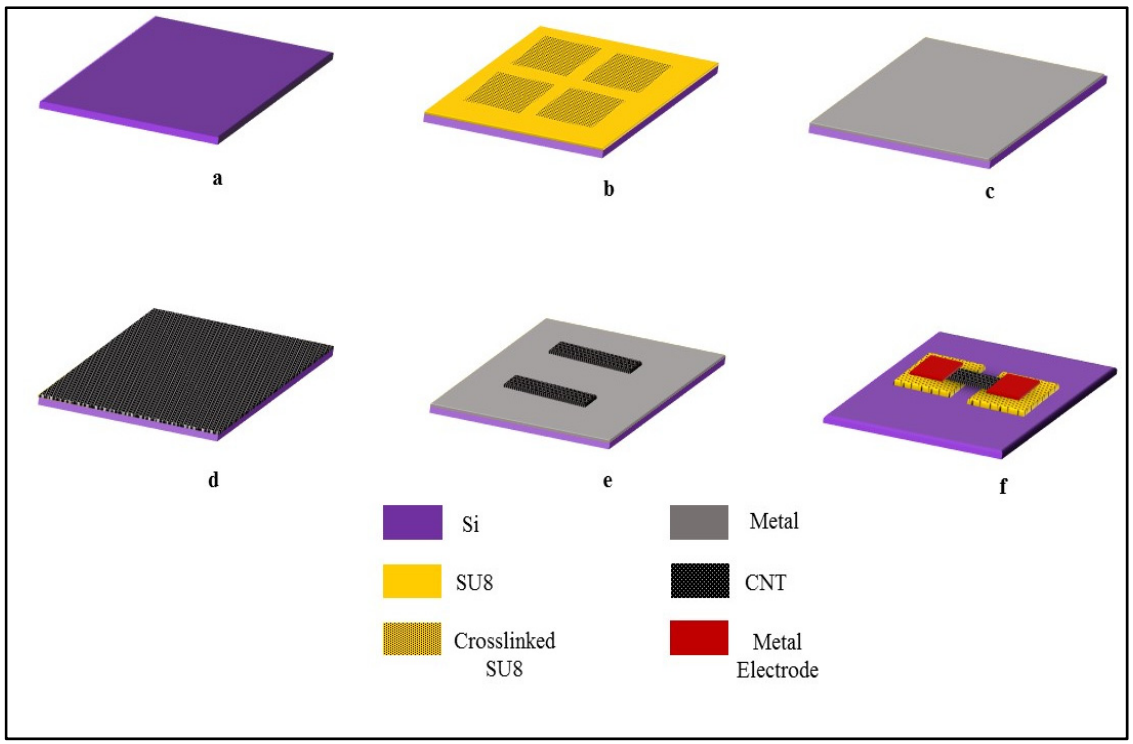

Figure 4.1 Process flow Schematic

Figure 4.1 shows the schematic of the fabrication process. The single-walled carbon nanotubes in this work were obtained from Carbon Solutions Inc. and used without any further modifications. The as obtained nanotubes were dispersed in a 1% Sodium Dodecyl Sulfate (SDS) solution and sonicated for 4 h.

After sonication, the solution is centrifuged for 60 min to remove any solid nanotube agglomerates. The top 80% of the centrifuged solution is decanted for further use. The process starts with a Silicon wafer with a 300 nm oxide (Figure 4.1 a). A 3.5 μm thick SU8 layer is spun and then it is selectively UV exposed using an OAI Hybralign system (Figure 4.2 b). The exposed SU8 crosslinks and acts as "pillars" for the nanotube beams. A 100 nm thick Aluminum layer is evaporated on top of the SU8 layer using filament evaporation, without developing the uncrosslinked SU8 (Figure 4.1 c). This metal layer acts as a barrier and protects the un-crosslinked SU8 from being attacked by organic solvents in future processing steps. The temperature inside the evaporation chamber is verified using temperature strips obtained from Thermax in order to ensure that the SU8 is not cross-linked during the evaporation process. The next step is to deposit the nanotube film (Figure 4.1 d). The carbon nanotube film was created using a simple vacuum filtration method (He et al. 2016; Wu, Chen, et al. 2004).

Vacuum filtration enables the formation of a uniform nanotube network and allows a precise control over the thickness of the film depending on the amount of solution used. More importantly, vacuum filtration is a room temperature deposition method and is of low-cost compared to other techniques. The nanotube film is deposited on a nitrocellulose membrane. After vacuum filtration, the film is washed in deionized (DI) water to remove any traces of surfactant that may be present on the surface. Then, the carbon nanotube film is transferred onto the substrate. The film is cut into the desired shape and size and transferred onto the substrate by dipping the nanotube film in chlorobenzene. The substrate is then dipped in acetone for 60 min to dissolve the nitrocellulose membrane. The resulting nanotube film thickness is between 0.5–0.7 μm depending on the amount of solution used. The nanotube film is then patterned by UV lithography. After development, the nanotube film is etched using oxygen plasma. After the plasma step, the barrier metal is etched by wet etching.

The next step of the process is to remove the uncrosslinked SU8 by dipping the substrate in Developer for 60 s to release the suspended structures, and the final step of the process is to deposit 50 nm thick Aluminum electrodes (Figure 4.1 f).

For the non-suspended carbon nanotubes, the nanotube film was directly transferred onto the substrate, patterned and etched using oxygen plasma using the same gas flow rates and chamber pressures as in the case of suspended carbon nanotube devices to minimize variability. Aluminum electrodes were then patterned onto the nanotubes for electrical measurements.

The concept of using SU8 as a sacrificial material was adopted from (Chung and Allen 2005). The reason for selecting SU8 as a sacrificial layer is the ease of availability and the thermal budget it provides. It also provides a very stable surface for further chemical processes and is also compatible with surface micromachining. Many polymeric materials as a sacrificial material were also considered, but it was found that using these materials lead to cracking of the metal barrier layer with the metal layer subsequently peeling off. This could be due to the thermal stress developed at the interface of the metal-polymer layer, which reduces the adhesiveness of the metal to the sacrificial layer. The other reason is the ease of removal of the SU8. Uncrosslinked SU8 can also be very selectively removed in the presence of other materials as mentioned in the referred work. Importantly, the process proposed in this work is low temperature and can be incorporated above CMOS integrated circuits.

4.4 Results and Discussion

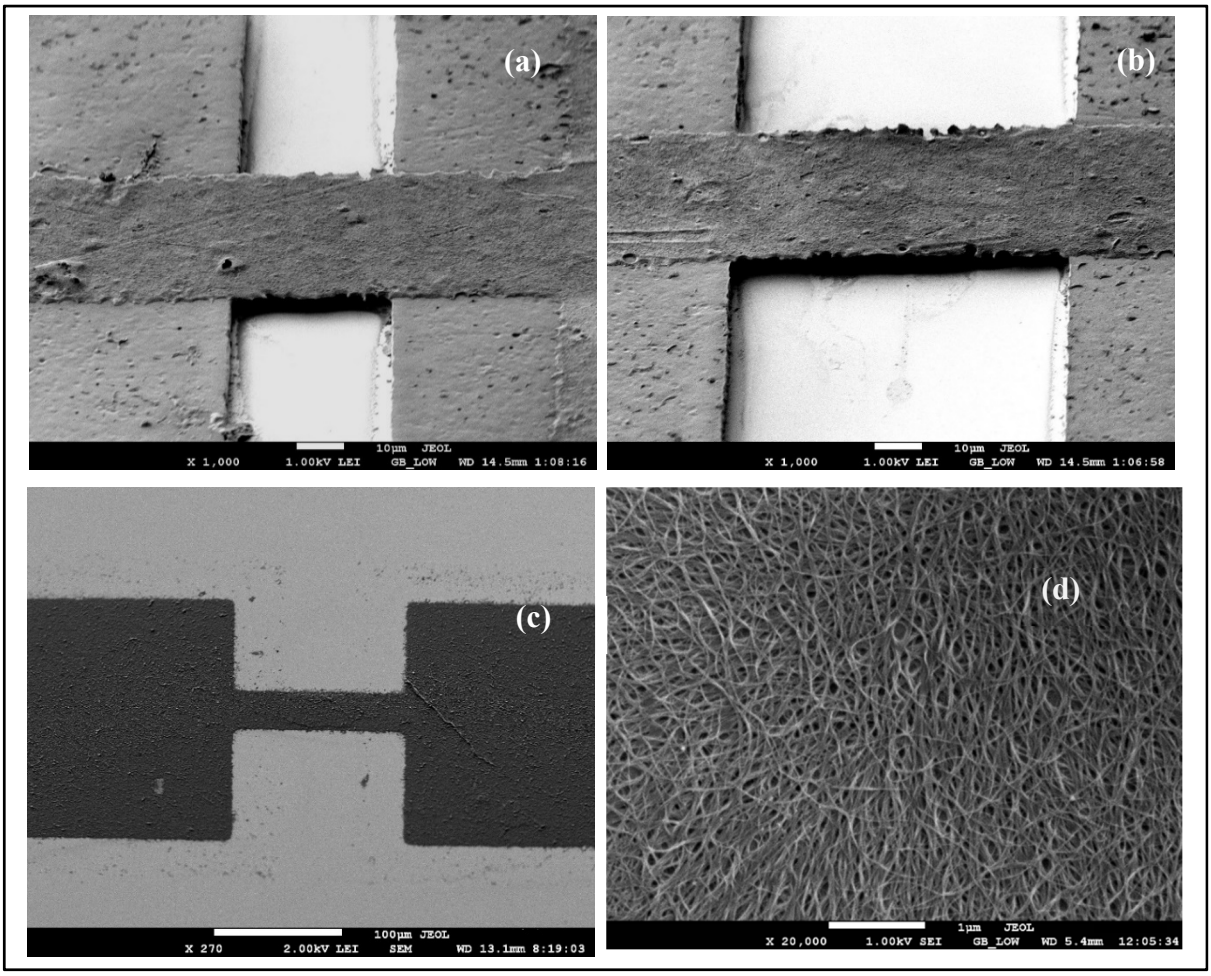

Figure 4.2 (a) and (b) Suspended beams with different suspension lengths,
(c) A normal Non-suspended nanotube beam, and,
(d) Networks of nanotubes that comprise the beam

The samples were imaged using a MEB 3600 Scanning Electron Microscope. The samples were metallized by sputtering a 20 nm Gold layer to make the nanotubes conductive for the SEM. It was found that the sputtering did not affect the properties of the nanotubes. Figure 4.2 (a, b) shows Scanning Electron Microscope (SEM) micrographs of suspended nanotube beams across the SU8 “pillars”. Figure 4.2 (c) shows a conventional non-suspended device, and

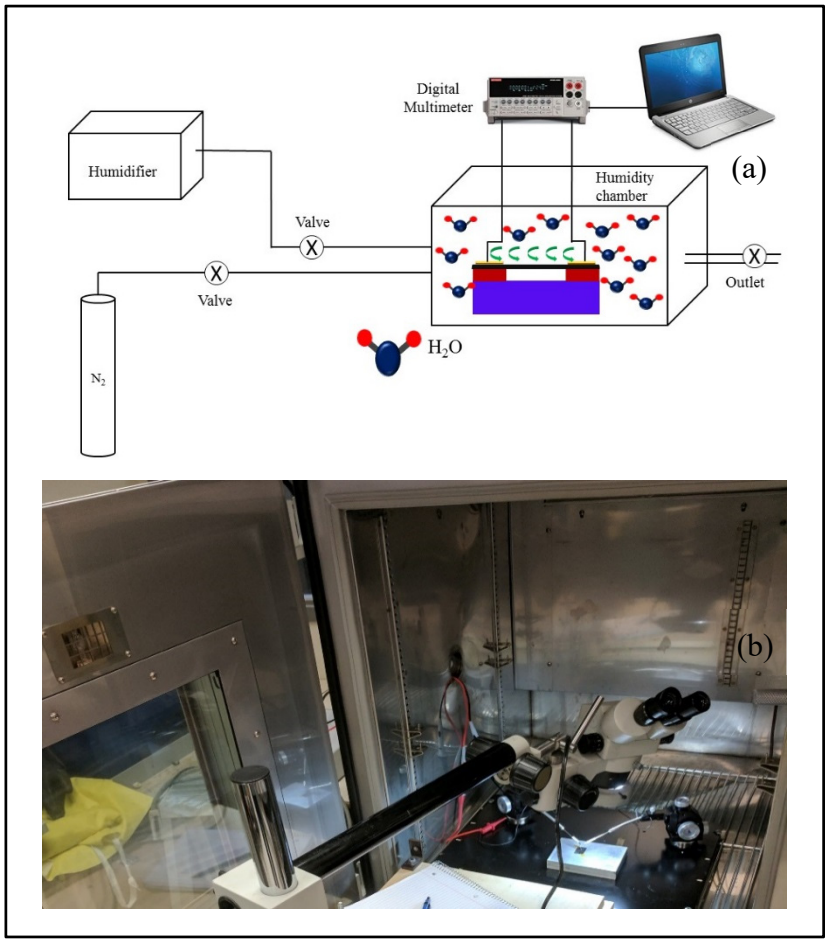

Figure 4.3 (a) Schematic of the test setup, and,
(b) Photograph of the device inside the test chamber

Figure 4.2 (d) shows a high magnification micrograph which shows the networks of nanotubes comprising the beam. The nanotube beam is suspended at a height of 3.5 µm above the substrate. After fabrication, the humidity-sensing characteristics of both types of sensors are recorded by measuring the change in resistance of the devices.

Figure 4.3 (a, b) shows the schematic of the test setup and a photograph of the setup used for the measurements. The sensors were interconnected using probes aligned with micro-positioners. A humidity chamber with an external humidity source was used for the measurements. The initial humidity was of 15% RH at 24ºC.

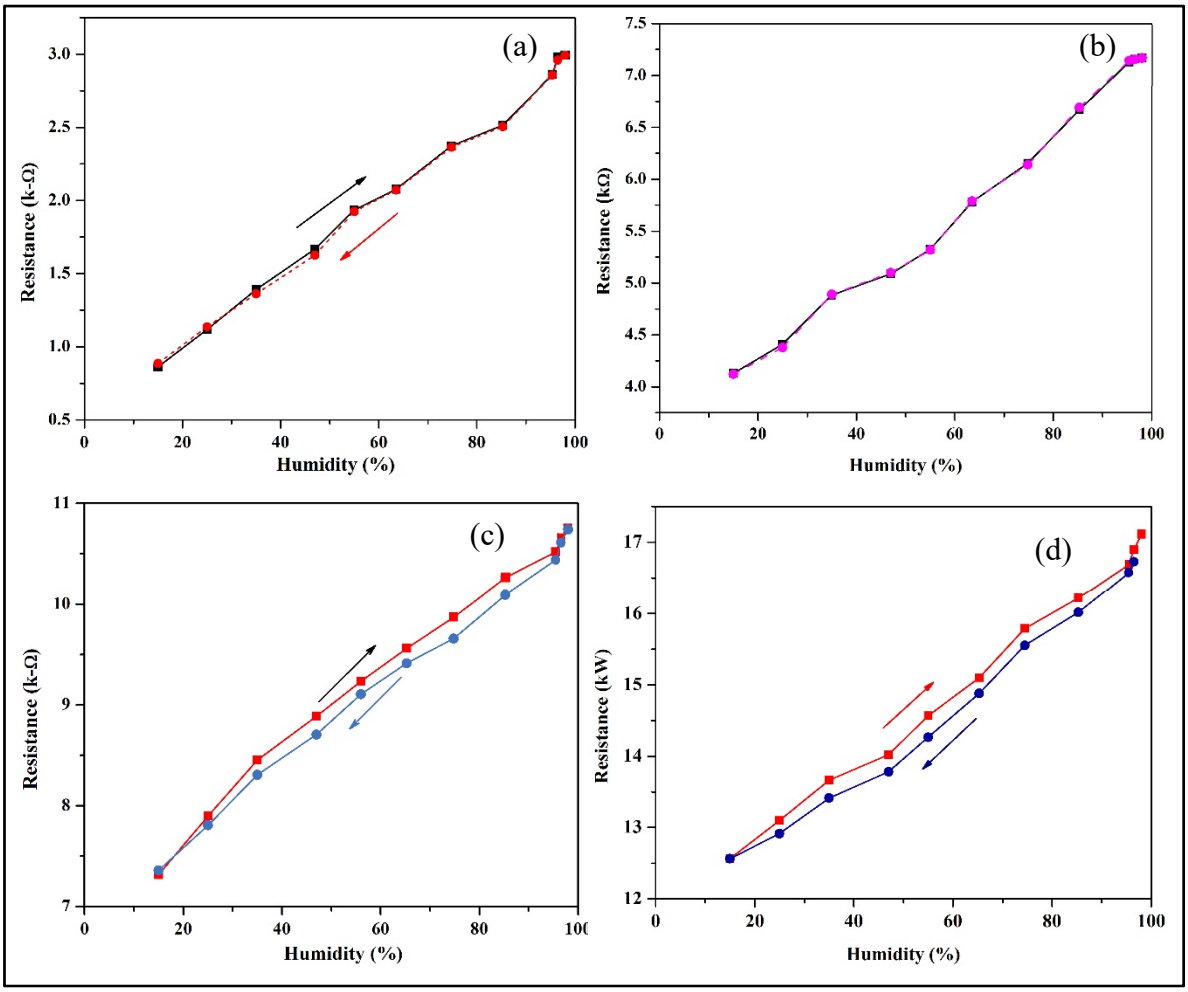

Figure 4.4 (a, b) Humidity response and Hysteresis for suspended carbon nanotubes (36 µm and 72 µm respectively), and,
(c, d) humidity response and hysteresis for non-suspended carbon nanotubes (36 µm and 72 µm respectively)

The percentage humidity inside the chamber was verified using a high-precision sensor embedded within the humidity chamber.

The compressor inside the humidity chamber could not be used to produce humidity since the vibrations led to the probes scratching the metal electrodes and destroying the devices. Accordingly, an external humidifier was used to inject water vapor into the chamber and a nitrogen tank was used to quickly flush out the humidity when required. Nitrogen was chosen as a carrier gas in order to maintain an inert environment within the chamber. The resistance of the devices was measured using a Keithley Digital Multimeter.

The multimeter was in-turn connected to a computer for data acquisition. The resistance was allowed to stabilize inside the chamber for 30 min prior to the first measurement.

Figure 4.4 shows the response of both suspended and non-suspended devices for relative humidity ranging from 15% to 98 % RH. Figure 4.4 (a, b) shows the hysteresis characteristics and average resistance values of suspended devices with different suspension lengths averaged for 10 up-and-down cycles respectively. The base resistance was around 0.86 kΩ for the 36 µm suspended tubes (Device A) and 4.12 kΩ for the 72 µm suspension length (Device B) at 15% humidity. At 98% humidity, the resistance for devices A and B are 2.991 kΩ and 7.167 kΩ, respectively. The suspended devices showed minimal hysteresis even after multiple humidity cycles. As shown in Figure 4.4 (c, d), for the non-suspended devices, devices with similar channel lengths of 36 µm (Device C) and 72 µm (Device D) had a base resistance of 7.3 kΩ and 12.56 kΩ respectively at 15% humidity. At 98% humidity, the resistance was 10.755 kΩ and 17.11 kΩ for devices C and D, respectively.

The devices showed an almost linear response to humidity. The non-suspended devices exhibit similar hysteresis characteristics. The hysteresis is caused by water molecules on the substrate, agreeing with the work reported in (Kim et al. 2003). The high resistance of the non-suspended devices is possibly due to the presence of charge traps and defects within the substrate which limit the flow of charge carriers in the network while in the case of suspended devices, the lack of substrate interactions provides a smoother pathway for charge carriers. The humidity-sensing mechanism of the nanotubes has been extensively studied and described in works such as (Zahab, Spina et al. 2000, Pati, Zhang et al. 2002). The nanotubes are inherently p-type having holes as the majority charge carriers.

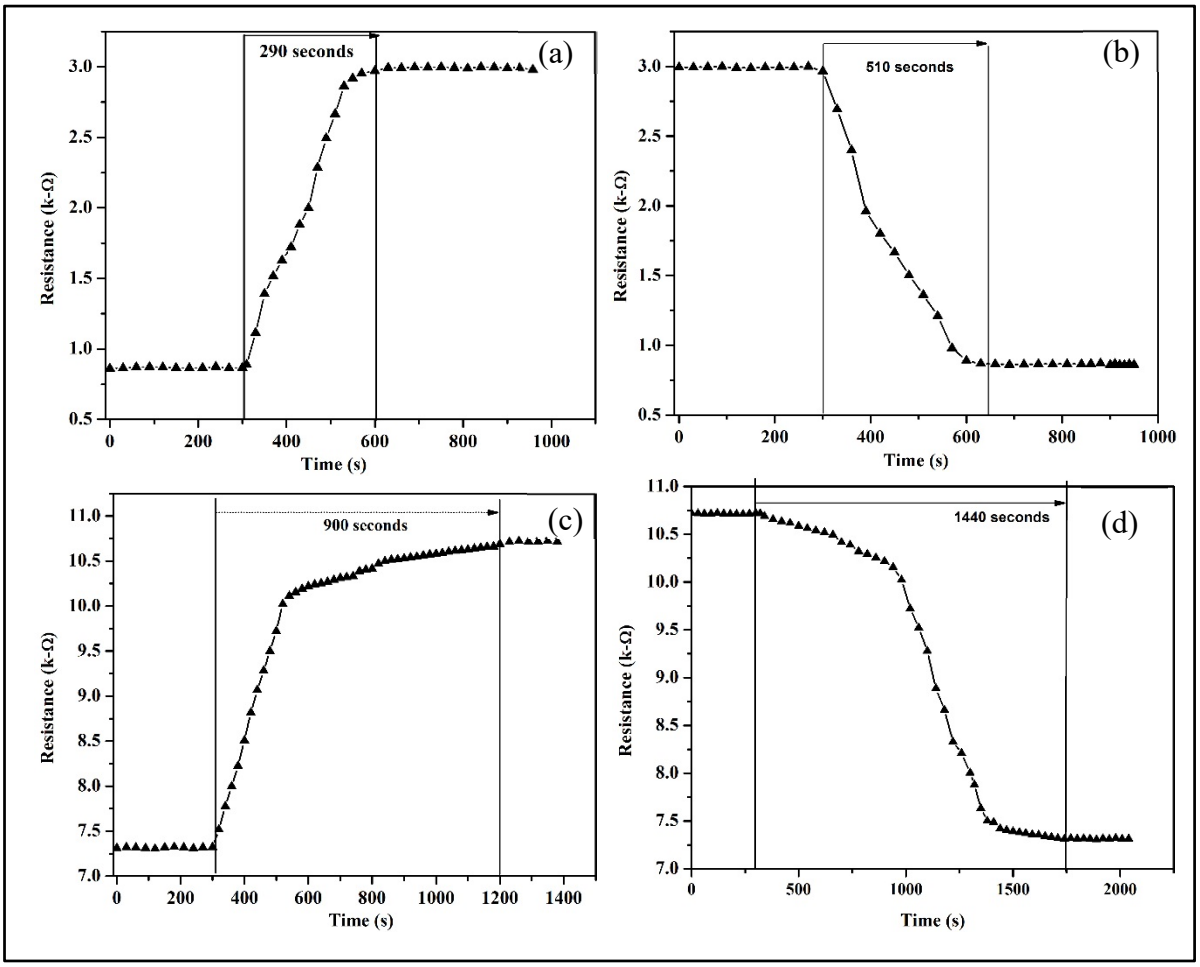

Figure 4.5 (a) Rise time and (b) fall times of suspended carbon nanotubes, and, (c) Rise time and, (d) fall times of non-suspended carbon nanotubes
The humidity was varied from 15% to 98% in steps of 10% RH increases every 20 s

When a water molecule interacts with the nanotube, it donates electrons to the nanotubes and because of electron transfer, the number of effective charge carriers in the nanotube decrease thereby increasing the resistance of the devices.

Figure 4.5 (a, b) and Figure 4.5 (c, d) show the rise and fall times of both types of sensors. The response time of the suspended structures is 290 s as compared to 900 s for the non-suspended devices. The faster rising response of suspended structure is due to the increased surface area of the device thanks to the flow of humidity below the beam enabled by the suspension of the nanotubes beam. The recovery or fall times are 510 s and 1440 s for suspended and non-suspended devices, respectively, outlining again the advantage of the suspended structure.

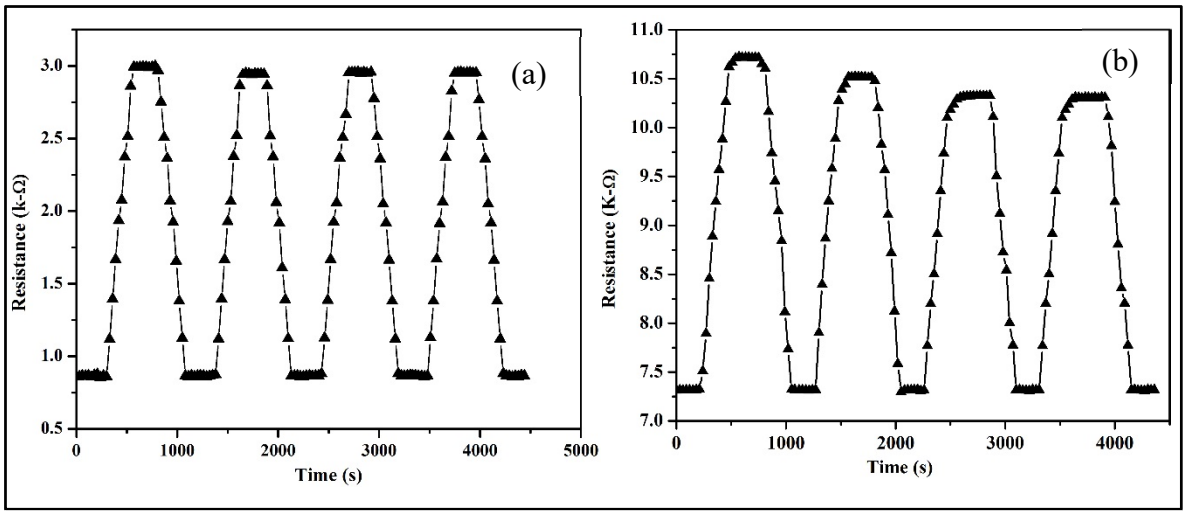

Figure 4.6 Repeatability of (a) suspended carbon nanotubes, and,
(b) non-suspended carbon nanotubes

The longer recovery time of the non-suspended devices could be due to the presence of water molecules on the nanotube network during the desorption process and to the reduced surface area available for desorption.

Figure 4.6 (a, b) shows repeatability of the devices by plotting resistance as a function of time for four continuous humidity cycles under continuous humidification from 15% to 98% RH. The resistance of each device was allowed to stabilize for a few minutes before the beginning of each cycle.

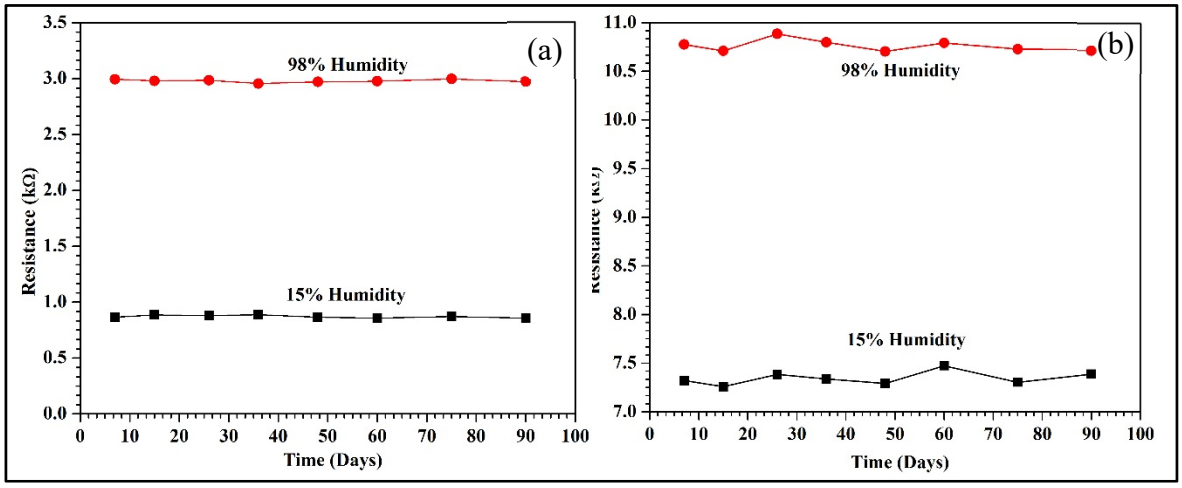

Figure 4.7 Long-term stability of (a) suspended sensors and,
(b) non-suspended sensors of 36 µm suspension

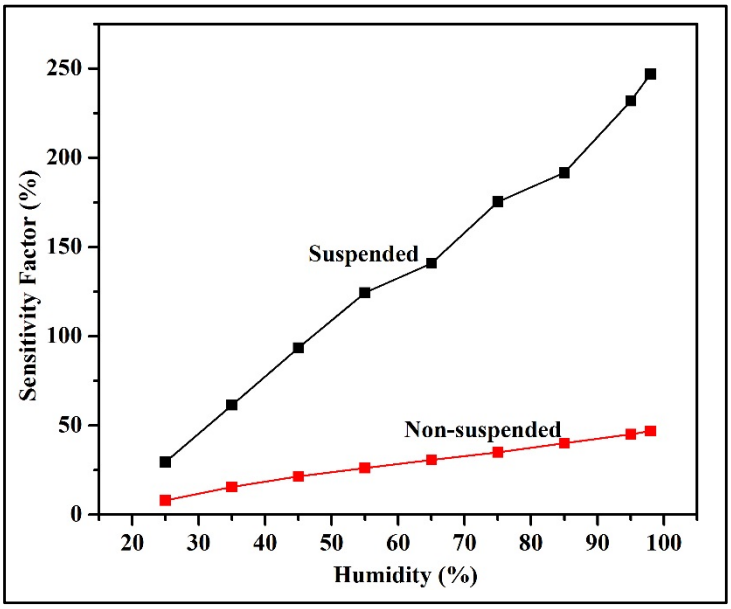

Figure 4.7 Sensitivities of suspended and non-suspended sensors

The suspended humidity sensor showed very consistent resistance values even after 3 cycles whereas the non-suspended sensor began to show drifting performance, outlining the compromised dynamics due to the reduced surface area and absent gas flow below the beam.

One of the most important parameters for gauging sensor performance is long-term stability. The sensor should show consistent values and response even after prolonged duration. To demonstrate long-term stability, the resistance of the suspended devices was measured after certain time intervals with similar testing conditions as the initial tests. The suspended nanotube sensors exhibited stable performance over the time period as shown in Figure 4.7

It has been shown in this work that the sensitivity of the sensor is improved by the suspension of the carbon nanotubes beam. The sensitivity factor, in percent, is given by:

$$S = \frac{R_H - R_0}{R_0} X100 \tag{4.1}$$

Where R_H is the resistance at the measured value of resistance, and R_0 is value of baseline resistance.

Since the suspended nanotubes beam is not connected to the substrate, the water molecules have both the top and bottom surface to adhere to which increases the sensitivity of the sensor. Figure 4.8 shows the plot of the sensitivity factor of both suspended and non-suspended sensors as a function of the relative humidity.

It can be gauged from this plot that the sensitivity of the suspended nanotubes is much greater than the non-suspended networks. From a base humidity of 15%, the increase in resistance at 98% humidity was of 246.9% for the suspended device compared to only 46.83% for the non-suspended devices. The results of this study are a clear indication that the use of suspended structures for sensing applications yields significant advantages in comparison to traditional substrate bound materials. It is clear that the response and recovery times presented in this work are not suitable for commercial use, as the nanotubes have not been functionalized. However, the aim of this work is to demonstrate the advantages of suspended nanotube networks, in terms of response time, hysteresis and sensitivity. Many functionalization schemes have been reported in literature (Han et al. 2012; Wang et al. 2014; Paul et al. 2013) and could be used to improve response time, while benefiting from the suspended structure. The recovery time can also be further improved by incorporating a micro-heater into the device to promote heating and therefore faster desorption. The comparison that is provided here does nonetheless outline the advantages of suspending the carbon nanotubes beam in order to improve response time, sensitivity and hysteresis.

4.5 Conclusion

Suspended carbon nanotubes have been investigated as an alternative to conventional non suspended devices. We have demonstrated an easy, low-temperature fabrication process to obtain suspended carbon nanotube beams using a common polymer sacrificial layer. Notably, the low-temperature of the process is well suited to the integrated of devices directly above CMOS integrated circuits. Moreover, this process with some modifications can also be used to create device such as nanotube micromechanical resonators.

It was found that suspended carbon nanotubes have better all-round humidity-sensing performance as compared to non-suspended architecture. The suspended nanotube sensor exhibited repeatable performance with good response times and recovery times as compared to the non-suspended sensor. The significantly reduced hysteresis in the suspended nanotube humidity sensor is a major advantage, along with their enhanced sensitivity and response time. The performance of the devices can be enhanced by chemical modification of the nanotube network and future work is to functionalize the nanotubes and study their humidity response in a suspended architecture.

Author Contributions: S.A performed all the experiments and measurements. A.A. Gupta contributed towards discussions and direction regarding the process flow and measurement setup. F.N and R.I contributed expertise, direction, materials and experiment tools.

CHAPTER 5

LOW-HYSTERESIS AND FAST RESPONSE TIME HUMIDITY SENSORS USING SUSPENDED CARBON NANOTUBES

Shiva ram Arunachalam[1], Frederic Nabki[1] and Ricardo Izquierdo[1]

[1]Department of Electrical Engineering, École de Technologie Supérieure,
1100 Notre Dame West, Montréal, Quebec, Canada H3C 1K3

Paper published in *MDPI Sensors*, February 2019

Preface

In the previous chapter, the concept of a suspended CNT humidity sensor was demonstrated. As compared to a traditional non-suspended device, the sensor showed excellent sensing characteristics in terms of response, recovery times and repeatability. Moreover, the suspended sensor also showed excellent stability for prolonged periods of time. Further, the suspended sensor experienced almost zero hysteresis after 10 cycles of operation. In comparison, the non-suspended sensor showed a large hysteresis which is undesirable.

However, in the previous work, the response and recovery times of the suspended sensor (290 s and 510 s respectively) is too high for real world applications. The high response time is because the CNTs were not chemically functionalized to make them selective to water vapor. In the following chapter, the issue of high response time of the sensor is addressed by using chemically functionalized CNTs making them much more sensitive to water vapor. The CNTs are directly obtained from a supplier, pre-functionalized, to save time and effort. The sensor is then fabricated using the same process flow as the previous work. The use of functionalized CNTs improves the response and recovery times significantly thereby solving the main issue at hand. The sensor still exhibits minimal hysteresis, good long-term stability and repeatability. Thus, we have demonstrated a fast, robust humidity sensor with zero hysteresis. This forms the second journal publication of this Ph.D. thesis and was published in MDPI Sensors.

5.1 Abstract

A humidity sensor using suspended carbon nanotubes (CNTs) was fabricated using a low-temperature surface micromachining process. The CNTs were functionalized with carboxylic acid groups that facilitated interaction of water vapor with the CNTs. The humidity sensor showed a response time of 12 s and a recovery time of 47 s, along with superior hysteresis and stable performance. The hysteresis curve area of the suspended structure is of 3.6, a 3.2 times reduction in comparison to the non-suspended structure. A comparative study between suspended and non-suspended devices highlights the advantages of using a suspended architecture.

Keywords: Carbon nanotubes; Suspended beam; Non-suspended beam; Humidity Sensing; Functionalized.

5.2 Introduction

Carbon nanotubes (CNTs), first discovered by Iijima (Iijima 1991), are one of the most studied materials for gas sensing applications (Cantalini et al. 2004) The inherent properties of CNTs, such as high surface area to volume ratio and a hollow structure, along with the ease of surface modification, have led to the use of both single- and multiwalled CNTs to detect a variety of gases with much success (Wang and Yeow 2009).

Sensing mechanisms can include change in resistance (Liang, Chen, and Wang 2004), capacitance (Chen et al. 2009a; Snow et al. 2005), frequency (Penza et al. 2008), etc. To date, most of the humidity sensors based on CNTs have been based on functionalized CNTs and have shown considerable promise for commercial usage. Humidity sensors have considerable usage in household, automotive, and medical applications (Ma et al. 1995). The performance and stability of sensors are important parameters that are the subject of continuous research using different materials and methods (Farahani, Wagiran, and Hamidon 2014).

Fast response and recovery times and low hysteresis of a humidity sensor are important parameters to consider, and recovery performance during prolonged exposure to high humidity levels is of interest for sensors to be commercially deployed. Accordingly, these parameters are considered in this work for the proposed devices.

There are many works in the literature focusing on the fabrication of humidity sensors based on CNTs. Multiwalled CNTs (MWCNTs) based humidity sensors were fabricated and studied by many research groups (Chen et al. 2009a; Cao et al. 2011; Tsai, Lu, and Li 2010). An ultrafast humidity sensor was fabricated by Chan et al. (Tang, Chan, and Zhang 2011) using composite films of polyimide and MWCNTs with a response time of 5 s and a recovery time of 8 minutes. Liu et al. (Liu et al. 2009) developed a MWCNTs based humidity sensor deposited by dielectrophoresis on interdigitated electrodes. Yeow et al. (Yeow and She 2006) used MWCNTs deposited on a stainless steel substrate to fabricate a capacitive humidity sensor with a response time of 75 s. An MWCNTs based humidity sensor was studied using different testing frequencies (AC current) with a response time of 16 s (Zhao et al. 2011). Researchers have also used single-walled CNTs to detect humidity (Mudimela et al. 2012). However, most of the works mentioned above focus on the hysteresis performance of the proposed sensors. Accordingly, this work aims at characterizing this important parameter as well.

Suspended CNTs have also been used previously to detect gases such as NO_2 (Chikkadi et al. 2014a) . One of the main advantages of using a suspended architecture is the significantly reduced hysteresis in the devices (Muoth et al. 2010). This combined with the increased surface area of adsorption is ideal for sensing applications. This has been demonstrated in our previous work (Arunachalam et al. 2018). Reduced hysteresis in a sensor leads to increased reliability and measurement consistency which are two important parameters for sensor performance. However, suspended CNTs are difficult to fabricate and require complex and often expensive tools. There is also the question of yield in traditionally followed methods to obtain suspended CNTs where individual CNTs or a cluster of CNTs are grown between pre-fabricated electrodes using high temperature chemical or physical vapor deposition processes.

This approach is generally used to study intrinsic properties such as transport phenomena (Cao, Wang, and Dai 2005), phonon interactions (Sapmaz et al. 2006), etc. Thus, suspended CNTs have rarely been used in sensing applications even though they offer significant inherent advantages.

In our previous work (Arunachalam et al. 2018), the advantages of pristine suspended CNTs have been demonstrated. The suspended CNTs showed near-zero hysteresis and better response and recovery times than non-suspended CNTs. Moreover, the fabrication process proposed had a low temperature budget, making the sensors suitable for integration above integrated circuits. However, the response and recovery times were relatively long, curtailing commercial viability. This work is an improvement over the previous work by using functionalized single walled CNTs. The suspended functionalized CNTs also showed near zero hysteresis, remarkable repeatability along with fast response and recovery times. To further demonstrate the advantages of using a suspended architecture, the device performance is compared to a traditional non-suspended CNT device using the same fabrication process.

5.3 Materials and Methods

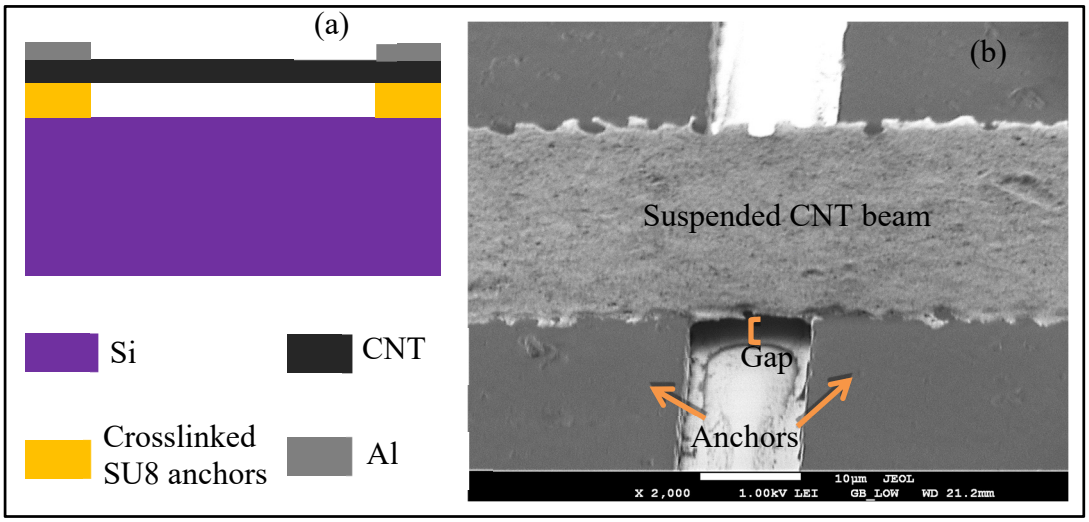

Figure 5.1 (a) Schematic of the suspended CNT beam and (b) SEM Micrograph

The detailed fabrication process has been discussed previously in (Arunachalam et al. 2018). Notably, the fabrication process features a very low temperature budget (i.e. below 110°C) and is amenable to integration above integrated circuits. The following is a brief overview of the fabrication process. The process is carried-out on a Silicon (Si) substrate. SU8, an epoxy based negative photoresist is used as a sacrificial layer to obtain suspended CNTs. SU8 was chosen as the sacrificial material due to its uniform surface profile and ease of availability. The SU8 is partially crosslinked by UV lithography. The Crosslinked SU8, of thickness 3.6 μm, is used as anchors for the CNT beam while the uncrosslinked SU8 is used as a sacrificial layer. The uncrosslinked SU8 is prevented from dissolving in further processing steps by depositing a 60 nm barrier layer of Aluminum by filament evaporation. The CNTs used in this work are obtained pre-functionalized with a carboxylic acid group (-COOH) from Carbon Solutions Inc. and used without any further material processing. 0.125 g of the as-obtained CNTs in powder form were dispersed in a 1 weight percent SDS solution. The as-prepared solution was then ultrasonicated for 6 hours at room temperature resulting in a uniformly dispersed CNT solution. The solution is then ultra-centrifuged at 47300 rpm for 60 minutes. The top half of the solution is then decanted for further use. Then, the CNT films are formed using vacuum filtration. Vacuum filtration enables the formation of a homogenous film with a uniform distribution of CNTs. This process also ensures strict control over film thickness. The CNT films used here are 0.7 μm thick. 20 nm thick aluminum (Al) electrodes are deposited on the CNTs before release to form the suspended CNT beams. The schematic of the resulting suspended CNT beam cross-section is shown in Fig. 5.1(a) and a SEM micrograph of a fabricated beam is shown in Fig. 5.1(b).

5.4 Results

The device characterization is done in a humidity chamber connected to an external humidifier, which acts as the humidity source. The sensors are interconnected using probes aligned using micro-positioners. The humidity percentage in the chamber was verified using a high-precision sensor embedded within the chamber. The resistance of the devices was measured using a Keithley Digital Multimeter connected to a computer for data acquisition.

5.4.1 Humidity Response

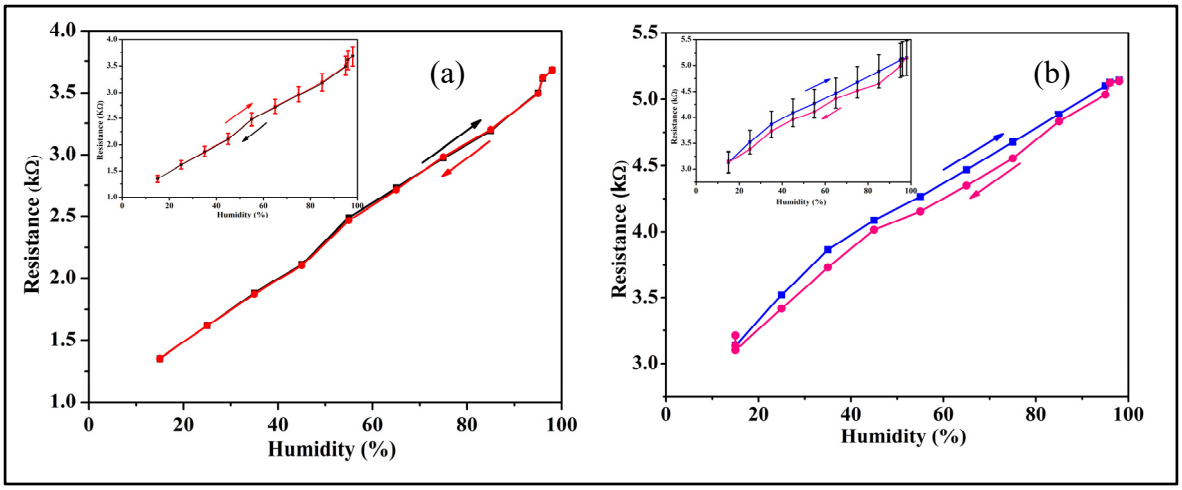

Figure 5.2 (a) Plot of the humidity response of the suspended CNTs, and,
(b) Plot of the humidity response of the non-suspended CNTs.
The hysteresis characteristic is also shown. The insets in each figure show the average hysteresis profile of 6 identical devices measured under similar testing conditions

To study the humidity sensing properties of the CNT based sensors, the resistance of the devices was measured as a function of relative humidity. The humidity was measured from a base of 15% RH to a maximum of 98% RH gradually increased in steps of ~10% RH per 2 Minutes. The results are shown in the plots of Fig. 2 for both suspended and non-suspended devices. The inset plots of Fig 5.2(a) and 2(b) show the average hysteresis profile of 6 measured devices of each type (i.e. suspended and non-suspended) while the outset shows the device response of a typical device of each type. A comparison of the hysteresis profile of a single device to the average profile shows that the suspended devices have a consistent response to humidity. The average base resistance of the suspended CNTs for 6 measured devices at 15% RH is 1.3 kΩ and it rises to an average of around 3.5 kΩ at 98% RH. In comparison, the non-suspended devices had an average base resistance of 3.3 kΩ at 15% RH and 5.1 kΩ at 98% RH. Moreover, the suspended devices exhibit minimal hysteresis with an average hysteresis curve area of 3.56, even after 8 measurement cycles. In comparison, the non-suspended sensors exhibited significant hysteresis, with an average hysteresis curve area of 11.21. This represents a 3.2x improvement in the hysteresis behavior of the suspended sensor over the non-suspended sensor.

The hysteresis curve area was calculated using the in-built Integrate function of the Origin software package. The lack of hysteresis in the suspended sensor can be attributed to the lack of substrate effects such as charge traps (Muoth et al. 2010) which could alter the pathway of the charge carriers in the nanotube network. The charge traps and grain boundaries within the substrate alter the conductivity and hence the non-suspended sensor also shows higher resistance.

5.5 Response time, Recovery time and Sensitivity

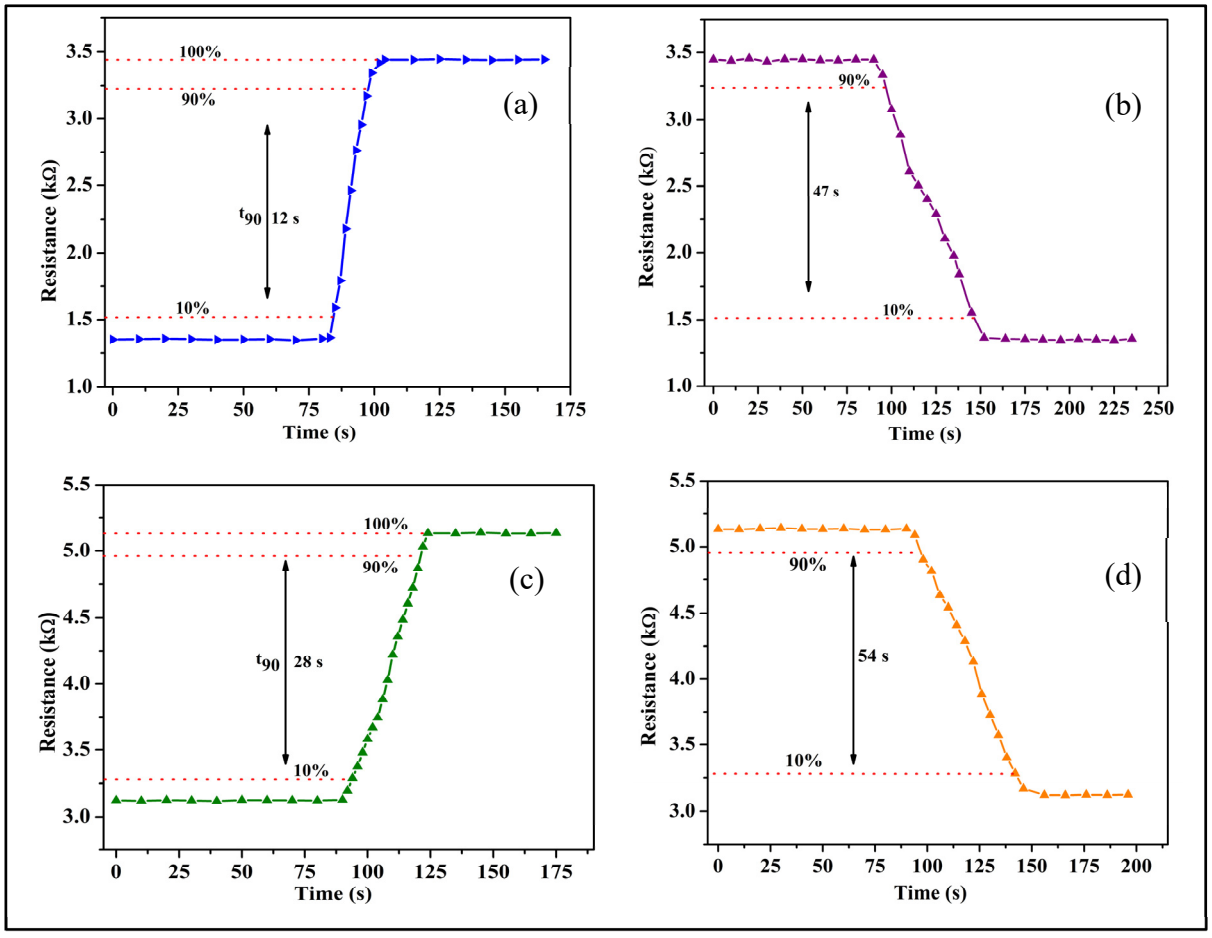

Figure 5.3 Response time and (b) recovery time of the suspended CNTs
(c) response time and (d) recovery time of the non-suspended CNTs
The humidity was increased gradually in steps of 10% RH

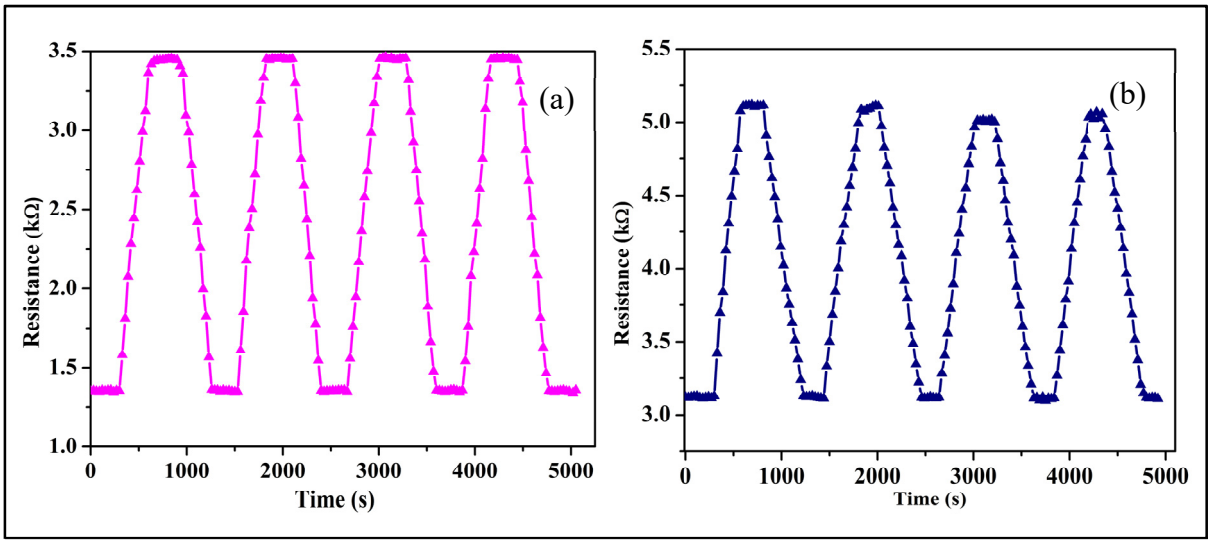

Figure 5.4 (a) Repeatability measurement over four humidity cycles for the suspended CNTs, and, (b) for the non-suspended CNTs

The response time, defined as the time taken to achieve 10–90% of the total resistance change, Is measured to be 12 s for the suspended sensors and around 28 s for the non-suspended sensors, as shown in Figure 5.3(a, c) respectively. The 2.3-fold shorter response time of the suspended sensors is due to the increased surface area for the adsorption of water molecules. Since the film is suspended, the molecules can adhere to both the top and bottom surface of the CNT beam. The recovery time, defined as the time taken by the sensor to go from 90% to 10% of its original resistance value is measured to be 47 s for the suspended sensors and 54 s for the non-suspended sensors, as shown in Figures 5.3 (b, d), respectively. Consistent performance of the sensor is necessary for long-term applications. Thus, repeatability of the sensors was verified by subjecting them to continuous humidity cycles by varying humidity from 15% to 98% RH and recording the resistance at an interval of every 5s.

As seen in Figure 5.4 (a), the suspended sensors showed remarkable stability and repeatability. In comparison, the non-suspended sensors showed relatively stable performance with a drift in performance after three humidity cycles, as shown in Figure 5.4 (b). This further demonstrates the advantages of using suspended CNTs over traditional non-suspended CNTs.

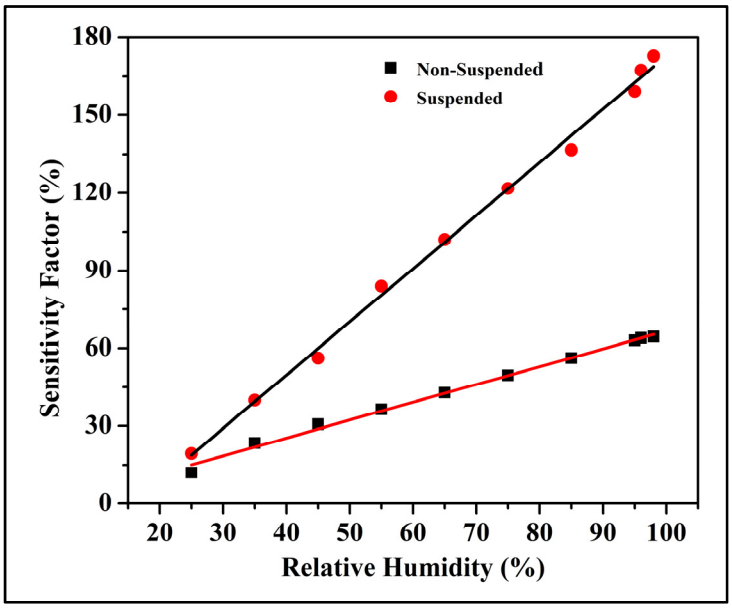

Figure 5.5 Sensitivity factors of suspended CNTs vs. non-suspended CNTs

The excellent repeatability is due to the ease of adsorption and desorption of the water molecules from the surface of the suspended CNT beam.

The humidity sensing mechanism of CNTs has been studied and discussed extensively in previous works (Cao et al. 2011). The sensing is primarily due to charge transfer within the CNT networks. The CNTs are inherently p-type. As the water molecules donate electrons to the CNTs as a result, the number of primary charge carriers in the CNTs (holes) decreases and thus the resistance increases in the sensor. The sensitivity factor is given by (Cao et al. 2011; Jung, Kim, and Lee 2015):

$$S = \frac{R_H - R_0}{R_0} X100 \tag{5.1}$$

Where R_H is the resistance at any given humidity, R_o is the starting resistance at 15% RH. The sensitivity factor comparison of the suspended and non-suspended sensors is shown in Figure 5.5. At 98% humidity, the sensitivity factor of the suspended sensor is 172.9% compared to 64.2% for the non-suspended sensor. This outlines a 2.7-fold improvement for the suspended structure.

The slope of the graph, which represents the percentage change in the resistance from the initial resistance per % RH change, for the suspended sensor is 2.05 compared to 0.68 for the non-suspended sensor, meaning the sensitivity of the suspended sensor is 3-fold greater than the non-suspended sensor. Demonstrably, the suspended sensor shows better performance in all aspects and thus is a better prospect for CNT-based humidity sensors. The acidic functionalization of CNTs shortens the CNTs, making ends open and introduces side wall defects, which facilitate water adsorption. The increased water adsorption capacity combined with shortened pathways for the charge carriers result in faster response times in the functionalized CNT sensor (Zhang et al. 2003).

5.6 Temperature Study

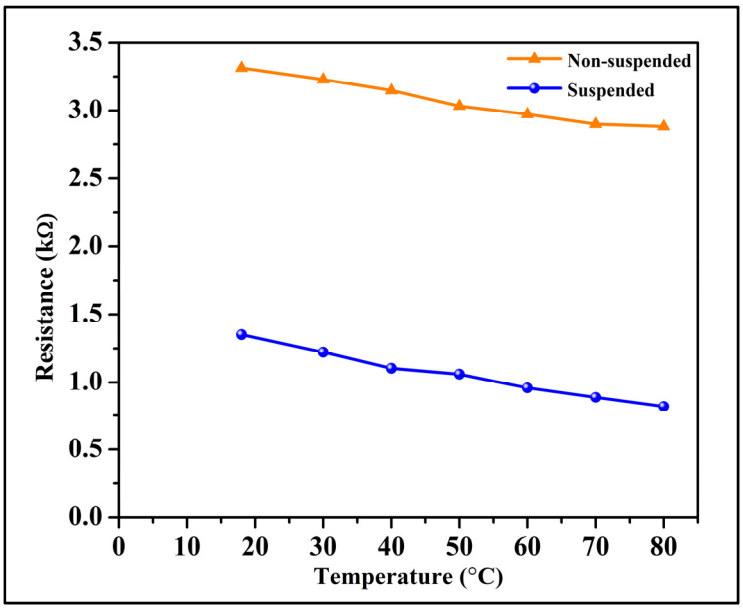

Figure 5.6 Resistance vs. temperature for suspended and non-suspended CNTs

The resistance of the suspended devices was measured at different temperatures to gauge the performance under different thermal operating conditions. In Figure 5.6, the resistance of the suspended and non-suspended sensors as a function of temperature is plotted. As can be seen, the resistance of the devices decreases with an increase in temperature.

This is attributed to a decrease in the number of water molecules available to interact with the CNT networks at higher temperatures. Moreover, the thermal energy of the electrons provided by the water molecules increases with increasing temperature. The imparted thermal energy is enough for the electrons to overcome the potential barrier between the CNTs in the network, which results in a decrease in the film's resistance (Benchirouf et al. 2016; Zhang et al. 2007).

5.7 Long term Stability

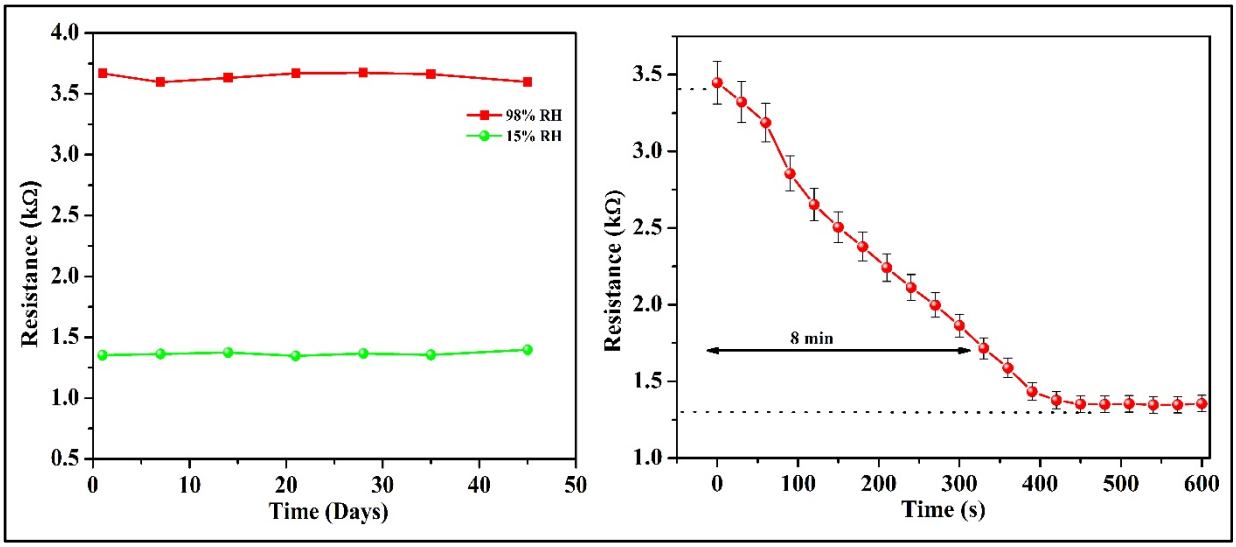

Figure 5.7 (a) Resistance as a function of time for suspended CNTs, indicating device stability, and (b) recovery time to 15% RH of the suspended CNTs after exposure to 98% RH for 24 h

The long-term stability of a sensor is a major factor in determining its performance. To gauge Long-term stability, the resistance of the suspended device was measured at regular intervals of seven to ten days. Figure 5.7 (a) shows the resistance value of the sensor at two different humidity levels over a 45-day period. This demonstrates the stability of the sensor over extended periods as the resistance fluctuates less than 3.32% over the timespan of the test. To gauge the sensor recovery time after prolonged exposure, the sensor was soaked in a humid environment at 98% RH for 24 h. The humidity was then flushed out and the sensor response was recorded. Figure 5.7 (b) shows the graph of the sensor recovery after prolonged exposure. The sensor took approximately 8 min to recover from 90% to 10% of its original resistance. In addition, no permanent shift in the sensor resistance was exhibited after recovery.

Table 5.1 shows a comparison of the response and recovery times of few of the different CNT humidity sensors in literature. The presented sensor exhibits good response and recovery times compared to other works. In addition, the device also exhibits enhanced sensitivity factor when compared to the other works and a 3-fold improved sensitivity than a non-suspended sensor.

Table 5.1 Comparison of the Response and Recovery times of different CNT humidity sensors

Publication	**Sensing Material**	**Response time (s)**	**Recovery time (s)**	**Sensitivity Factor (%)**
This work	Functionalized Single- walled CNTs	12	47	172.9
Jung et al. (Jung, Kim, and Lee 2015)	Metal oxide coated CNTs	30	25	~60
Cao et al. (Cao et al. 2011)	Multiwalled CNTs	50	140	124
Mudimela et al.(Mudimela et al. 2012)	Single-walled CNTs	180	240	N/A
Zhang et al. (Zhang et al. 2005)	Multiwalled CNTs	60	70	80
Moraes et al. (C. Moraes et al. 2014)	Functionalized Multiwalled CNTs	3	90	135
Chen et al. (Chen et al. 2009a)	Multiwalled CNTs	16	8	29.9
Arunachalam et al. (Arunachalam et al. 2018)	Single-walled CNTs	290	510	246.9

5.8 Conclusions

In this work, a humidity sensor based on a suspended carbon nanotube has been demonstrated. The suspended sensor showed good performance with near-zero hysteresis, fast response and recovery times, and exhibited good long-term stability. To demonstrate the advantages of using a suspended architecture, the performance of suspended CNTs was compared to a non-suspended sensor under similar testing conditions. Evidently, the suspended sensors showed superior humidity sensing characteristics such as near-zero hysteresis, and significantly improved sensitivity owing to lack of substrate effects and more surface area for adsorption.

Moreover, the work improved the response time of the devices as compared to our previous work in (Arunachalam et al. 2018) by more than 10-fold due to the chemical functionalization of the nanotubes making them more sensitive to the water molecules.

The suspended humidity CNT sensor presented here also compares favorably in terms of response and recovery times to other literary works. The proposed sensor design thus has the potential of yielding high-performance humidity sensors that are suitable to integration with integrated circuits.

Author Contributions

S.A. did all the experimental work, data acquisition, and analysis. F.N. and R.I. contributed expertise, direction, materials, and experimental tools.

CHAPTER 6

IONIZATION GAS SENSOR USING SUSPENDED CARBON NANOTUBE BEAMS

Shiva ram Arunachalam[1], Frederic Nabki[1] and Ricardo Izquierdo[1]

[1]Department of Electrical Engineering, École de Technologie Supérieure,
1100 Notre Dame West, Montréal, Quebec, Canada H3C 1K3

Paper published in *MDPI Sensors*, March 2020

Preface

In this chapter, we present a gas sensor based on a field ionization process. The proposed sensor is an evolution of our previous device design with the addition of an electrode underneath the beam. Ionization sensors have a big advantage over traditional chemical sensors since the sensing principle is not based on chemical interactions but by ionization of the analyte molecules by the sensing material. This means that ionization sensors do not have the problem of cross-sensitivity. Further, since there is no adsorption or desorption phenomena involved, the response and recovery times of ionization sensors are very low. Another advantage is that ionization sensors can also be used to detect noble gases.

In previous CNT ionization sensors, the CNTs are grown vertically on a pre-patterned substrate with a metal electrode, mostly by high temperature vapor deposition methods. The challenge with using such growth methods is the yield and integration with ancillary electronics in real world applications. This work proves that it is not necessary to have vertically grown CNTs for ionization sensors. It also eliminates the need for any high temperature growth or processing methods. This work contributed to the third journal publication of this Ph.D. project. A variety of gases were tested, and the results were verified accordingly. This work constitutes the third journal publication which has been submitted for peer review.

6.1 Abstract

An Ionization sensor based on Suspended Carbon Nanotubes (CNTs) is presented. A suspended CNT beam is fabricated by a low temperature surface micromachining process using SU8 photoresist as the sacrificial layer. Application of a bias to the CNT beam generates very high non-linear electric fields near the tips of individual CNTs sufficient to ionize target gas molecules and initiate a breakdown current. The sensing mechanism of the CNT ionization sensor is discussed. The sensor response was tested in air, nitrogen, argon and helium ambients. Each gas demonstrates a unique breakdown signature. Further, the sensor is tested with gaseous mixtures. The sensor exhibited good long-term stability and had comparable performance to other reported CNT based ionization sensors in literature which use high temperature vapor deposition methods to grow CNTs. The sensor notably allowed for lower ionization voltages due to its reduced ionization gap size.

Keywords: Suspended; Carbon nanotubes; ionization

6.2 Introduction

Carbon nanotube (CNT) based gas sensors have been the subject of much research in the past few decades owing to their excellent electrical and mechanical properties. A host of sensing principles (Chen et al. 2009a; Penza et al. 2008; Cantalini et al. 2004; Liang, Chen, and Wang 2004) and device designs have been proposed to develop gas sensors based on CNTs with high performance metrics (Rana et al. 2017). Other materials that have been used in gas sensing applications include metal oxides (Comini 2006; Fine et al. 2010) and polymers (Han et al. 2016; Meyerhoff 1980). Although every gas-sensing material possess their advantages, they are also associated with certain drawbacks such as cross-sensitivity, performance degradation over time and shelf-life. CNT based sensors have overcome these drawbacks and have proven to be excellent gas sensing elements (Kerdcharoen and Wongchoosuk 2013). Suspended chemical CNT chemical gas sensors have also been previously fabricated (Chikkadi et al. 2014a; Lee et al. 2012). Chikkadi et al. fabricated a NO_2 sensor using a single suspended CNT across prefabricated electrodes.

Li et al.(Li et al. 2015) fabricated suspended CNT microlines on a polymeric substrate using a wet contact printing method. More recently, suspended chemical CNT sensors have been used to sense humidity (Arunachalam et al. 2018) with minimal hysteretic effects, due to mitigation of substrate effects (Soares and Jorio 2012). The increase in surface area for adsorption of the analyte also results in better sensitivity and long-term stability of the sensor. However, most chemical sensors are still prone to chemical poisoning and cross-sensitivity to other gases.

Ionization gas sensors operate by detecting gases based on their ionization properties and the field emission properties of the sensing elements. Townsend first studied and postulated the concept of gaseous breakdown thereby formulating the understanding of this sensing principle's physics and its operation (Townsend 1910). Ionization occurs due to the migration of electrons from cathode to anode under an applied electric field between two electrodes. The main advantage of ionization gas sensors is their independence on absorption characteristics of the sensing material or chemical interaction between species. Thus, they have faster response and recovery time and are also sensitive to inert gases. Some drawbacks of ionization sensors include relatively high voltage operation, bulky architecture and performance degradation over time. Metal oxides, ceramics and more recently, Carbon based materials have been used to fabriate ionization gas sensors. CNT based ionization sensors work on the principle of the formation of a corona on the tips of the individual CNTs due to very high electric fields near the tips that favor discharges at lower voltages than that of typical ionization sensors. On the contrary, typical ionization sensors based on metal electrodes suffer from high power consumption and high temperature operation (Hernandez-Ramirez et al. 2011; Hackner et al. 2009; Mohammadpour, Ahmadvand, and Iraji zad 2014). A CNT based ionization sensor was proposed in 2003 by (Modi et al. 2003) using vertically aligned multi-walled CNTs. The sensor showed good sensitivity to various gases. A comparative study showed that the breakdown voltages for CNT based sensor are much lower than a sensor with metal electrodes. However, no information is provided about the long-term stability of the sensor, which is a very important performance metric of gas sensors. Other CNT based ionization sensors have been developed to detect humidity, NO_2, etc. (Jiahao et al. 2008; Song, Li, and Li 2018; Song, Li, and Wang 2018; Bohr-Ran, Tzu-Ching, and Ying-Kan 2010).

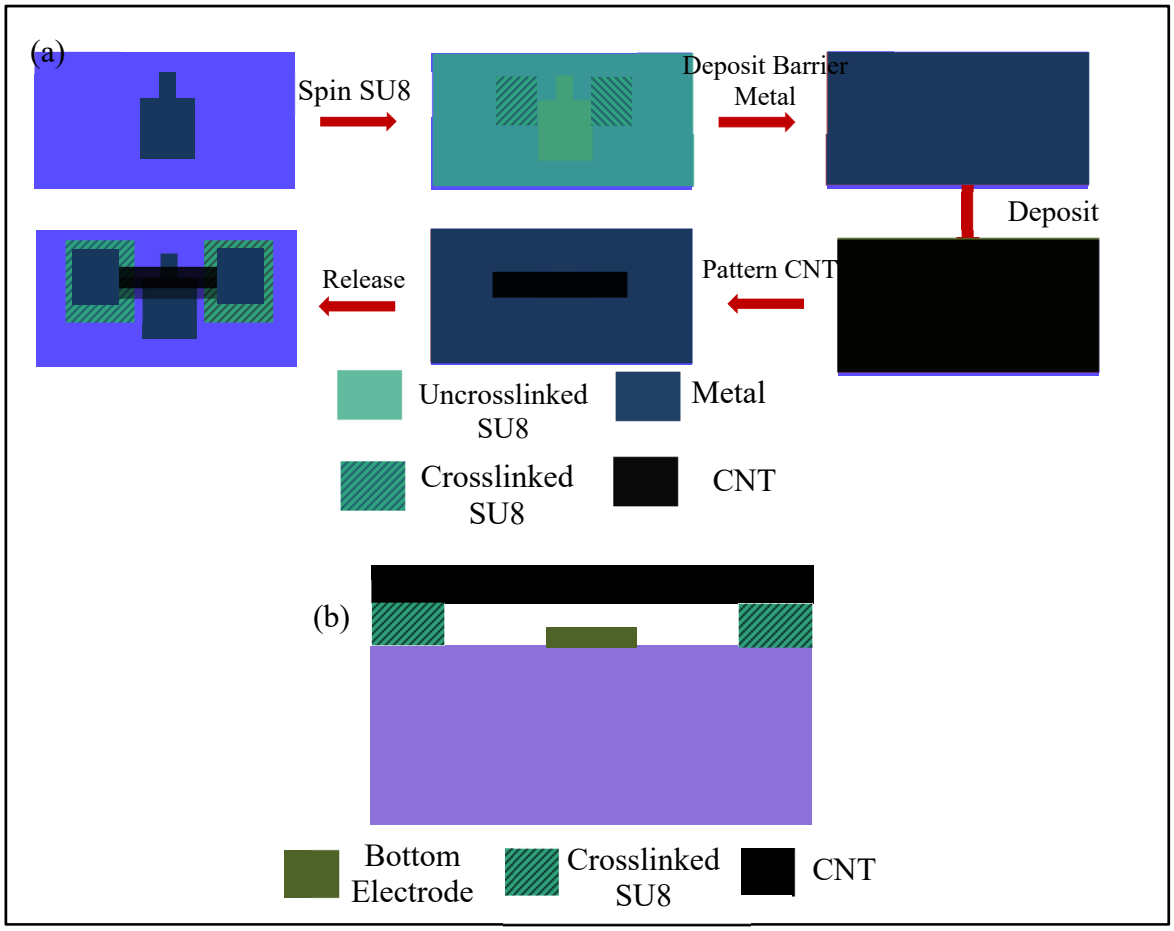

Figure 6.1 (a) Process Flow Schematic.
Taken from (Arunachalam, Izquierdo, and Nabki 2019) and,
(b) Schematic of the cross section of the device.

In all the articles mentioned above, the CNTs are grown vertically using very high temperature-based vapor deposition techniques. These growth techniques have a risk of low yield. Moreover, these deposition techniques are not suited to integration of the sensor with a wide range of substrates, which can reduce their degree of integration in a full implementation. In this work, we present an ionization gas sensor based on suspended single walled CNTs that are arranged horizontally, instead of being vertically aligned like previously mentioned publications. The resultant sensor showed similar behavior to vertically aligned CNT ionization sensors. It is worthwhile to note that the fabrication process has a temperature budget that is below 115 °C, and as such has advantage if the sensor is to be integrated with a wide range of substrates or various metallizations.

6.3 Materials and Methods

The fabrication process uses uncrosslinked SU8 photoresist as a sacrificial layer. The process was originally developed to obtain suspended nanotube beams and is shown in Figure 6.1 (a) and a cross-section of the device is shown in Figure 6.1 (b). To begin, a 30 nm-thick aluminum layer is deposited onto a silicon substrate by thermal evaporation using a Joule evaporator and patterned into an electrode shape using contact UV lithography and wet etching, using an Aluminum Etchant (Sigma Aldrich) etching solution. Then, a 3.6 µm-thick SU-8 2010 photoresist, obtained from Microchem and diluted with cyclopentanone in the ratio 1:4, is spun on top of the metal electrode and partially cross-linked by UV contact lithography using a OAI aligner to form pillar anchors for the CNT beam. The dilution was necessary to achieve the desired thickness using the thicker SU8 2010 resist Following this step, a 30 nm-thick barrier aluminum metal layer (Al) is deposited over the SU8 by thermal evaporation using a Joule effect evaporator. This barrier metal helps prevent the dissolution of the SU8 in future processing steps, more specifically during the CNT film transfer onto the substrate. The CNTs used in this work were obtained from Carbon Solutions Inc. (P2-SWNT) and a solution of CNTs in water was prepared by dispersing CNTs in a 1 wt% solution of Sodium Dodecyl Sulfate (SDDS) (obtained from Sigma Aldrich) in water and ultrasonicated for 6 hours followed by centrifugation for 60 minutes followed by decantation.

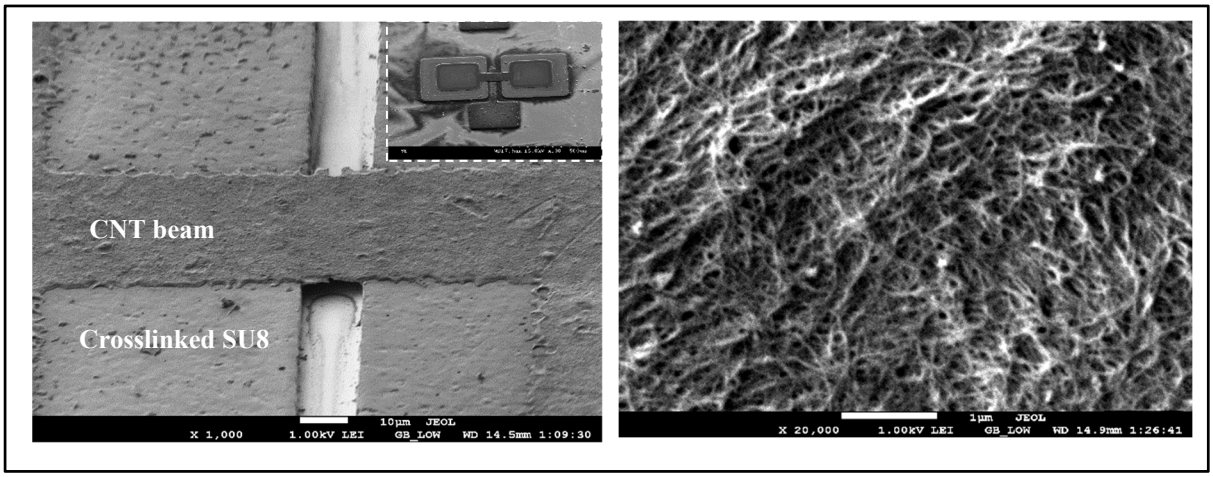

Figure 6.2 (a) SEM Micrograph of the device and,
(b) High Magnification SEM micrograph of the CNTs comprising the beam

Then, a thin film of CNTs was prepared by vacuum filtration with a thickness of 0.48 μm verified by profilometry. The reason for using the vacuum filtration technique is the easiness of processing and the ability to control the film thickness precisely depending on the amount of solution filtered. The film was then washed with DI water, air-dried and transferred onto the substrate. The CNT beams were patterned by UV lithography followed by oxygen plasma ashing. 20 nm-thick aluminum film is deposited, again by thermal evaporation and contacts are then patterned via lithography and wet etching onto the beam's extremities, above the anchors.

Finally, the barrier metal is etched using wet etching, and this followed by a removal of the uncrosslinked SU-8 in RemoverPG obtained from Microchem to release the CNT beams. The SEM Micrograph of the fabricated device is shown in Figure 6.2(a). This yields a gap between the suspended CNT beam and the bottom electrode of 3.6 μm. All the processing steps are below a temperature budget of 115 °C, making the process amenable to monolithic integration with electronics or other sensors. This fabrication process has been adopted from (Arunachalam, Izquierdo, and Nabki 2019) and is derived from the process in (Arunachalam et al. 2018) used to fabricated CNT humidity sensors. However, the fabrication process diverges from the work in (Arunachalam et al. 2018) by adding the bottom electrode layer to implement the ionization sensor The inset of the figure shows the overall device structure. Figure 2(b) shows a high magnification SEM image of the CNT networks that comprise the overall beam structure. Evidently, the SEM Micrograph in Figure 6.2(b) shows the intertwined CNTs that form a network aiding in the ionization process.

6.3.1 Test Setup

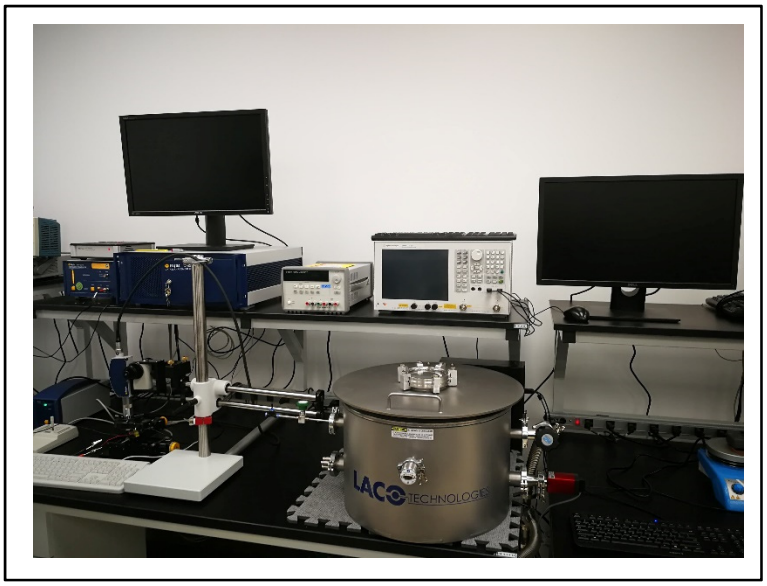

Figure 6.3 Photograph of the test setup used for the measurements showing the gas chamber, the multimeter and the computer for data acquisition.

Figure 6.3 shows the photograph of the test setup. The setup consists of a custom gas chamber obtained from Laco Technologies in which the device was placed. Two DC probes were placed within the chamber along with micro-positioners to align the probes. The chamber is evacuated using a vacuum pump. Gas lines were connected to the chamber in order to inject different gases for sensor characterization. The gas flow is controlled via Mass Flow Controllers. The DC probes were in-turn connected to a Keithley 2290-5 series high voltage DC source limited to 5000 V in order to extract the ionization voltage. The concentration of the gas inside the chamber was measured using a commercial sensor embedded within the chamber.

6.4 Results

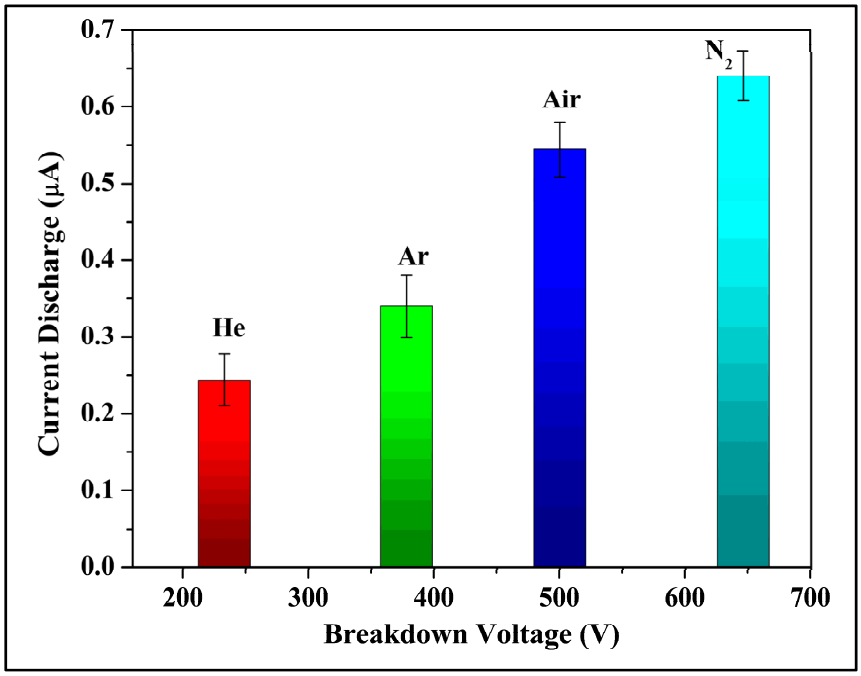

Figure 6.4 Breakdown signatures of Various gases as tested. Taken from (Arunachalam, Izquierdo, and Nabki 2019). The trend of breakdown voltages is similar to that observed by (Modi et al. 2003)

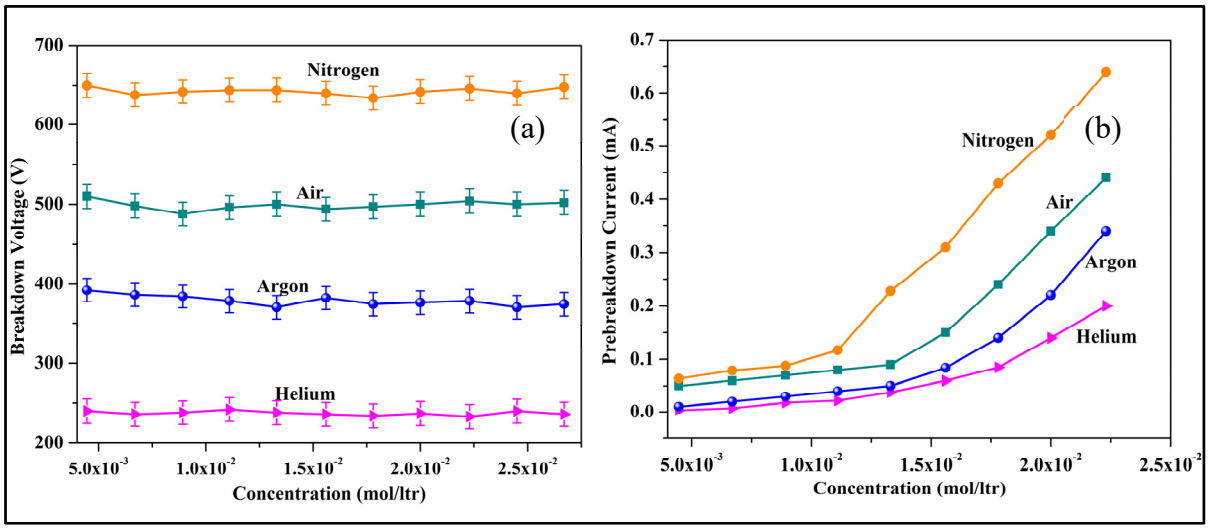

Figure 6.5 (a) Gas concentration vs breakdown voltage which shows that the breakdown voltage of the gas is independent of the gas concentration, and (b) discharge current increases as a function of concentration due to increasing gas molecules available for conduction.

A plot of the breakdown voltages of each tested gas as a function of the discharge current is shown in Figure 6.4. For 6 measured devices, the average breakdown in air was observed at a voltage of 500 V with a discharge current of 0.44 mA. In vacuum, there was no observed breakdown for a voltage sweep between 150 V and 1000 V. This is expected since in vacuum there are not enough gaseous molecules in the chamber for ionization to occur.

Then, when nitrogen was introduced into the chamber and the average breakdown was observed at 646 V, with a discharge current of 0.618 mA. In argon ambient, the average breakdown was observed at 378 V with a discharge current of 0.32 mA and for helium, the average breakdown was 233 V. The measurements were made multiple times in order to verify the stability of the breakdown voltages and to determine repeatability of the sensor. The trend of the breakdown voltage of the tested gases is similar to other reports in literature (Modi et al. 2003). This corresponds to the theory of different gases having different breakdown "signatures". The ionization of different gases occurs via a Townsend discharge where there is an electron avalanche due to the ionization. The avalanche effect depends on the mean free path of gas molecules which varies depending on the gas density. Hence, different gases show breakdown at different voltages. The effect of gas concentration on the breakdown voltages of each gases is shown in Figure 6.5(a). The breakdown voltages did not change significantly with varying the concentration.

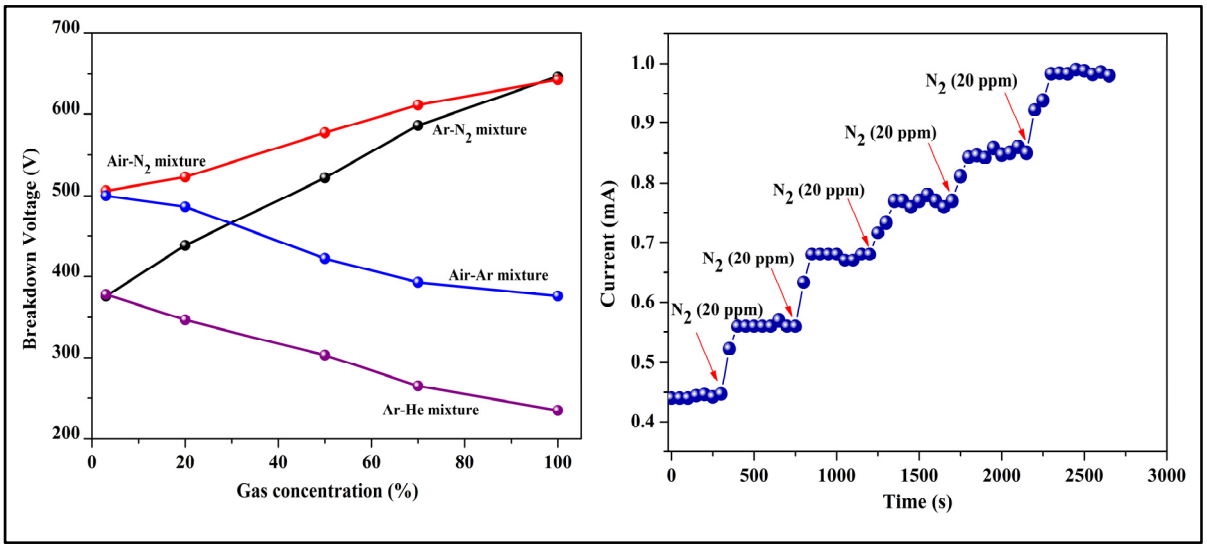

Figure 6.6 (a) Breakdown Voltage variation with different gas-air mixtures and (b) Dynamic sensing Curves of the sensor for N_2

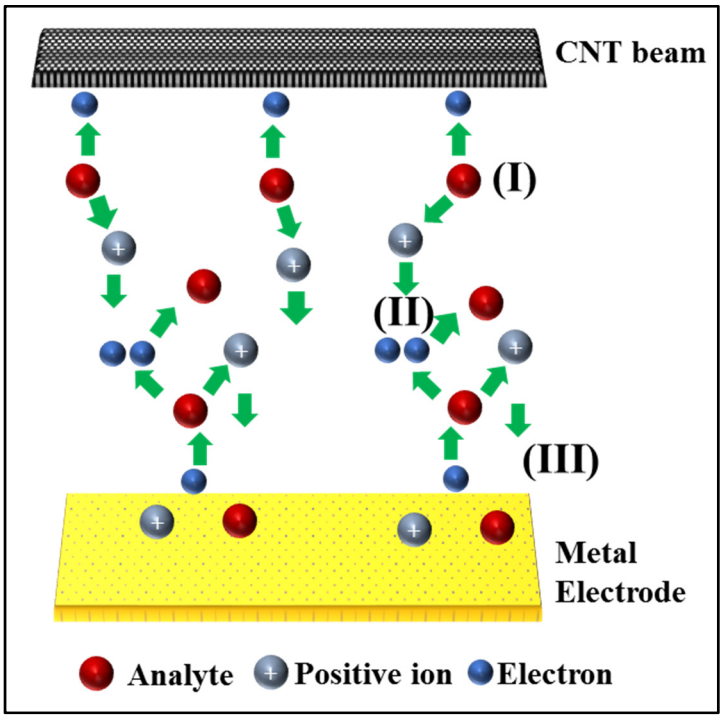

Figure 6.7 Sensing mechanism with a positive nanotip: (I) Nanotip Ionization, (II) Impact Ionization and (III) Electron Recombination

This is because the breakdown behavior is dominated by the generation of highly non-linear electric fields at the tips of the CNTs. The electric field bridges the inter-electrode gap thereby mitigating the effect of gas concentration on the breakdown voltage. Figure 6.5(b) shows the discharge current as a function of gas concentration. The discharge current increases logarithmically as the concentration increases which is because the generated current at breakdown is a property related to the number of gas molecules amenable to conduction at the time of the breakdown. Thus, the self-sustained discharge can also be used to quantify the gas concentration. The device was also tested for sensitivity to gaseous mixtures as shown in Figure 6.6 (a). Here the gas concentration percentage outlines the mixture ratio of the second gas listed in each mixture to the overall mixture. In the first case, Argon was pumped into the chamber already containing air. For greater than 50% Argon concentration in the chamber, the ionization voltage converged to the value obtained for standalone Argon measurements, indicating the increased presence of argon gas in the chamber.

As the relative concentration of Argon is reduced, the voltage increases towards 500 V, a value characteristic of the ionization voltage measured for air. Then, the air-Argon mixture was pumped out and a mixture air-Nitrogen was pumped into the chamber. As the amount of N2 was increased, the voltage increased towards the breakdown voltage of 646 V for nitrogen. As the concentration of nitrogen is decreased gradually, the breakdown voltage also decreased. Similarly, the sensor was also tested in other gaseous mixtures such as Argon-Helium. In this case, the recorded voltage shifted towards 378 V with decreasing Helium concentration and towards the standalone value of 233 V as the Helium concentration increased, as predicted. Figure 6.6 (b) shows the dynamic sensing curve of the sensor for air-nitrogen mixture. The current increases from 0.44 mA in air ambient to 0.93 mA for 100 ppm of N_2.

The sensitivity of the sensor defined as the ratio of the gas concentration to change in the current and is given by:

$$S = \frac{C}{I_g - I_a} \quad (6.1)$$

Where S is the sensitivity, C is the concentration, I_g is the current in the gas ambient and I_a is the pre-breakdown current in air. The sensitivity of the sensor is about 0.2ppm / 0.01 mA. Thus, the limit detection of the sensor is about 0.2 ppm. The schematic of Figure 6.7 shows the possible sensing mechanism with a positive CNT nanotip. The tips of the CNTs produce strong electric fields which ionize the target gas analyte and results in the release of an electron. The released electron is absorbed at the positive CNT tip while the ion moves towards the negative electrode (metal). On the metal surface, the ion recombines with an electron. Further, the kinetic energy of the ion induces an electron emission from the negative electrode (also called the γ process). The emitted electron now has enough energy to ionize other gas molecules on its path. This process is called impact ionization. The pre-breakdown current is due to the ionization at the nanotip which is amplified by the impact ionization. Thus, the working voltage of the device can be reduced (Huang et al. 2009). When the CNTs are biased as the negative electrode, electron emission occurs from the CNT nanotips followed by impact ionization and recombination which would further aid in decreasing the working voltage of the device.

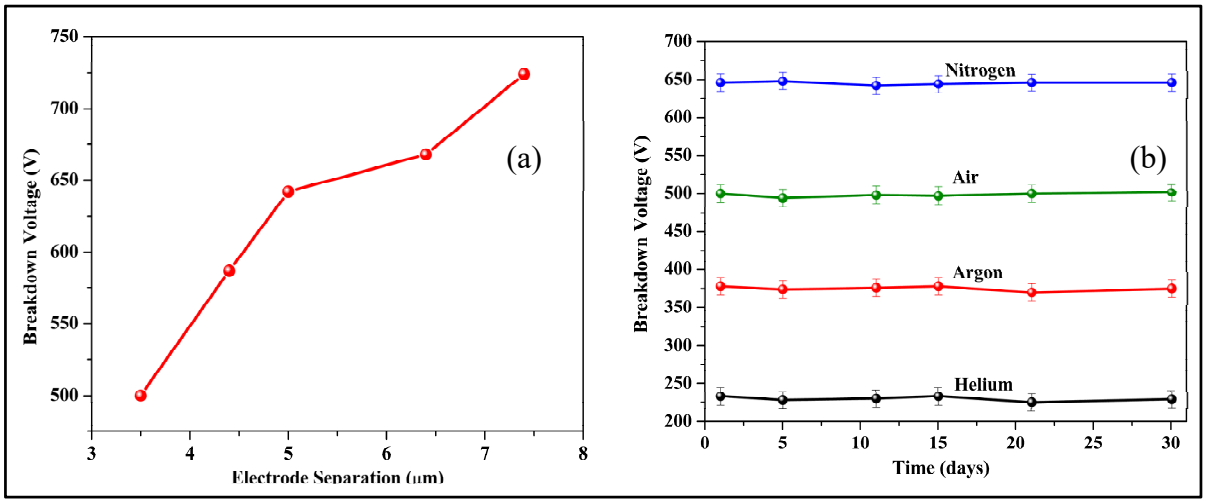

Figure 6.8 (a) Effect of inter-electrode distance on the Breakdown Voltage, and, (b) Long term stability of the sensor

When the CNTs were biased negatively, the breakdown voltage in air reduced to 242 V while for nitrogen the breakdown was observed at 328 V in agreement with (Huang et al. 2009) and (Saheed, Mohamed, and Burhanudin 2014) .The one-dimensional structure of CNTs aid in amplifying the electric field and induce discharge at a lower voltage as compared to traditional metallic ionization sensors. This is in accordance with (Modi et al. 2003) where the use of two metallic electrodes in air for ionization yielded breakdown at 1,050 V as compared to 354 V for CNTs for similar inter-electrode separation. Figure 6.8 (a) shows the effect of interelectrode separation on the breakdown voltage. The different electrode spacing was achieved by varying the SU8 pillar thickness during the fabrication process. The breakdown voltage for the gases was found to decrease with the reduction in the inter-electrode spacing. For air, the breakdown voltage was observed at 725 V for a spacing of 7.4 µm and decreases to 500 V for a spacing of 3.6 µm. The breakdown voltage could then further be reduced by decreasing the inter-electrode distance. In this case, the limitation was the beam collapse onto the bottom electrode below a height of 3.6 µm, possibly due to stiction issues.

The inter-electrode distance can also be decreased by using thinner resists as sacrificial materials, and this is currently being investigated with thinner SU8 variants. The reason for using SU8 as the sacrificial material is its ease of availability and its ease of processing.

Further, SU8 also allows for a higher thermal budget and provides a stable surface for chemical processing. The long-term stability of the sensor was gauged by measuring the breakdown voltage of all gases after intervals of 5 days for a period of 30 days. The sensor exhibited stable and consistent behavior for each measurement phase for all tested gases as shown in Figure 6.8 (b). The sensor was also tested for performance degradation under a constant applied voltage of 500 V. The sensor showed consistent behavior for 150 breakdown cycles at 500 V after which the CNT network seemed to degrade. It remains to be seen if increasing the thickness of the CNT layer influences the degradation time of the sensor.

6.5 Discussion

The work presented here shows the application of suspended CNTs to ionization gas sensing. In comparison to metallic ionization gas sensors, CNTs offer advantages such as room temperature operation, reduced operating voltages and miniature size. Ionization sensors can be advantageous in applications which require instant and consistent gas detection. The generation of strong non-linear electric fields at the tips of CNTs under applied bias reduces the breakdown voltages of target gases in comparison to metallic ionization sensors. Under positive bias, the sensing proceeds via three different steps namely: the ionization of the CNT tips, the ionization of the gas due to impact with the electron and the recombination. It is important to acknowledge that that the operation of the presented ionization sensor is not readily applicable in all sensing systems, due to the still high breakdown voltages required. However, in comparison to other CNT based ionization sensors (21, 23, 24), the presented suspended CNT sensor demonstrates lower breakdown voltages and represents a step towards mitigating this limitation. Methods to reduce the breakdown voltage even further are being investigated to widen the applications of the sensor. The sensor also shows predictable behavior on exposure to gaseous mixtures. The analyte concentration can be quantified by monitoring the breakdown current. Ionization sensors could be used in place of gas chromatography systems which are often bulky and expensive, provided the working voltage is of the order of a few volts. The high working voltage of ionization sensors hinders them from being used as-is in such an application.

Further, sensor decay also remains an issue to be studied. It could be interesting to see if the sensor can also be used to sense Volatile Organic Compounds (VOCs), thereby providing an alternative for Gas Chromatography systems. Further, the operation of the sensor in various temperature ranges and humidity needs to be studied.

6.6 Conclusions

In this work, an ionization gas sensor based on suspended CNTs was demonstrated as an alternative to conventional CNT ionization sensors. A metal electrode is placed under the suspended beam and is used as one electrode with the suspended beam acting as the other electrode. The CNT beam was biased both positively and negatively and the sensor was able to sense various inorganic gases based on their breakdown voltages. In comparison to metallic ionization sensors, the use of CNTs lowered the working voltage of the sensor, charting a path towards a more compact and wider application space for such sensors. The demonstrated sensor can be used for applications such as environmental monitoring and gas sensing in industrial and domestic environments.

Author Contributions: S.A. performed all the experiments, data acquisition and analysis. F.N. and R.I. contributed expertise, direction, materials and experimental tools.

CONCLUSION

Summary

In the introductory portion of this thesis, an overview of MEMS and its significance was presented. This is followed by describing in detail the main motivation behind this Ph.D. work. Further, the main problems with current gas sensing technologies is described followed by the objectives that this Ph.D. work aims to accomplish.

In Chapter 1, a detailed introduction about MEMS is presented including fundamental techniques, materials used in MEMS, etc. with the aim of familiarizing the reader with the meaning and significance of MEMS technologies.

In Chapter 2, a detailed discussion is presented on Carbon Nanotubes. CNTs are wondrous materials with applications in many walks of life. CNTs are the main sensing material in the sensors fabricated in this Ph.D. work and this necessitate a separate discussion. Thus, Chapter 2 details the important properties of CNTs especially applicable to the area of sensing. This is followed by a section detailing the potential applications of CNTs.

In Chapter 3, a literature survey of the application of CNTs in gas sensing is presented. A variety of methods and principles can be found in literature for CNTs based gas sensing. They range from electrical, capacitive, acoustic and even optical based sensing. These methods are studied and analyzed in detail. Keeping in line with the theme of the Ph.D. research, a sub-section reviewing and analyzing the use of CNTs in humidity sensing is also described.

Chapter 4 details the first journal publication of this project. A humidity sensor based on a suspended SWCNT bridge, fabricated by a low-temperature surface micromachining process is fabricated and tested for humidity. The CNTs used to fabricate the sensor are in the form of a thin film thereby eliminating the need for expensive and high temperature processes such as chemical vapor deposition. The fabrication process to attain suspended devices is also described in detail. The humidity sensor is shown to have minimal hysteresis even after multiple gas adsorption and desorption cycles, which was one of the main aims of this work.

The hysteresis effect can be observed in almost all the humidity sensors reported in literature and is undesirable for repeatability and long-term use. The sensor is subjected to various tests to gauge its performance and is compared to other works in literature.

Chapter 5 further expands on the work done in the previous work and constitutes the second journal publication of this Ph.D. While the previous work successfully addressed the issue of hysteresis, some performance metrics of the sensor such as the response and recovery time were too high to be deemed useful for real world use. This issue is addressed by the use of chemically functionalized CNTs thereby making them more sensitive and selective to water vapor. The chemical functionalization facilitates efficient chemical interaction between the water molecules and the CNT surface. To save time and effort, the CNTs in this work were obtained pre-functionalized. As expected, the fabricated sensor exhibited fast response and recovery times comparable to other works in literature, if not quicker.

In Chapter 6, a CNT based ionization sensor is demonstrated. This work demonstrates the evolution of the device design and flexibility of the demonstrated microfabrication process for fabricating different devices. The ionization sensor identifies gases based on ionization voltages or commonly known as “fingerprints”. The sensor is tested for sensitivity to various gases and the results are reported. One major advantage of this device is that it does not involve the use of high temperature growth methods and vertical growth of CNTs as used in other ionization-based sensors. This not only helps with device yield but also enables above IC integration. This work contributed towards the third journal publication of this Ph.D. work.

Original Contributions

Some original contributions of this work are mentioned below:

1. A novel below 115ºC microfabrication process to obtain suspended MEMS structures.
2. Development of a humidity sensor with near-zero hysteresis, fast response, recovery times and excellent long-term stability.
3. Demonstrated the use of photoresist as a sacrificial material in surface micromachining process.
4. Demonstrated a horizontally aligned SWCNT ionization sensor using a suspended CNT beam, a first of its kind in literature.

Discussion

In this Ph.D. work, we have demonstrated the application of single walled CNTs in gas sensing. Although there are demonstrated works in literature that use CNTs for gas sensing, most of them use multi walled CNTs, since they are cheaper to produce and the ability to modify their surface chemistry which makes them amenable for chemical interaction with the analyte molecules. In terms of device architecture, most of the works grow CNTs using vapor deposition techniques on substrate. The use of high temperature growth methods inhibits their integration with Integrated Circuits and sensor systems. Another drawback to using this method is the yield and quality of the CNTs obtained during the deposition process. Another major drawback which has been demonstrated is hysteresis in the sensor, primarily due to the substrate which has shown to limit charge transfer within the CNT network thereby affecting the sensor performance. Defect free substrates, although possible to produce involve expensive equipment and methodologies which in turn would add to the fabrication cost of the sensor. Thus, it is not a viable alternative to use a defect free substrate.

Another alternate to overcoming this issue is to eliminate the influence of the substrate in the sensing process. This can be achieved by suspending the sensing material so that it is not in contact with the substrate during the sensing process.

Suspended structures have historically been created by bulk micromachining techniques, wherein parts of the substrates are etched away to create grooves and then depositing the sensing material, like CNTs or Graphene over these grooves by various deposition methods that usually require high temperatures. Further, bulk micromachining also involves use of expensive equipment for lithography (e-beam) and etching. In addition, the number of usable devices in a given die can never be accurately determined because the growth of materials such as CVD is random and not necessarily over the often-predefined trenches. Also, in most of the cases, individual strands of CNTs are suspended over the trenches, which may not aid in high sensitivity.

The work done and published in this Ph.D. work tries to address all or most of the above-mentioned challenges. A new microfabrication process for fabricating suspended structures has been demonstrated. The complete process is done under a temperature of 120°C without the use of any high temperature deposition techniques. The materials used are also commonly available in any cleanroom environment and are inexpensive to purchase. To support our hypothesis of eliminating hysteretic effects, a suspended humidity sensor was fabricated and is compared to a non-suspended CNT sensor. As predicted, the suspended CNT sensor showed minimal hysteresis whereas the non-suspended sensor suffered from hysteretic effects like other sensors in literature. In addition, the suspended sensor was shown to be atleast 3 times more sensitive than a non-suspended sensor, due to the increased surface area available for analyte adsorption and desorption.

The developed device was envisioned to have different applications with minor modifications to the fabrication process. In this regard, an ionization gas sensor was realized and was tested for response to various gases. Traditionally, CNT based ionization sensors are realized by growing vertically grown CNTs on a substrate. In our work, we have demonstrated an ionization sensor in which the CNTs are horizontally aligned. To the best of the author's knowledge, this is the first instance in literature where a horizontally aligned CNT ionization

sensor has been realized. The sensor was fabricated by adding just one extra step in the fabrication process which proves the flexibility of the developed process.
The observed ionization voltages are broadly in the range of other literary works. In addition, the operating voltage can be further lowered by decreasing the inter-electrode distance.

Future work

In this work, we have used suspended CNTs to show their advantages over non-suspended sensors. In the future, it will be interesting to see if a film of graphene can be used to build a similar kind of device and then compare the performance metrics of CNTs and graphene for similar sensing applications. Further, it will also be interesting to delve into inkjet printing of the CNT network in the shape of a beam on pre-patterned photoresist features and then release the beam to create an inkjet printed suspended CNT sensor. A similar approach can be taken to print graphene-based gas sensors. This may have the potential to be one of the first printed suspended gas sensors in literature.

Here, we have only demonstrated the proof of concept for the suspended sensor as a humidity sensor. However, this work can be furthered to detect multiple gases through surface functionalization of the CNTs and building a custom gas chamber for sensing measurement. In our studies, we did not conduct studies for cross-sensitivity due to unavailability of appropriate gases at the time of testing. Thus, it is of interest and would add value if the suspended sensor exhibits minimal cross-sensitivity to gases other than the analyte.

To evolve and further the research, a similar suspended device architecture can be used to develop a SWCNT beam resonator. Although preliminary work was done to realize this device, the inter-electrode gap was deemed to be high to achieve any type of resonance. Thus, fabricating a device with reduced electrode spacing should help further the cause. This device has the potential to be one of the first SWCNT resonator fabricated by a low temperature process with a suspended CNT beam. A preliminary simulation using ANSYS has already been done to gauge an understanding of the resonant frequency of the device. The simulations showed a resonant frequency of 7.5 MHz for the first node for a suspension length of 40 μm. This needs to be corroborated with real world device testing.

LIST OF PUBLICATIONS

Arunachalam, Shivaram, Anubha Gupta, Ricardo Izquierdo, and Frederic Nabki. 2018. 'Suspended Carbon Nanotubes for Humidity Sensing', *Sensors,* 18: 1655.

Arunachalam, Shivaram, Ricardo Izquierdo, and Frederic Nabki. 2019. 'Low-Hysteresis and Fast Response Time Humidity Sensors Using Suspended Functionalized Carbon Nanotubes', *Sensors (Basel, Switzerland)*, 19: 680.

Arunachalam, Shivaram, Ricardo Izquierdo, and Frederic Nabki. 2020. 'Ionization Gas Sensor using Suspended Carbon Nanotube Beams' Submitted to *Sensors*, January 2020.

Gupta, Anubha A., Shivaram Arunachalam, Sylvain G. Cloutier, and Ricardo Izquierdo. 2018. 'Fully Aerosol-Jet Printed, High-Performance Nanoporous ZnO Ultraviolet Photodetectors', *ACS Photonics*, 5: 3923-29.

BIBLIOGRAPHY

Aimi, Marco F., Masa P. Rao, Noel C. MacDonald, Abu Samah Zuruzi, and David P. Bothman. 2004. 'High-aspect-ratio bulk micromachining of titanium', *Nature Materials*, 3: 103-05.

An, K. H., S. Y. Jeong, H. R. Hwang, and Y. H. Lee. 2004. 'Enhanced Sensitivity of a Gas Sensor Incorporating Single-Walled Carbon Nanotube–Polypyrrole Nanocomposites', *Advanced Materials*, 16: 1005-09.

Archives.caltech.edu. 2016. 'The Encyclopedia Britannica on the head of a pin?', Accessed March 4.

Arunachalam, S., R. Izquierdo, and F. Nabki. 2019. "Fabrication of an Ionization Gas Sensor using Suspended Carbon Nanotubes." In *2019 IEEE SENSORS*, 1-4.

Arunachalam, Shivaram, Anubha Gupta, Ricardo Izquierdo, and Frederic Nabki. 2018. 'Suspended Carbon Nanotubes for Humidity Sensing', *Sensors*, 18: 1655.

Ballschmiter, K., and M. Zell. 1980. 'Analysis of polychlorinated biphenyls (PCB) by glass capillary gas chromatography', *Fresenius' Zeitschrift für analytische Chemie*, 302: 20-31.

Bandaru, Prabhakar R. 2007. 'Electrical properties and applications of carbon nanotube structures', *Journal of nanoscience and nanotechnology*, 7: 1239-67.

Baratto, C., E. Comini, G. Faglia, G. Sberveglieri, M. Zha, and A. Zappettini. 2005. 'Metal oxide nanocrystals for gas sensing', *Sensors and Actuators B: Chemical*, 109: 2-6.

Barone, Paul W., Seunghyun Baik, Daniel A. Heller, and Michael S. Strano. 2004. 'Near-infrared optical sensors based on single-walled carbon nanotubes', *Nature Materials*, 4: 86.

Bauhofer, Wolfgang, and Josef Z. Kovacs. 2009. 'A review and analysis of electrical percolation in carbon nanotube polymer composites', *Composites Science and Technology*, 69: 1486-98.

Bekyarova, Elena, Mikhail E. Itkis, Nelson Cabrera, Bin Zhao, Aiping Yu, Junbo Gao, and Robert C. Haddon. 2005. 'Electronic Properties of Single-Walled Carbon Nanotube Networks', *Journal of the American Chemical Society*, 127: 5990-95.

Benchirouf, Abderrahmane, Saravanan Palaniyappan, Rajarajan Ramalingame, Poornima Raghunandan, Torsten Jagemann, Christian Müller, Michael Hietschold, and Olfa Kanoun. 2016. 'Electrical properties of multi-walled carbon nanotubes/PEDOT:PSS nanocomposites thin films under temperature and humidity effects', *Sensors and Actuators B: Chemical*, 224: 344-50.

Bohr-Ran, Huang, Lin Tzu-Ching, and Yang Ying-Kan. 2010. "Gas ionization sensors with CNT/Ni field cathodes." In *2010 3rd International Nanoelectronics Conference (INEC)*, 535-36.

C. Moraes, Marcos, Elisabete Galeazzo, Henrique Peres, Javier Ramirez-Fernandez, and Michel Dantas. 2014. *Development of Fast Response Humidity Sensors Based on Carbon Nanotubes*.

Camponeschi, Erin, Richard Vance, Marwan Al-Haik, Hamid Garmestani, and Rina Tannenbaum. 2007. 'Properties of carbon nanotube–polymer composites aligned in a magnetic field', *Carbon*, 45: 2037-46.

Cantalini, C., L. Valentini, I. Armentano, J. M. Kenny, L. Lozzi, and S. Santucci. 2004. 'Carbon nanotubes as new materials for gas sensing applications', *Journal of the European Ceramic Society*, 24: 1405-08.

Cao, C. L., C. G. Hu, L. Fang, S. X. Wang, Y. S. Tian, and C. Y. Pan. 2011. 'Humidity Sensor Based on Multi-Walled Carbon Nanotube Thin Films', *Journal of Nanomaterials*, 2011: 5.

Cao, Jien, Qian Wang, and Hongjie Dai. 2005. 'Electron transport in very clean, as-grown suspended carbon nanotubes', *Nature Materials*, 4: 745.

Cao, Qing, and John A. Rogers. 2009. 'Ultrathin Films of Single-Walled Carbon Nanotubes for Electronics and Sensors: A Review of Fundamental and Applied Aspects', *Advanced Materials*, 21: 29-53.

Chen, Jian, Mark A. Hamon, Hui Hu, Yongsheng Chen, Apparao M. Rao, Peter C. Eklund, and Robert C. Haddon. 1998. 'Solution Properties of Single-Walled Carbon Nanotubes', *Science*, 282: 95-98.

Chen, Wei-Ping, Zhen-Gang Zhao, Xiao-Wei Liu, Zhong-Xin Zhang, and Chun-Guang Suo. 2009a. 'A Capacitive Humidity Sensor Based on Multi-Wall Carbon Nanotubes (MWCNTs)', *Sensors (Basel, Switzerland)*, 9: 7431-44.

Chen, Zhihong, Joerg Appenzeller, Joachim Knoch, Yu-ming Lin, and Phaedon Avouris. 2005. 'The Role of Metal−Nanotube Contact in the Performance of Carbon Nanotube Field-Effect Transistors', *Nano Letters*, 5: 1497-502.

Chikkadi, K., M. Muoth, and C. Hierold. 2013. "Hysteresis-free, suspended pristine carbon nanotube gas sensors." In *2013 Transducers & Eurosensors XXVII: The 17th International Conference on Solid-State Sensors, Actuators and Microsystems (TRANSDUCERS & EUROSENSORS XXVII)*, 1637-40.

Chikkadi, Kiran, Matthias Muoth, Wei Liu, Verena Maiwald, and Christofer Hierold. 2014a. 'Enhanced signal-to-noise ratio in pristine, suspended carbon nanotube gas sensors', *Sensors and Actuators B: Chemical*, 196: 682-90.

Choi, W. B., D. S. Chung, J. H. Kang, H. Y. Kim, Y. W. Jin, I. T. Han, Y. H. Lee, J. E. Jung, N. S. Lee, G. S. Park, and J. M. Kim. 1999. 'Fully sealed, high-brightness carbon-nanotube field-emission display', *Applied Physics Letters*, 75: 3129-31.

Chou, Kan-Sen, Tzy-Kuang Lee, and Feng-Jiin Liu. 1999. 'Sensing mechanism of a porous ceramic as humidity sensor', *Sensors and Actuators B: Chemical*, 56: 106-11.

Chu, Jin, Xiaoyan Peng, Peter Feng, Yong Sheng, and Jianting Zhang. 2013. 'Study of humidity sensors based on nanostructured carbon films produced by physical vapor deposition', *Sensors and Actuators B: Chemical*, 178: 508-13.

Chung, Charles, and Mark Allen. 2005. 'Uncrosslinked SU-8 as a sacrificial material', *J. Micromech. Microeng*, 15: 1-5.

Comini, Elisabetta. 2006. 'Metal oxide nano-crystals for gas sensing', *Analytica Chimica Acta*, 568: 28-40.

Dong, Xiaochen, Dongliang Fu, Moawia O. Ahmed, Yumeng Shi, S. G. Mhaisalkar, Sam Zhang, Shabbir Moochhala, Xinning Ho, John A. Rogers, and Lain-Jong Li. 2007. 'Heme-Enabled Electrical Detection of Carbon Monoxide at Room Temperature Using Networked Carbon Nanotube Field-Effect Transistors', *Chemistry of Materials*, 19: 6059-61.

Eneman, G., M. Wiot, A. Brugere, O. Sicart I Casain, S. Sonde, D. P. Brunco, B. De Jaeger, A. Satta, G. Hellings, K. De Meyer, C. Claeys, M. Meuris, M. M. Heyns, and E. Simoen. 2008. 'Impact of Donor Concentration, Electric Field, and Temperature Effects on the Leakage Current in Germanium p $+/$n Junctions', *IEEE Transactions on Electron Devices*, 55: 2287-96.

Farahani, Hamid, Rahman Wagiran, and Mohd Hamidon. 2014. 'Humidity Sensors Principle, Mechanism, and Fabrication Technologies: A Comprehensive Review', *Sensors*, 14: 7881.

Fine, George F., Leon M. Cavanagh, Ayo Afonja, and Russell Binions. 2010. 'Metal Oxide Semi-Conductor Gas Sensors in Environmental Monitoring', *Sensors*, 10: 5469-502.

Fischer, J. E., H. Dai, A. Thess, R. Lee, N. M. Hanjani, D. L. Dehaas, and R. E. Smalley. 1997. 'Metallic resistivity in crystalline ropes of single-wall carbon nanotubes', *Physical Review B*, 55: R4921-R24.

Fung, C. K. M., M. Q. H. Zhang, R. H. M. Chan, and W. J. Li. 2005. "A PMMA-based micro pressure sensor chip using carbon nanotubes as sensing elements." In *18th IEEE International Conference on Micro Electro Mechanical Systems, 2005. MEMS 2005.*, 251-54.

Gojny, F. H., M. H. G. Wichmann, U. Köpke, B. Fiedler, and K. Schulte. 2004. 'Carbon nanotube-reinforced epoxy-composites: enhanced stiffness and fracture toughness at low nanotube content', *Composites Science and Technology*, 64: 2363-71.

Gu, Lei, Qing-An Huang, and Ming Qin. 2004. 'A novel capacitive-type humidity sensor using CMOS fabrication technology', *Sensors and Actuators B: Chemical*, 99: 491-98.

Hackner, A., A. Habauzit, G. Muller, E. Comini, G. Faglia, and G. Sberveglieri. 2009. 'Surface Ionization Gas Detection on Platinum and Metal Oxide Surfaces', *IEEE Sensors Journal*, 9: 1727-33.

Han, Jin-Woo, Beomseok Kim, Jing Li, and M. Meyyappan. 2012. 'Carbon Nanotube Based Humidity Sensor on Cellulose Paper', *The Journal of Physical Chemistry C*, 116: 22094-97.

Han, Shijiao, Xinming Zhuang, Wei Shi, Xin Yang, Lu Li, and Junsheng Yu. 2016. 'Poly(3-hexylthiophene)/polystyrene (P3HT/PS) blends based organic field-effect transistor ammonia gas sensor', *Sensors and Actuators B: Chemical*, 225: 10-15.

He, Xiaowei, Weilu Gao, Lijuan Xie, Bo Li, Qi Zhang, Sidong Lei, John M. Robinson, Erik H. Hároz, Stephen K. Doorn, Weipeng Wang, Robert Vajtai, Pulickel M. Ajayan, W. Wade Adams, Robert H. Hauge, and Junichiro Kono. 2016. 'Wafer-scale monodomain films of spontaneously aligned single-walled carbon nanotubes', *Nature Nanotechnology*, 11: 633.

Helbling, T., R. Pohle, L. Durrer, C. Stampfer, C. Roman, A. Jungen, M. Fleischer, and C. Hierold. 2008. 'Sensing NO2 with individual suspended single-walled carbon nanotubes', *Sensors and Actuators B: Chemical*, 132: 491-97.

Helbling, Thomas, Christofer Hierold, Lukas Durrer, Cosmin Roman, Roland Pohle, and Maximilian Fleischer. 2008. 'Suspended and non-suspended carbon nanotube transistors for NO2 sensing – A qualitative comparison', *physica status solidi (b)*, 245: 2326-30.

Hernandez-Ramirez, Francisco, Juan Daniel Prades, Angelika Hackner, Thomas Fischer, Gerhard Mueller, Sanjay Mathur, and Joan Ramon Morante. 2011. 'Miniaturized ionization gas sensors from single metal oxide nanowires', *Nanoscale*, 3: 630-34.

Heyd, R., A. Charlier, and E. McRae. 1997. 'Uniaxial-stress effects on the electronic properties of carbon nanotubes', *Physical Review B*, 55: 6820-24.

Hone, J., M. C. Llaguno, N. M. Nemes, A. T. Johnson, J. E. Fischer, D. A. Walters, M. J. Casavant, J. Schmidt, and R. E. Smalley. 2000. 'Electrical and thermal transport properties of magnetically aligned single wall carbon nanotube films', *Applied Physics Letters*, 77: 666-68.

Hong, Guosong, Shuo Diao, Alexander L. Antaris, and Hongjie Dai. 2015. 'Carbon Nanomaterials for Biological Imaging and Nanomedicinal Therapy', *Chemical Reviews*, 115: 10816-906.

Huang, Jiarui, Junhai Wang, Cuiping Gu, Kun Yu, Fanli Meng, and Jinhuai Liu. 2009. 'A novel highly sensitive gas ionization sensor for ammonia detection', *Sensors and Actuators A: Physical*, 150: 218-23.

Iijima, Sumio. 1991. 'Helical microtubules of graphitic carbon', *Nature*, 354: 56.

Iijima, Sumio, and Toshinari Ichihashi. 1993. 'Single-shell carbon nanotubes of 1-nm diameter', *Nature*, 363: 603-05.

Inpil, Kang, J. Schulz Mark, H. Kim Jay, Shanov Vesselin, and Shi Donglu. 2006. 'A carbon nanotube strain sensor for structural health monitoring', *Smart Materials and Structures*, 15: 737.

Janas, Dawid. 2018. 'Towards monochiral carbon nanotubes: a review of progress in the sorting of single-walled carbon nanotubes', *Materials Chemistry Frontiers*, 2: 36-63.

Javey, Ali, Jing Guo, Qian Wang, Mark Lundstrom, and Hongjie Dai. 2003. 'Ballistic carbon nanotube field-effect transistors', *Nature*, 424: 654-57.

Jensen, K., Kwanpyo Kim, and A. Zettl. 2008. 'An atomic-resolution nanomechanical mass sensor', *Nature Nanotechnology*, 3: 533.

Jiahao, Wu, Liu Hai, Wang Yanyan, Xu Dong, and Zhang Yafei. 2008. "A MEMS-based ionization gas sensor using carbon nanotubes and dielectric barrier." In *2008 3rd IEEE International Conference on Nano/Micro Engineered and Molecular Systems*, 824-27.

Jiangbo, Zhang, Xi Ning, Chan Hoyin, and Li Guangyong. 2006. "Single Carbon Nanotube Based Ion Sensor for Gas Detection." In *2006 Sixth IEEE Conference on Nanotechnology*, 790-93.

Jung, Daewoong, Jinhong Kim, and Gil S. Lee. 2015. 'Enhanced humidity-sensing response of metal oxide coated carbon nanotube', *Sensors and Actuators A: Physical*, 223: 11-17.

Kaiser, A. B., G. Düsberg, and S. Roth. 1998. 'Heterogeneous model for conduction in carbon nanotubes', *Physical Review B*, 57: 1418-21.

Kawano, Takeshi, Heather C. Chiamori, Marcel Suter, Qin Zhou, Brian D. Sosnowchik, and Liwei Lin. 2007. 'An Electrothermal Carbon Nanotube Gas Sensor', *Nano Letters*, 7: 3686-90.

Kerdcharoen, Teerakiat, and Chatchawal Wongchoosuk. 2013. 'Carbon nanotube and metal oxide hybrid materials for gas sensing.' in.

Kim, Woong, Ali Javey, Ophir Vermesh, Qian Wang, Yiming Li, and Hongjie Dai. 2003. 'Hysteresis Caused by Water Molecules in Carbon Nanotube Field-Effect Transistors', *Nano Letters*, 3: 193-98.

Klinger, Colin, Yogeshwari Patel, and Henk W. Ch Postma. 2012. 'Carbon Nanotube Solar Cells', *PLOS ONE*, 7: e37806.

Ko, Hyunhyub, and Vladimir V. Tsukruk. 2006. 'Liquid-Crystalline Processing of Highly Oriented Carbon Nanotube Arrays for Thin-Film Transistors', *Nano Letters*, 6: 1443-48.

Kong, Jing, Nathan R. Franklin, Chongwu Zhou, Michael G. Chapline, Shu Peng, Kyeongjae Cho, and Hongjie Dai. 2000. 'Nanotube Molecular Wires as Chemical Sensors', *Science*, 287: 622-25.

Krishnan, A., E. Dujardin, T. W. Ebbesen, P. N. Yianilos, and M. M. J. Treacy. 1998. 'Young's modulus of single-walled nanotubes', *Physical Review B*, 58: 14013-19.

Kumar, S., J. Y. Murthy, and M. A. Alam. 2005. 'Percolating Conduction in Finite Nanotube Networks', *Physical Review Letters*, 95: 066802.

Lee, Dongjin, Zhijiang Ye, Stephen A. Campbell, and Tianhong Cui. 2012. 'Suspended and highly aligned carbon nanotube thin-film structures using open microfluidic channel template', *Sensors and Actuators A: Physical*, 188: 434-41.

Li, Bo, Xin Wang, Hyun Young Jung, Young Lae Kim, Jeremy T. Robinson, Maxim Zalalutdinov, Sanghyun Hong, Ji Hao, Pulickel M. Ajayan, Kai-Tak Wan, and Yung Joon Jung. 2015. 'Printing Highly Controlled Suspended Carbon Nanotube Network on Micro-patterned Superhydrophobic Flexible Surface', *Scientific Reports*, 5: 15908.

Li, Jing, Yijiang Lu, Qi Ye, Martin Cinke, Jie Han, and M. Meyyappan. 2003. 'Carbon Nanotube Sensors for Gas and Organic Vapor Detection', *Nano Letters*, 3: 929-33.

Liang, Y. X., Y. J. Chen, and T. H. Wang. 2004. 'Low-resistance gas sensors fabricated from multiwalled carbon nanotubes coated with a thin tin oxide layer', *Applied Physics Letters*, 85: 666-68.

Lima, Márcio D., Shaoli Fang, Xavier Lepró, Chihye Lewis, Raquel Ovalle-Robles, Javier Carretero-González, Elizabeth Castillo-Martínez, Mikhail E. Kozlov, Jiyoung Oh, Neema Rawat, Carter S. Haines, Mohammad H. Haque, Vaishnavi Aare, Stephanie Stoughton, Anvar A. Zakhidov, and Ray H. Baughman. 2011. 'Biscrolling Nanotube Sheets and Functional Guests into Yarns', *Science*, 331: 51-55.

Liu, Litao, Xiongying Ye, Kang Wu, Rui Han, Zhaoying Zhou, and Tianhong Cui. 2009. 'Humidity Sensitivity of Multi-Walled Carbon Nanotube Networks Deposited by Dielectrophoresis', *Sensors*, 9: 1714.

Ma, X., H. Ning, N. Hu, Y. Liu, J. Zhang, C. Xu, and L. Wu. 2015. 'Highly sensitive humidity sensors made from composites of HEC filled by carbon nanofillers', *Materials Technology*, 30: 134-39.

Ma, Yuhua, Shuangyu Ma, Tieliu Wang, and Weiling Fang. 1995. 'Air-flow sensor and humidity sensor application to neonatal infant respiration monitoring', *Sensors and Actuators A: Physical*, 49: 47-50.

Meitl, Matthew A., Yangxin Zhou, Anshu Gaur, Seokwoo Jeon, Monica L. Usrey, Michael S. Strano, and John A. Rogers. 2004. 'Solution Casting and Transfer Printing Single-Walled Carbon Nanotube Films', *Nano Letters*, 4: 1643-47.

Meyerhoff, Mark E. 1980. 'Polymer membrane electrode based potentiometric ammonia gas sensor', *Analytical Chemistry*, 52: 1532-34.

Minot, E. D., Yuval Yaish, Vera Sazonova, Ji-Yong Park, Markus Brink, and Paul L. McEuen. 2003. 'Tuning Carbon Nanotube Band Gaps with Strain', *Physical Review Letters*, 90: 156401.

Modi, Ashish, Nikhil Koratkar, Eric Lass, Bingqing Wei, and Pulickel M. Ajayan. 2003. 'Miniaturized gas ionization sensors using carbon nanotubes', *Nature*, 424: 171-74.

Mohammadpour, Raheleh, Hassan Ahmadvand, and Azam Iraji zad. 2014. 'A novel field ionization gas sensor based on self-organized CuO nanowire arrays', *Sensors and Actuators A: Physical*, 216: 202-06.

Monthioux, Marc, Philippe Serp, Emmanuel Flahaut, Manitra Razafinimanana, Christophe Laurent, Alain Peigney, Wolfgang Bacsa, and Jean-Marc Broto. 2007. 'Introduction to Carbon Nanotubes.' in Bharat Bhushan (ed.), *Springer Handbook of Nanotechnology* (Springer Berlin Heidelberg: Berlin, Heidelberg).

Mudimela, Prasantha R., Kestutis Grigoras, Ilya V. Anoshkin, Aapo Varpula, Vladimir Ermolov, Anton S. Anisimov, Albert G. Nasibulin, Sergey Novikov, and Esko I. Kauppinen. 2012. 'Single-Walled Carbon Nanotube Network Field Effect Transistor as a Humidity Sensor', *Journal of Sensors*, 2012: 7.

Muoth, M., T. Helbling, L. Durrer, S. W. Lee, C. Roman, and C. Hierold. 2010. 'Hysteresis-free operation of suspended carbon nanotube transistors', *Nature Nanotechnology*, 5: 589.

Novak, J. P., E. S. Snow, E. J. Houser, D. Park, J. L. Stepnowski, and R. McGill. 2003. *Nerve agent detection using networks of single-walled carbon nanotubes*.

Park, Steve, Michael Vosguerichian, and Zhenan Bao. 2013. 'A review of fabrication and applications of carbon nanotube film-based flexible electronics', *Nanoscale*, 5: 1727-52.

Paul, A., B. Pramanick, B. Bhattacharya, and T. K. Bhattacharyya. 2013. 'Deoxyribonucleic Acid Functionalized Carbon Nanotube Network as Humidity Sensors', *IEEE Sensors Journal*, 13: 1806-16.

Penza, M., R. Rossi, M. Alvisi, P. Aversa, G. Cassano, D. Suriano, M. Benetti, D. Cannata, F. Di Pietrantonio, and E. Verona. 2008. "SAW Gas sensors with carbon nanotubes films." In *2008 IEEE Ultrasonics Symposium*, 1850-53.

Qi, Qi, Tong Zhang, Qingjiang Yu, Rui Wang, Yi Zeng, Li Liu, and Haibin Yang. 2008. 'Properties of humidity sensing ZnO nanorods-base sensor fabricated by screen-printing', *Sensors and Actuators B: Chemical*, 133: 638-43.

Rana, Masud, Shehu Dauda, Mohd Asyraf Mohd Razib, Sams Jarin, and A. N. M. Tomal. 2017. 'A review on recent advances of CNTs as gas sensors', *Sensor Review*, 37: 127-36.

Rosenblatt, Sami, Yuval Yaish, Jiwoong Park, Jeff Gore, Vera Sazonova, and Paul L. McEuen. 2002. 'High Performance Electrolyte Gated Carbon Nanotube Transistors', *Nano Letters*, 2: 869-72.

Saheed, M. Shuaib M., Norani Muti Mohamed, and Zainal Arif Burhanudin. 2014. 'Breakdown voltage reduction by field emission in multi-walled carbon nanotubes based ionization gas sensor', *Applied Physics Letters*, 104: 123105.

Saile, Volker, Ulrike Wallrabe, Osamu Tabata, and Jan Korvink. 2009. *LIGA and its applications*.

Saito, Riichiro, Mitsutaka Fujita, G. Dresselhaus, and M. S. Dresselhaus. 1992. 'Electronic structure of graphene tubules based on ${\mathrm{C}}_{60}$', *Physical Review B*, 46: 1804-11.

Sapmaz, S., P. Jarillo-Herrero, Ya M. Blanter, C. Dekker, and H. S. J. van der Zant. 2006. 'Tunneling in Suspended Carbon Nanotubes Assisted by Longitudinal Phonons', *Physical Review Letters*, 96: 026801.

Sazonova, Vera, Yuval Yaish, Hande Üstünel, David Roundy, Tomás A. Arias, and Paul L. McEuen. 2004. 'A tunable carbon nanotube electromechanical oscillator', *Nature*, 431: 284-87.

Schroeder, Vera, Suchol Savagatrup, Maggie He, Sibo Lin, and Timothy M. Swager. 2018. 'Carbon Nanotube Chemical Sensors', *Chemical Reviews*.

Science and Society. 2004. 'World's Smallest Motor: The McLellan Micromotor', Accessed March 4.

Sinha, Niraj, Jiazhi Ma, and John T. W. Yeow. 2006. 'Carbon Nanotube-Based Sensors', *Journal of Nanoscience and Nanotechnology*, 6: 573-90.

Slade, P. G., and E. D. Taylor. 2001. "Electrical breakdown in atmospheric air between closely spaced (0.2 /spl mu/m-40 /spl mu/m) electrical contacts." In *Proceedings of the Forth-Seventh IEEE Holm Conference on Electrical Contacts (IEEE Cat. No.01CH37192)*, 245-50.

Snow, E. S., F. K. Perkins, E. J. Houser, S. C. Badescu, and T. L. Reinecke. 2005. 'Chemical Detection with a Single-Walled Carbon Nanotube Capacitor', *Science*, 307: 1942.

So, Hye-Mi, Jin Woo Sim, Jinhyeong Kwon, Jongju Yun, Seunghyun Baik, and Won Seok Chang. 2013. 'Carbon nanotube based pressure sensor for flexible electronics', *Materials Research Bulletin*, 48: 5036-39.

Soares, Jaqueline S., and Ado Jorio. 2012. 'Study of Carbon Nanotube-Substrate Interaction', *Journal of Nanotechnology*, 2012: 10.

Song, Hui, Kun Li, and Quanfu Li. 2018. 'A tripolar-electrode ionization gas sensor using a carbon nanotube cathode for NO detection', *Journal of Micromechanics and Microengineering*, 28: 065010.

Song, Hui, Kun Li, and Chang Wang. 2018. 'Selective Detection of NO and NO_2 with CNTs-Based Ionization Sensor Array', *Micromachines*, 9: 354.

Star, Alexander, J. Fraser Stoddart, David Steuerman, Mike Diehl, Akram Boukai, Eric W. Wong, Xin Yang, Sung-Wook Chung, Hyeon Choi, and James R. Heath. 2001. 'Preparation and Properties of Polymer-Wrapped Single-Walled Carbon Nanotubes', *Angewandte Chemie International Edition*, 40: 1721-25.

Tang, Qing-Yuan, Y. C. Chan, and Kaili Zhang. 2011. 'Fast response resistive humidity sensitivity of polyimide/multiwall carbon nanotube composite films', *Sensors and Actuators B: Chemical*, 152: 99-106.

Townsend, John. 1910. *The theory of ionization of gases by collision* (Constable & Co.: London).

Treacy, M. M. J., T. W. Ebbesen, and J. M. Gibson. 1996. 'Exceptionally high Young's modulus observed for individual carbon nanotubes', *Nature*, 381: 678.

Tsai, Jeff T. H., Chih-Cheng Lu, and Jason G. Li. 2010. 'Fabrication of humidity sensors by multi-walled carbon nanotubes', *Journal of Experimental Nanoscience*, 5: 302-09.

Wang, Dayue, Ying Huang, Wenting Cai, Min Tian, Ping Liu, and Yugang Zhang. 2014. 'Functionalized multi-wall carbon nanotubes/silicone rubber composite as capacitive humidity sensor', *Journal of Applied Polymer Science*, 131.

Wang, Yun, and John T. W. Yeow. 2009. 'A Review of Carbon Nanotubes-Based Gas Sensors', *Journal of Sensors*, 2009: 24.

Wei, Chen, Liming Dai, Ajit Roy, and Tia Benson Tolle. 2006. 'Multifunctional Chemical Vapor Sensors of Aligned Carbon Nanotube and Polymer Composites', *Journal of the American Chemical Society*, 128: 1412-13.

Weiser, Eric. 2013. 'Degradation of multiwall carbon nanotube epoxy composites', Accessed December 19.

Wong, Eric W., Paul E. Sheehan, and Charles M. Lieber. 1997. 'Nanobeam Mechanics: Elasticity, Strength, and Toughness of Nanorods and Nanotubes', *Science*, 277: 1971-75.

Wu, Jian, Ji Zang, Brian Larade, Hong Guo, X. G. Gong, and Feng Liu. 2004. 'Computational design of carbon nanotube electromechanical pressure sensors', *Physical Review B*, 69: 153406.

Wu, Zhuangchun, Zhihong Chen, Xu Du, Jonathan M. Logan, Jennifer Sippel, Maria Nikolou, Katalin Kamaras, John R. Reynolds, David B. Tanner, Arthur F. Hebard, and Andrew G. Rinzler. 2004. 'Transparent, Conductive Carbon Nanotube Films', *Science*, 305: 1273-76.

Yang, Mujie, Yang Li, Xiaowei Zhan, and Mingfang Ling. 1999. 'A novel resistive-type humidity sensor based on poly(p-diethynylbenzene)', *Journal of Applied Polymer Science*, 74: 2010-15.

Yeow, J. T. W., and J. P. M. She. 2006. 'Carbon nanotube-enhanced capillary condensation for a capacitive humidity sensor', *Nanotechnology*, 17: 5441.

Yu, Min-Feng, Bradley S. Files, Sivaram Arepalli, and Rodney S. Ruoff. 2000. 'Tensile Loading of Ropes of Single Wall Carbon Nanotubes and their Mechanical Properties', *Physical Review Letters*, 84: 5552-55.

Zhang, Hai-Long, Jing-Feng Li, Bo-Ping Zhang, Ke-Fu Yao, Wei-Shu Liu, and Heng Wang. 2007. 'Electrical and thermal properties of carbon nanotube bulk materials: Experimental studies for the $328--958\phantom{\rule{0.3em}{0ex}}\mathrm{K}$ temperature range', *Physical Review B*, 75: 205407.

Zhang, Jin, Hongling Zou, Quan Qing, Yanlian Yang, Qingwen Li, Zhongfan Liu, Xinyong Guo, and Zuliang Du. 2003. 'Effect of Chemical Oxidation on the Structure of Single-Walled Carbon Nanotubes', *The Journal of Physical Chemistry B*, 107: 3712-18.

Zhang, Yongsheng, Ke Yu, Rongli Xu, Desheng Jiang, Laiqiang Luo, and Ziqiang Zhu. 2005. 'Quartz crystal microbalance coated with carbon nanotube films used as humidity sensor', *Sensors and Actuators A: Physical*, 120: 142-46.

Zhao, B., H. Hu, and R. C. Haddon. 2004. 'Synthesis and Properties of a Water-Soluble Single-Walled Carbon Nanotube–Poly(m-aminobenzene sulfonic acid) Graft Copolymer', *Advanced Functional Materials*, 14: 71-76.

Zhao, Zhen-gang, Xiao-wei Liu, Wei-ping Chen, and Tuo Li. 2011. 'Carbon nanotubes humidity sensor based on high testing frequencies', *Sensors and Actuators A: Physical*, 168: 10-13.

Zhou, Gengheng, Joon-Hyung Byun, Youngseok Oh, Byung-Mun Jung, Hwa-Jin Cha, Dong-Gi Seong, Moon-Kwang Um, Sangil Hyun, and Tsu-Wei Chou. 2017. 'Highly Sensitive Wearable Textile-Based Humidity Sensor Made of High-Strength, Single-Walled Carbon Nanotube/Poly(vinyl alcohol) Filaments', *ACS Applied Materials & Interfaces*, 9: 4788-97.